UNCLASSIFIED

AD NUMBER

AD506209

CLASSIFICATION CHANGES

TO: unclassified

FROM: confidential

LIMITATION CHANGES

TO:

Approved for public release, distribution unlimited

FROM:

Distribution: Controlled: all requests to Director, Naval Research Lab., Attn: Code 102-OS. Washington, D. C. 20390.

AUTHORITY

ONR ltr., ser93/160, 10 Mar 1999; ONR ltr., ser93/160, 10 Mar 1999

THIS PAGE IS UNCLASSIFIED

CONFIDENTIAL

AD 506209L

CLASSIFICATION CHANGED
TO: CONFIDENTIAL
FROM: SECRET
AUTHORITY:

DoD 5200.1-R
Oct 80

CONFIDENTIAL

SECRET
NOFORN

MC REPORT 003
Volume 1

AD506209

THE PARKA I EXPERIMENT

November 1969

Special Handling Required
Not Releasable to Foreign Nationals

DDC
WHITE
HEADQUARTERS

466930

DEC 31 1969

DDC CONTROL
NO. 93975

OCEAN SCIENCE PROGRAM

MAURY CENTER FOR OCEAN SCIENCE
Department of the Navy
Washington, D.C.

Downgraded at 12 year intervals;
Not automatically declassified.

SECRET

In addition to security requirements which apply to this document and must be met, it may be further distributed by the holder *only* with specific prior approval of the Director, Long Range Acoustic Propagation Project (ONR Code 102-OS).

SECURITY

This document contains information affecting the national defense of the United States within the meaning of the Espionage Laws, Title 18, U.S.C., Sections 793 and 794. The transmission or revelation of its contents in any manner to an unauthorized person is prohibited by law.

SECRET

MC Report 003
Volume 1
Copy No. [redacted] of 125 Copies

LONG RANGE ACOUSTIC PROPAGATION PROJECT

THE PARKA I EXPERIMENT

PACIFIC ACOUSTIC RESEARCH KANEOHE-ALASKA

NOVEMBER 1969

THIS DOCUMENT CONTAINS
DEFENSE OF THE UNITED
ESPIONAGE LAWS,
ITS TRANSMISSION
REVELATION TO AN UNAUTHORIZED

OCEAN SCIENCE PROGRAM
MAURY CENTER FOR OCEAN SCIENCE
Department of the Navy
Washington, D.C.

DDC CONTROL
NO. 93975

SECRET

CONTENTS

Acknowledgments iii
Foreword iv
Summary v

The PARKA I Experiment
Introduction 1
Objective 1
Experiment Plan 2
Organization and Personnel 3
Experimental Procedures 5
Field Operations 6

Calculations of Propagation Loss
Introduction 10
Propagation Loss Model 12
Construction of the Sound Velocity Profiles 13
The Sound Velocity Structure 14
The Oceanic Environment 14
Oceanographic Results 15
The Sampling Program 19
Data Quality and Reliability 24
Oceanographic Results 24
Geophysical Results 24
Sound Velocity Along PARKA I Track 26
Calculated Propagation Loss 28

Acoustic Results
Introduction 34
Source Levels 34
The Drift of FLIP 38
Propagation Loss Results 38
Discussion of Propagation Loss Results 54
Effects of Hydrophone Depth and Location 54
Effect of Source Depth 60
Comparison of Phase 1 and Phase 2 Results 62
Effects of Frequency 62
SUS Charge Studies 65
Comparison of Projector and Charge Results 66
Ambient Noise 66

Measured and Computed Propagation Loss
Introduction 74
Average Loss 74
Convergence Zones 75
Discussion 75
Summary and Conclusions 76

ACKNOWLEDGMENTS

On behalf of Navy Managers responsible for the PARKA I experiment, the contributions of senior officers of the Navy, members of the scientific community who participated in PARKA I, and seafaring men, both naval and civilian, who contributed in various ways to the experiment are gratefully acknowledged.

Vice Admiral C. B. Martell, USN (Ret.); Vice Admiral T. Caldwell, USN; Vice Admiral H. G. Bowen, USN; and other senior officers supported and encouraged the planning and execution of the whole PARKA series.

Dr. R. H. Nichols, Bell Telephone Laboratories, served as Chief Scientist, and in that role was responsible for the scientific planning and execution of PARKA I. Mr. R. W. Hasse, Navy Underwater Sound Laboratory, was the Deputy Chief Scientist. Mr. G. H. Fisher, Hudson Laboratories, served as Project Coordinator, and was assisted by Mr. K. W. Lackie in the coordination of oceanographic operations. Captain R. H. Smith, USN, and Lieutenant E. E. Flesher, USN, ASWFORPAC, directed naval aspects of the operations. Broad scientific planning was accomplished by a group including Dr. F. N. Spiess, Marine Physical Laboratory; Mr. W. Annis, Office of Naval Research; Mr. J. I. Ewing, Lamont-Doherty Geological Observatory; Dr. G. P. Woollard, Hawaii Institute of Geophysics; Dr. E. E. Hays, Woods Hole Oceanographic Institution; Mr. W. B. Randlett, Naval Oceanographic Office; Dr. J. C. Munson, Naval Research Laboratory; Captain Paul Wolff, Fleet Numerical Weather Central; and Mr. E. L. Smith, Navy Undersea Research and Development Center.

The Commanding Officer, Fleet Weather Central, Pearl Harbor, and his staff provided data handling facilities which acted as the necessary link between the data-gathering ships at sea and the data-processing facilities at FNWC. Commander, Fleet Air Wing Two and his staff and aircraft crews provided a most important series of quick looks at the ocean structure during the experiment, and are continuing to fly similar flights to obtain seasonal data. The Commanding Officers, Masters, and crews of the ships, and the commands responsible for platforms and shore stations participated, in most instances, continuously during the two-month period of the experiment; their attention to detail and ability to adapt to changing requirements provided the continuity and responsiveness necessary to meet the scientific objectives of the experiment.

Valuable administrative assistance in logistics, materiel procurement and schedule coordination was provided by Lieutenant Commander J. J. Holt, USN, and Mr. A. E. Molloy of the Office of Naval Research.

Obviously, many other individuals and organizations have contributed to the planning and execution of the experiment. Although it is not practical to list them all here, their contributions are most gratefully acknowledged.

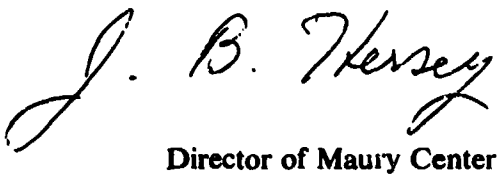

Director of Maury Center

FOREWORD

This Report, like the PARKA I Experiment itself, was achieved by the cooperative efforts of many individuals from the organizations which participated. It is bound in two volumes. Volume I presents a description of the experiment, the results of the oceanographic and acoustic measurements, the predicted (computed) transmission loss characteristics based on a particular mathematical model, and a comparison of calculated and measured results. This volume was produced by interweaving and editing the writing of a number of authors, in particular, R. W. Hasse, W. B. Randlett, K. W. Lackie, Capt. P. M. Wolff, and the undersigned.

Volume II comprises a set of Appendices which generally are directed toward presenting information about the operations conducted and the results obtained by a number of the individual organizations. In many cases they amplify and extend in greater detail the material in Volume I. The authors of each Appendix in Volume II are identified by a by-line.

Acknowledgment is also due the several hundred individuals who contributed directly or indirectly to the Report through their participation in a multitude of ways in the PARKA I Experiment.

R. H. Nichols

R. H. NICHOLS
Chief Scientist, PARKA

SUMMARY

(C) The PARKA I Experiment was designed for the purpose of providing simultaneous, detailed acoustic and oceanographic data for testing acoustic propagation models to ranges out to 2000 miles, and specifically, to test the interim model for predicting long range sound propagation which has been programmed for the CDC 6500 computer at Fleet Numerical Weather Central (FNWC), Monterey, California. It was a cooperative venture of 16 laboratories and other organizations, involving a total of eight ships, several aircraft, and two large oceanographic buoys, FLIP and the Monster Buoy from the Scripps Institution of Oceanography. The experiment comprised a series of intensive, simultaneous acoustic and oceanographic measurements along a north-south track from Oahu, Hawaii, to Alaska. Hydrophones suspended at depths of 300, 2500 and 10,800 ft from FLIP at a point 350 miles north of Kaneohe (Oahu) were the principal receivers. Looking north, the oceanographic properties were such that acoustic transmission was not bottom limited, and a rising sound channel improved the coupling to shallow sources at long ranges. Looking south from FLIP, transmission was severely bottom limited. Secondary receivers were the MILS hydrophones on the bottom at a depth of 2070 ft on the slope off Kaneohe. Sound sources were explosive shots detonated at 60 and 500 feet, 1/3-mile apart along the track and, in a separate exercise, a continuous tone projector (178 Hz) towed at 500 feet over the entire 2000 mile track. The data were all reduced at sea and the final results have been available for various uses since the end of PARKA I in late September 1968.

Model Validation

(C) At ranges from about 600 n.m. to the end of the track at 1700 n.m. the agreement between average loss computed on the basis of simultaneous environmental measurements and average measured loss at 100 Hz is generally good, within 0 to 3 dB with occasional divergences of perhaps 4 to 5 dB.

(C) At ranges less than 600 n.m. (where convergence zones are strong), the agreement between computed and measured averages is not as good. This could be due to use of too high a bottom loss in the model, or to lack of accounting in the model for leakage. Some of the deviations in averages might also be due to FLIP's drifting during the measurements.

(C) At 200 and 400 Hz there is a consistent pattern of computed average losses increasing with range over measured average losses, to maximum differences of 8 dB and 18 dB, respectively, at 1200 n.m. There is evidence that this is due to use of too high a value for attenuation per mile.

(C) Measured and computed convergence zones spacings agree within 1 or 2 percent.

(C) Computed losses at convergence zone peaks are 0 to 10 dB less than measured losses at 100 Hz and 0 to 5 dB at the higher frequencies. These discrepancies might be corrected by making the limiting values of one of the terms in the ray tracing program ("L", p. 13) dependent on frequency.

(C) Computed losses for the regions between convergence zones are greater than measured losses by as much as 18 dB at 100 Hz to 55 dB at 400 Hz. The losses at these ranges are strongly dependent on bottom reflection loss and to some extent on leakage. The table of reflection losses used in the model is based on published data; additional measured values from this and other experiments should serve to improve prediction capability. Some provision may need to be made in the model to account for leakage paths.

Acoustic Features Relevant to System Design

(C) In addition to the general validation of the model, a number of important features were found in the sound propagation characteristics at 100 Hz along this track:

(C) 1. For the 60 ft source, reception was best at the 10,800 ft FLIP hydrophone.

(C) 2. For the 500 ft source, reception was more range dependent: Reception at the 10,800 ft hydrophone was equal to or better than at the 2500 ft hydrophone out to about 500 nm and poorer at the longer ranges.

(C) 3. Reception from the 60 ft source at the 2500 ft hydrophone was 5 to 12 dB poorer than from the 500 ft source. At the 10,800 ft hydrophone also, reception from the 500 ft source was poorer, by 0 to 10 dB.

(C) 4. For very long ranges, reception at the Kaneohe hydrophone at 2070 ft was about equal to that at the 2500 ft FLIP unit, because of good source coupling to the rising sound channel in northern waters.

(C) 5. For sources in the portion of the track between Kaneohe and FLIP, reception at both locations was severely bottom limited, and very sensitive to hydrophone position and depth. (Plots showing these acoustic features may be found in the Acoustic Summary, Figs. 63-79, pp. 55 to 70.)

(S) The acoustic results demonstrate that, for a given combination of the environment and the surveillance needs, there is an optimal depth and position of receiver to minimize the propagation loss. This, in turn, points up the desirability of structures for mounting surveillance system arrays which will allow complete freedom of choice of position, depth and orientation in the ocean.

Oceanographic Program

(U) The program of oceanographic measurements provided data in support of updating the FNWC propagation loss calculations. As was intended, the density and scope of the oceanographic data proved to be far greater than current modelling procedure requires. The data can serve, therefore, along with the associated acoustical results, as a useful data bank for future extension and improvement of modelling. The ability to reduce and transmit such large quantities of data as fast as they were acquired was well demonstrated. FNWC's predictions of sound velocity values agreed well with those measured. In turn, the measurements with different systems aboard the different ships agreed well among themselves. The expendable bathythermographs, XBT's and AXBT's, proved to be very useful from the standpoint of speed and convenience. However, as is well known, they do have greater inaccuracies and greater failure rates than the STD and velocimeter systems.

(U) The sound velocity profile in the deep ocean, below 2500 m, was found to be very constant, both in time and in distance over the PARKA I track. The mixed surface layer was well defined and was between 30 and 50 m deep at both the northern and southern end regions of the track. In the center, it was thin and variable and did not exist at all in small local areas.

Data Tapes

(U) All of the acoustic and oceanographic data have been recorded on digital magnetic tapes, copies of which may be made available to qualified users upon approval of the Deputy Assistant Oceanographer for Ocean Science, Code 102-OS, Office of Naval Research.

Introduction

(S) The PARKA I Experiment is part of the Long Range Acoustic Propagation Project (LRAPP). This project is part of Advanced ASW Surveillance, budget category 6.3, Program Element 63701N, Project 2408, in RDT&E, Advanced Development. The Project Manager is J. B. Hersey, ONR, Deputy Assistant Oceanographer for Ocean Science.

(S) The objective of the LRAP Project is to conduct an advanced development program in long range acoustic propagation to support current ASW detection systems (such as SOSUS, JEZEBEL, DIFAR and moored sonobuoys) and the systems of the 1970's. Specifically, the major objectives of the program are to establish the technical feasibility and operational utility of:

a. An environmental/acoustic model, which can be used to reliably predict the performance of and assure the most advantageous location of both fixed and deployable sonar systems.
b. Appropriate facilities for the purpose of collection, storage, analysis and dissemination of acoustic and oceanographic data and predictions relating to the performance of fixed and deployable sonar systems.

(S) The end objectives are validated technological options for systems, techniques, survey procedures, and facilities to provide substantial improvements in determining the performance of long-range active and passive sonar systems.

The Objective of PARKA I

(C) When LRAPP was first established, no acoustic propagation model had been tested against propagation measurements to distances greater than about 300 miles. Furthermore, no propagation model was available to the Navy that had been validated thoroughly to any range. There were, however, several variants of both ray and normal mode theory models that might be able to do the job. Accordingly, a first responsibility of LRAPP was to establish an interim model for the prediction of propagation loss and initiate a measurements program of validation and improvement.

(C) The first model was based on ray theory; the total archival data bank on sound velocity in the ocean; ocean bathymetry from NAVOCEANO, ESSA, and other sources; bottom loss data from the Marine Geophysical Survey; and near-surface conditions based on the forecasting procedures of the FNWC at Monterey. FNWC completed a ray program to cover ranges to 125 nautical miles, and, through FIXWEX and various other measurement programs its validity was tested.

(S) The two to three thousand mile SOSUS detection ranges obtained over the past few years immediately demanded a suitable prediction model usable over the same distance. Simultaneous acoustic structure and propagation loss data were required over a comparable range and the range should include as diverse a set of environmental conditions as practical. For this purpose, a north-south line from Oahu to the Alaska Peninsula was chosen, and a detailed program of measurements called the PARKA Experiment was planned and performed during FY 1968 and 1969 under the direction of R. H. Nichols of Bell Telephone Laboratories as Chief Scientist and R. W. Hasse of Navy Underwater Sound Laboratory as Deputy Chief Scientist.

(S) PARKA is an acronym for *P*acific *A*coustics *R*esearch *K*aneohe *A*laska. In addition to the environmental considerations, this

area is known to be a holding area for Soviet submarines, and, hence, is of special interest for us to know well. The original PARKA Experiment has been completed, but, in the process, other experiments have been planned. Hence, this first one has become known as PARKA I.

(S) The primary objective of the PARKA I Experiment was to test and improve the acoustic prediction model for surveillance systems. PARKA I was devoted almost exclusively to this objective. Thus, the approach employed in the PARKA I Experiment was to compare measured propagation loss with propagation loss computed by means of the model based on two sets of data: first, *forecasts* of the sound velocity structure of the water and on bottom topography from previous surveys, and second, *measurements* of near-surface and deep-water structure, and bottom topography made during the acoustic tests. The acoustic measurements of propagation loss and the oceanographic measurements on which computed values of propagation loss were based were made simultaneously along the same path to maximize the interrelationship.

The PARKA I Experiment Plan

(C) The PARKA I experiment was designed to test the ability to predict propagation loss from oceanographic and environmental data by use of an acoustic ray theory model. The experiment consisted of two parallel parts: one, a set of simultaneous acoustical and oceanographic measurements at sea, and the other, a set of calculations ashore based on the model. At sea, the experiment comprised the collection of extensive oceanographic data along a specific track across the ocean and the concurrent measurement of acoustic propagation loss along the identical track. Ashore, propagation loss along the track was computed from the environmental data inputs, and its accuracy evaluated by comparing it directly with the real measured acoustic propagation loss. Figure 1 indicates schematically the nature of the experiment.

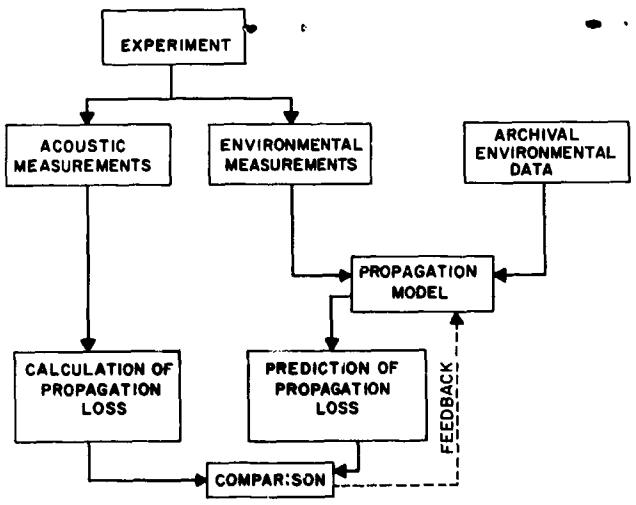

Fig. 1 — Diagram of experiment (U)

(C) It was desired that the track should not only provide conditions of specific interest to present and future systems, but also provide a wide variety of environmental conditions so as to make the test of the model a severe one. One matter of particular interest is the propagation over long ranges (i.e., 2000 n.m.) from high northern latitudes to semi-tropical waters. This path is characterized by a deepening sound channel axis in going from north to south. Another matter of particular interest is the effect produced by propagation through oceanic fronts or water-mass boundary regions with high temperature and/or salinity gradients. Such regions in themselves place stress on the modeling techniques. It was decided to

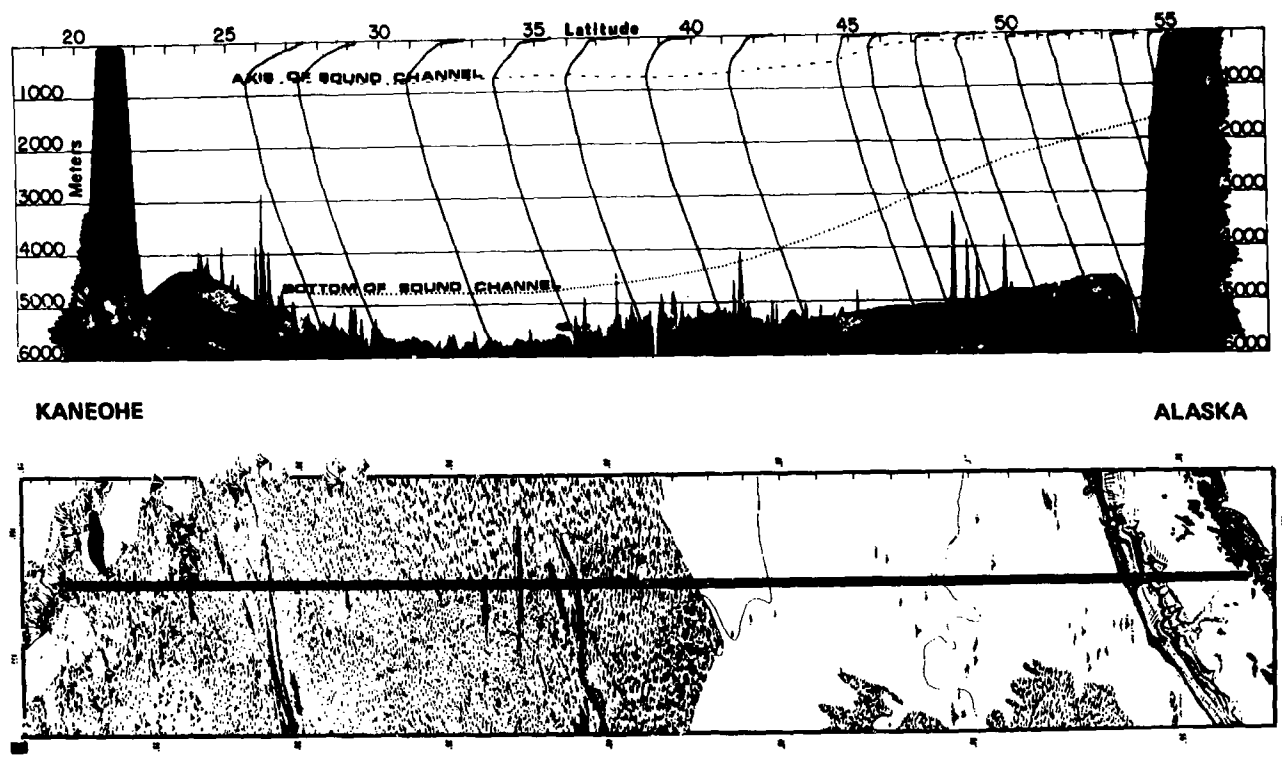

Fig. 2 – PARKA track and its acoustic environment (U)

provide additional stress as well as greater generality by choosing a track and receiver site for the experimental acoustic measurements which would permit study of both bottom-limited and non-bottom-limited types of propagation.

(U) These environmental features are all to be found along the PARKA I track; they are described in broad outline in Section IV on the calculation of propagation loss, and in detail in the Appendices of Volume II.

(U) By suspending receivers at 27°30′N on this track, which is at a point about 330 n.m. north of Kaneohe (Fig. 2), it is possible to have bottom-limited propagation conditions looking south from the receivers, and non-bottom-limited conditions looking north from the receivers.

Organization and Personnel

(U) The PARKA I experiment was planned and carried out by the cooperative efforts of personnel from sixteen civilian and military laboratories and agencies. Overall direction and coordination of the project were in the hands of:

Director: J. B. Hersey, Deputy Asst. Oceanographer for Ocean Science

Chief Scientist: R. H. Nichols, Bell Telephone Laboratories

Deputy Chief Scientist: R. W. Hasse, U.S. Navy Underwater Sound Lab.

Project Coordinator: G. H. Fisher, Hudson Laboratories.

The Principal Scientists in charge of the activities of individual organizations were:

Marine Physical Laboratory
F. N. Spiess
USN Underwater Sound Laboratory
R. L. Martin
W. R. Schumacher
Lamont-Doherty Geological Observatory
J. I. Ewing
Hawaii Institute of Geophysics
G. P. Woollard
R. C. Latham
Undersea Surveillance Oceanographic Center, Naval Oceanographic Office
W. B. Randlett
K. W. Lackie
Woods Hole Oceanographic Institution
E. E. Hays
T. L. Whalen
Scripps Institution of Oceanography
R. W. Schwartzlose
Navy Undersea Warfare Center (San Diego)
E. L. Smith
Naval Research Laboratory
J. C. Munson
H. L. Peterson
A. T. McClinton
Bell Telephone Laboratories
G. R. Fox
Fleet Numerical Weather Central
Capt. P. M. Wolff
Lt. N. L. Perkins
Fleet Weather Central (Pearl Harbor)
Capt. W. E. Hubert
Lt. Cdr. V. Buschmann
Anti-Submarine Warfare Forces, Pacific
Capt. R. H. Smith
Lt. E. E. Flesher

Lt. Flesher was Officer Conducting the Exercise (OCE) for the field operations.

(U) Senior Scientists on board ships and aircraft during the experimental operations were:

R/V TERITU
R. Budd
R/V MIKIMIKI (Phases I, II and III)
R. C. Latham
R/V MIKIMIKI (Phase III for NRL)
F. F. Horner
USS REXBURG and USS MARYSVILLE (Phase 0)
E. L. Smith
USS MARYSVILLE (Phases I and II)
T. L. Whalen
R/V CONRAD (Phases I, II and III)
J. I. Ewing
R/V CONRAD (Phase II, for NRL)
C. W. Searfoss
R/V FLIP
W. R. Whitney
USNS SANDS
R. L. Martin
M/V PACIFIC APOLLO
E. Squier
USS RADFORD
J. McElroy
ASWEPS Aircraft
C. F. Beckner

In addition to the Principal Scientists and Senior Scientists, others who made special contributions to the experiment were:

Hawaii Institute of Geophysics
N. J. Thompson
Pacific Missile Range, Kaneohe
L. R. Fairbanks
R. Lunderville
Naval Undersea Research and Development Center
K. W. Nelson

Bell Telephone Laboratories
Miss H. M. Walkinshaw
H. J. Young
Fleet Numerical Weather Central
LCDR G. M. Griswold
Fleet Numerical Weather Central
LCDR P. R. Tatro
Fleet Numerical Weather Central
LT T. J. McCloskey

Experimental Procedures

(C) The primary set of five receivers for PARKA I was suspended on a vertical cable from FLIP: one hydrophone at 300 feet depth, a group of three at about 2500 feet (with a spacing of 46 feet between the first two and 184 feet between the second and third), and a fifth unit at a depth of 10,800 feet. The individual hydrophone outputs were multiplexed up the cable to FLIP, and were thence sent by radio telemetry to SANDS for on-line real-time processing, analysis, and print-out of propagation loss vs. range plots. FLIP was tethered to SANDS by a one-mile nylon cable, and SANDS was moored to keep FLIP from drifting unduly.

(C) Secondary acoustic receivers were the two Pacific Missile Range (PMR) Kaneohe Hydrophones located on the bottom at 21°47′N, 157°50′W at a depth of 2070 feet. Their outputs came ashore directly by cable to the PMR Facility Kaneohe, which was Operation Control Center for the PARKA I experiment. The output signals were passed through suitable bandpass filters and recorded on both a graphic level recorder, for on-line visual monitoring, and on a magnetic tape recorder. The magnetic tape was processed post-exercise on the identical equipment used on SANDS for the on-line processing of FLIP hydrophone outputs during the experiment, to insure comparable results.

(C) The acoustic signals were generated by three types of underwater impulse sources fired at regular intervals, (a) the Lamont-Doherty Geological Observatory (LDGO) towed airgun, (b) 3-lb fused TNT charges, (c) MK 59 pressure detonated explosive charges, and by one type of high-power towed CW source at 178 Hz. CONRAD handled impulse sources only, starting at 22°N and proceeding to 55°N. After that run was completed RADFORD towed the CW source over the same path, also dropping charges at regular 10-mile intervals.

(C) In order to obtain concurrent measurements of sound velocity as a function of depth in the water through which the sound was being transmitted, oceanographic data designed to provide sound velocity profiles were taken along the track by three ships and an aircraft, in addition to data taken by the source ship and receiving ships. One oceanographic ship (PACIFIC APOLLO or MARYSVILLE) took deep oceanographic casts to the bottom twice a day, at positions about halfway between the source and the receiver (maintaining an average SOA about half that of the source ship). Another ship (MIKIMIKI) took stations about halfway between the source ship and the water mass boundary at 43°N *after* the source ship had passed the boundary on its way north. A third ship (TERITU) made measurements along the part of the track south of FLIP.

(C) This combination of ships insured that the conditions on each side of one of the principal water mass boundaries were under observation; meanwhile, a fourth ship, REXBURG, patrolled back and forth through the boundary region, from 41° to 45°N with a towed thermistor chain to maintain surveillance of the

velocity structure in that region (the sub-arctic front). In addition, comprehensive oceanographic data down to 500 m depth were reported every 6 hrs from the Scripps-Convair Monster Buoy, which was moored on the track at 43°N, near the center of the same water mass boundary region.

(U) Aircraft (from Fleet Air Wing Two) made AXBT drops at 25-mile spacing along the track on alternate days. This type of measurement yielded what was essentially a snapshot of the velocity structure at a given time down to a depth of 1000 feet over the entire acoustic propagation path. These data were digitized at Fleet Weather Central (FWC) at Pearl Harbor and transmitted by cable to FNWC at Monterey after each aircraft run. Two runs were also made over the track by a Naval Oceanographic Office airplane equipped with an airborne radiation thermometer (ART) to measure surface temperatures.

(U) Oceanographic data at regular six-hour intervals were sent by radio from the oceanographic ships at sea to FWC via a military channel or via the PARKA civilian channel as appropriate to the individual ship. At FWC the data were inspected, coded and transmitted by cable to FNWC. FNWC then used all the incoming data as appropriate to update their information for computing values of propagation loss vs. range, for comparison with the measured results from FLIP/SANDS immediately after the experiment.

(U) Detailed descriptions of the instrumentation and the signal processing, and analysis procedures will be found in the individual reports of the activities of participating organizations, which make up Volume II of this report.

Field Operations

(C) The PARKA I experiment comprised four phases, as follows:

PHASE O: 1 January to 15 August
Oceanographic measurements only, along the entire PARKA track

PHASE 1: 15 August to 24 August
Acoustic measurements with impulse source (air gun and/or charges) and concurrent oceanographic measurements from ships and aircraft.

PHASE 2: 27 August to 5 September
Acoustic measurements with CW source and concurrent oceanographic measurements from ships and aircraft.

PHASE 3: 5 September to 22 September
Acoustic measurements only: (a) Measurements of bottom reflectivity vs. angle vs. frequency at 3 characteristic areas along the PARKA track; (b) Long baseline coherence measurements at PMR hydrophones at Midway, Kaneohe, and Pt. Sur, using pseudo-random noise signals from the CW source at 5 points along the PARKA track.

The operations in each Phase were as follows:

Phase 0: 1 January to 15 August

(U) TERITU made three bathymetric profiles from 22°N to 30°N. Single vertical sound velocity profiles were measured at 20 n.m. intervals along the same tracks. CONRAD transitted the PARKA I track from 55°N to 22°N, taking STD readings from the surface to the bottom at 100 n.m. intervals and taking continuous seismic and bathymetric profiles. MARYSVILLE towed the 800-foot thermistor chain over the entire PARKA I track from north to south.

Phase 1: 15 August to 24 August

(C) CONRAD proceeded at 10 knots from 22°N to 55°N along the track. It had been planned to tow the air-gun all the way at 60 ft depths. However, the sound level was found to be insufficient in the frequency bands employed and so the run was made dropping 3-lb TNT charges once every two minutes, at 60 ft and 500 ft alternately, except for a 5-minute silent period once every hour to permit measurement of ambient noise. Signals received by FLIP were radio-telemetered to SANDS. Abroad SANDS, the impulse signals from each hydrophone were filtered into the following frequency bands:

Bandwidth	Center
1 octave	31 Hz
1/3 octave	100
	200
	400

The output of each hydrophone in each filter band was squared and integrated, and the resulting propagation loss values, (the "total energy" received, corrected by the calibration of the source at 1 yd) were plotted vs. range for each impulse.

(C) The output of the Kaneohe PMR hydrophone No. 14 was filtered in bands:

(a) 1 octave wide centered at 40 Hz
(b) 1/3 octave wide centered at 100 Hz
(c) 1/3 octave wide centered at 400 Hz
(d) Broad-band

(C) Hydrophone No. 16 was operated broad-band only. The outputs of both hydrophones were recorded on the graphic recorder and the magnetic tape recorder. On-line monitoring of propagation loss vs. range was done by means of peak received levels read from the graphic recorder charts. The broad-band tapes from Kaneohe were analyzed aboard SANDS during her homeward-bound journey. Methods and instrumentation were identical to those employed in the on-line analysis of the FLIP data.

(U) Oceanographic measurements were made concurrently during Phase 1 by PACIFIC APOLLO, REXBURG, MIKIMIKI, TERITU and by ASWFORPAC aircraft:

PACIFIC APOLLO: took deep sound velocimeter casts to the bottom twice a day at stations approximately halfway between the source ship CONRAD and the listening ships FLIP/SANDS, about every 60 miles.

REXBURG: towed the thermistor chain back and forth along the track between 41°N and 45°N to maintain running oceanographic surveillance of the thermal front region.

MIKIMIKI: took deep velocimeter casts to the bottom from south to north at stations along the track, departing a few days before the start of PHASE 1 so as to be overtaken by CONRAD at about 43°N. From there northward she took velocimeter stations twice a day at points about halfway between 43°N and CONRAD, at intervals of about 60 miles, until the end of Phase 1.

TERITU: made deep STD casts to the bottom along the track from 22°N to 30°N.

ALL SHIPS: made 2500-foot XBT drops every 6 hours.

ASWFORPAC AIRCRAFT: made AXBT drops along the track at 25 mile intervals on alternate days. The first two runs were from 22°N to 43°N. The remainder were over the whole track from 22°N to 55°N.

SCRIPPS-CONVAIR MONSTER BUOY: meteorological data and oceanographic data were reported every 6 hours by radio telemetry to SIO and thence by radio to FNWC. The sub-surface data included current, temperature, pressure and conductivities at points from the surface down to 500 m, but not all quantities at all depths.

Phase 2: 27 August to 5 September

(C) The pattern of operations in this phase was similar to that of PHASE 1, except for the acoustic signals used and the ships employed. RADFORD towed a 178 Hz CW sine-wave source at 10 knots at 500 feet depth from 22°N to 55°N along the track. The source had a capability of radiating 1000 watts of acoustic power in the water (102 dbμb at 1 yd). The level was held constant at that value throughout the run. Fused TNT charges of 3 lbs were also dropped at 60′ and 500′ depths at regular 10-mile intervals to provide acoustic path structure information. In addition, MK 59 SUS charges were detonated at the sound-channel-axis at 10-mile intervals for purposes of acoustic attenuation measurements. The acoustic schedule for PHASE 2 was based on a repeated hourly cycle, as follows:

45 minutes CW projector on
5 minutes CW projector off, to allow ambient noise measurement
5 minutes – one 60′ and one 500′ charge
5 minutes – two MK 59 SUS charges

The cycle was repeated continuously along the track except for a 5-minute period at noon and at midnight each day during which pseudo-random noise signals were transmitted for preliminary long baseline correlation measurements. Some breaks occurred in the schedule, as indicated in the narrative log of the experiment (Appendix A). The acoustic receiving systems for the projector signals employed a bandpass filter 1 Hz wide at the signal frequency.

(U) During this phase, oceanographic measurements were made from MARYSVILLE, which took stations about halfway between RADFORD and FLIP and from MIKIMIKI, which took stations halfway between RADFORD and 43°N on the northern end of the track. ASWFORPAC aircraft flew the track on alternate days as in PHASE 1, from 22°N to 43°N the first two times, and then over the whole track for the rest of the runs. Data from the Scripps-Convair buoy were transmitted regularly as in PHASE 1.

(U) REXBURG continued her thermistor-chain patrol of the 41°-45°N segment of the track as long as fuel permitted, and then returned to Pearl Harbor, towing the chain from 32°N to 26°20′N on the way.

Phase 3: 2 September to 22 September

(C) Upon completion of PHASE 2, RADFORD, CONRAD, and MIKIMIKI proceeded to Kodiak to rendezvous in preparation for the two parts of PHASE 3, (a) bottom reflectivity measurements, and (b) long baseline coherence measurements.

a. Bottom reflectivity measurements

(C) MIKIMIKI acted as the source ship, and CONRAD as the receiving ship. CONRAD took stations successively at three locations along the track:

52°30′N	157°50′W
45°45′N	157°50′W
24°30′N	157°50′W

At each station she suspended two hydrophones, one at a depth of 500 ft and the other at 1000 ft. MIKIMIKI dropped explosive charges at a depth of 1000 ft, starting at a point 1000 yards or less from CONRAD and proceeding away along the track to a range of 30 n.m. The charges were spaced to give increments in grazing angle of approximately 2°. The bottom-reflected explosive signals were recorded aboard CONRAD for later analysis. These will be analyzed to determine reflectivity in 1/3 octave frequency bands from 50 Hz to 5 kHz for grazing angles at the bottom ranging from nearly 90° to about 0.5°. These will be reported at a later date.

b. Long baseline correlation measurements

(C) For the long baseline correlation measurements, the 178 Hz sound source was operated at a depth of 500 ft from RADFORD. It was energized with a pseudo-random noise signal (PRN) of about 15 Hz bandwidth, centered at 178 Hz. The cycle interval of the PRN was such that the line components within the band were about 0.83 Hz apart. RADFORD operated at each of four stations:

45°30'N	157°50'W	(12 September)
35°00'N	157°50'W	(13 September)
27°00'N	157°50'W	(15 September)
24°00'N	157°50'W	(15 September)

At each station the source was operated 2 hours with the ship held stationary, and 7. hours under tow at 10 knots on ten different headings to introduce Doppler shifts. The acoustic signals were received and recorded on magnetic tape at three locations: Pacific Missile Range (PMR) Kaneohe, PMR Midway, and the U.S. Naval Facility at Pt. Sur, California, for post-exercise analysis. The results from these experiments will be reported at a later date.

Introduction

(U) Estimates of propagation loss in underwater acoustics have generally been made by assuming that propagation could be described in a vertical plane and by assuming the ocean to be a layered space in which the sound velocity gradient and density are imagined to be constant everywhere on any given line normal to that plane. Both vertical and horizontal changes in velocity and density are then described in the required detail. Since 1945, the favorite propagation models of a host of investigators have been based on elaborations and extensions of ray theory or normal mode theory. Up to the present, ray theory has been more readily applicable to problems in which arbitrary spatial variations in sound velocity or density structure of the medium must be taken into account. Low frequency sound propagation over hundreds of miles of deep ocean fits into this category, and ray theory has been used almost exclusively thus far in developing the long range propagation model. The exceptions are propagation in the surface mixed layer, or in shallow water, where normal mode theory has been widely employed.

(U) In the present report, the calculations of propagation loss are based on the particular combined ray and normal mode digital-computer program developed at FNWC during the past three years. It should be remembered, however, that this program is based on research and development activity going back many years and, more immediately, on current R&D programs in both Navy and contract laboratories. Without this previous research, the development activities reported here would have been impossible.

(C) The FNWC model, described in broad outline below, is designed to employ a vertical profile of sound velocity in the water and a profile of the bottom, both in the vertical plane of propagation from source to receiver. No other use is made of density variations in the water, and, at the bottom, sound is assumed to reflect as though the bottom were an infinite plane inclined only in the plane of propagation at the local angle of slope. Reflection loss is treated empirically, the loss being dependent on the grazing angle and frequency in accordance with the graphs of Fig. 3, by interpolation. These are based on an analysis by FNWC of the Marine Geophysical Survey (MGS) data of the Naval Oceanographic Office. The selection of bottom class is based on estimates of bottom roughness from echo soundings. The method of estimating roughness has not been suitably quantified at this writing nor is the relationship understood. At present, the choice is based in part on trial and error. Initial estimates of roughness for the PARKA track are given in the section describing geological and geophysical results. Since this experiment is intended, in part, to provide data for extending the model, the structure of the sea floor has been measured by seismic reflection, and bottom samples and photographs have been taken. In the present calculations of propagation loss, however, only the profile provided by echo sounding has been used.

(U) The velocity profile or structure of the water along the PARKA track has been provided by an intensive measurements program whose complexity has already been indicated in the section on experimental procedures. The results of these measurements have been used to construct velocity profiles for calculating propagation loss during Phase 1 and Phase 2 as though the structure remained fixed during each phase, but was allowed to change between the two phases.

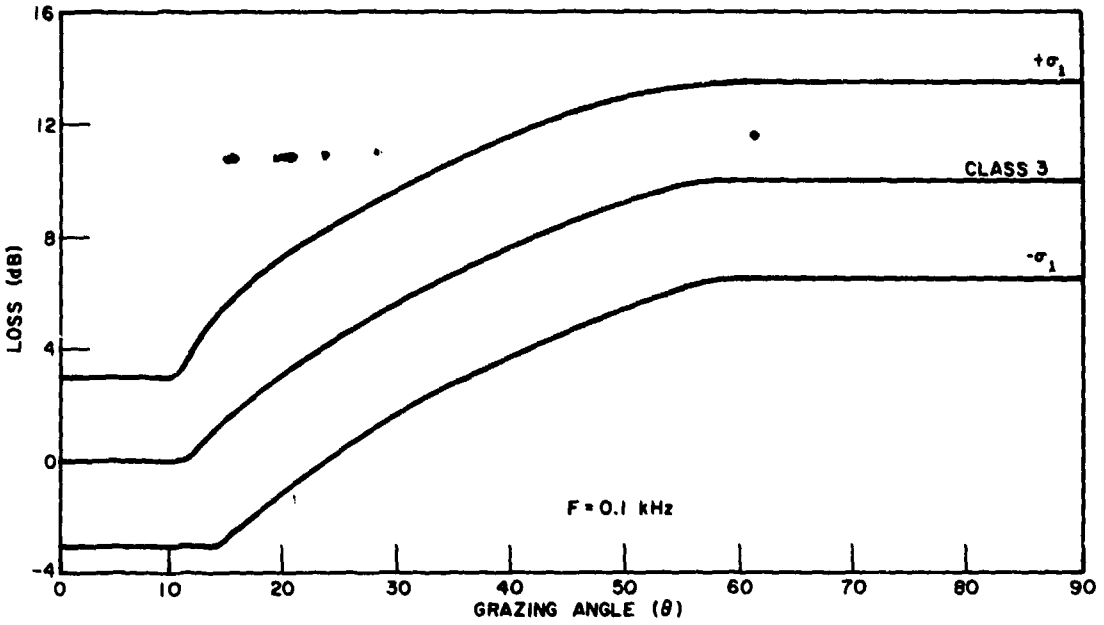

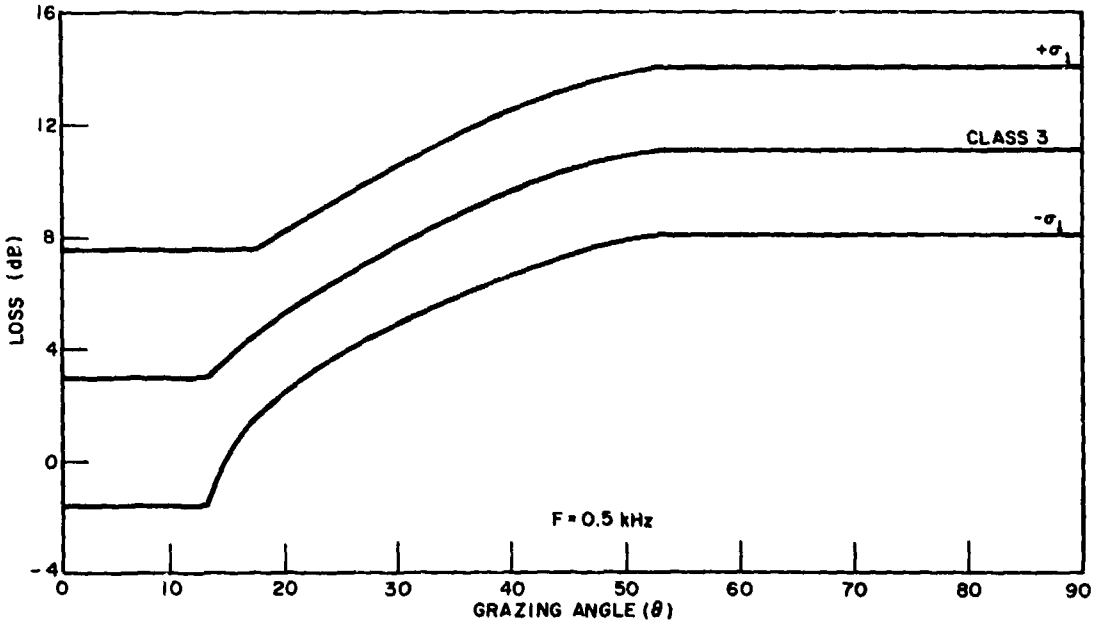

Fig. 3 – Bottom reflection loss vs grazing angle for a class 3 bottom (C)

Propagation Loss Model

(U) The FNWC long range model was used to calculate propagation loss for comparison with the PARKA I measured acoustic data. The ray theory portion of this model, for purposes of description, may be divided into two phases: (1) ray tracing, and (2) propagation loss.

Ray Tracing

(U) Input data consist of temperature and salinity profiles or sound velocity profiles, bottom profile, and bottom loss classes.

(U) Sound velocity is computed from temperature and salinity profiles using Wilson's equation or taken from direct velocimeter measurements. Profiles are described as accurately in the vertical and spaced as closely in the horizontal as the data justify. A third-order vertical and linear horizontal interpolation scheme is utilized to determine the velocity at points interior to the grid of data in the range-depth plane. The stability of the water column at each profile is checked for quality control of the input data.

(U) Bathymetric data are entered as closely-spaced as data permits. All PARKA calculations were based upon depth specifications at one mile intervals. Depths between specified points are calculated by linear interpolation. At each interaction of a ray with the bottom, the slope angle is sensed and the angle of reflection is modified accordingly. A bottom reflectivity class is specified which keys a table containing bottom loss per reflection as a function of frequency and angle of incidence.

(U) The ray trace program is a numerical integration of the Eikonal equation, incorporating an earth curvature correction, with a precision of 1 part in 10^6 in the horizontal and 1 part in 10^4 in the vertical at a range of 1000 miles. For PARKA, rays were computed from the receiver as though it were the source. This makes computation simpler, and the necessary assumption of reciprocity in the medium does not produce appreciable errors in estimated propagation loss.

(C) The initial ray bundle used for calculation was from +90° to −90° in quarter-degree increments. These initial calculations were used to identify critical areas; in these areas a ray spacing of 1/100 degree was utilized. Additional critical areas were defined, and successively more rays added, until a convergent solution was obtained: i.e., until additional rays produced no further changes in the magnitude or detail of the computed propagation loss.

(C) Surface reflections are assumed to be specular reflections from a horizontal, plane, perfectly-reflecting surface. Bottom reflections are assumed to be from a linearly-sloping plane surface. Rays reflecting backward are terminated; other reflecting rays are continued until their total accumulated loss exceeds 220 db or until they reach maximum range.

(C) Rays cycling in the surface duct are terminated after 200 n.m. of continuous travel in the layer because of the high duct leakage losses associated with the low frequencies of interest to PARKA (below 400 Hz).

(C) Output data include initial angle, range, depth, local angle, travel time, path length, geometric spreading in the range-depth plane, and accumulated bottom loss. Output data are recorded on magnetic tape for each of the following events:

(a) initial point
(b) each crossing of a depth of interest
(c) surface reflection

(d) bottom contact
(e) minimum depth turn
(f) maximum depth turn
(g) maximum range

Propagation Loss

(C) Propagation loss is calculated in the computer by summing the intensities over all existing paths to each range interval. Interpolation in range is made only between rays with the same history. Where a surface duct exists a normal mode solution is used in computing propagation loss for this mode of propagation. A ray trace approach was employed in determining propagation loss for the following paths:

(a) convergence zone paths, RSR and RRR
(b) bottom bounce paths
(c) paths with mixed histories

For all paths other than the surface duct, loss along each ray within a class is determined from the formula:

$$\text{Loss} = 10 \log R + 10 \log L + \alpha R + N \cdot \text{BOTLOS (db)}$$

where

$10 \log R$ = the cylindrical spreading loss assumed to occur in the horizontal plane

$10 \log L$ = the geometric spreading loss in the range-depth plane

αR = the attenuation loss which is due to the combined effects of scattering and absorption*

$N \cdot \text{BOTLOS}$ = the accumulated bottom loss as a function of roughness, frequency, and grazing angle.

(U) The attenuation coefficient, α, is calculated according to the semi-empirical expression reported by Thorp (1967).

(U) L is the ratio of the perpendicular distance between two adjacent rays with the same history at range R, determined from ray tracing, to the perpendicular distance between the same two rays at a range of one yard. As two RSR or RRR rays approach an intersection, L is allowed to decrease only to a value of R/100 but never less than 250. This lower bound was determined empirically from a study of the available literature on the intensity of convergence zones. For bottom bounce rays, L has a lower bound of R/10 or 250. This lower bound is rarely needed, since the L/R ratio for bottom bounce rays is seldom much less than one.

(U) Propagation loss within the surface duct is calculated from an empirical analytic expression whose results closely approximate a normal mode solution.

(U) The output of the model is propagation loss as a function of range in either digital or plotted format.

Construction of the Sound Velocity Profiles

(U) One of the objectives of the experiment was to forecast the velocity structure prior to the measurements and to use the FNWC model just described to predict the propagation loss based on the forecast. The forecast was made several weeks prior to Phase 1 and is discussed later in this section. It proved impractical during the experiment

*J. W. Horton, Fundamentals of Sonar, p. 75, United States Naval Institute, Annapolis, Maryland, 1957. (NAVSHIPS 92719)

to make full acoustical predictions because the model was by then only partially converted from a 125-n.m. program to one for 2000-n.m. The conversion was completed in October. It has been used without alteration since that time for the calculations of propagation loss discussed in this report.

The Sound Velocity Structure

General

(U) Until recently, sound velocity in the ocean has been determined indirectly through the measurement of salinity and temperature. Profiles along a ship's track in the ocean have been constructed by measuring a series of single vertical profiles along the track, usually separated by several miles to tens of miles. At present, continuous sampling in depth is possible by means of salinity-temperature-depth (STD) sensors or sound velocimeters. Bathythermographs have long provided continuous temperature-depth information from which velocity-depth information can be computed if the salinity-temperature correlation is accurately known. Their usefulness is well-established even though they cannot be relied upon for refined measurements either of temperature or sound velocity. All of these techniques have been employed in PARKA I as indicated under the sections on experimental procedures and operations.

(U) The principal features of the water masses that control sound velocity structure will be described in terms of temperature and salinity. This description will be followed by an abbreviated description of the environmental data taken during PARKA I and a discussion of the same features in acoustical terms of sound velocity, sound channels and their properties, and the general features of the effect of the sea floor. Volume 2 contains the detailed data on which the description of the sound velocity structure and the topography and reflectivity of the sea floor are based. The current FNWC propagation loss model uses these data.

(U) Volume 2 also contains a detailed discussion of observations of weather conditions, sea state, sea surface temperature and extensive geophysical examination of subseafloor properties made during PARKA I. These properties of the medium do affect sound propagation, and it is important to have observed and analyzed them so that their influence can be properly evaluated in future improvements to long range propagation models.

The Oceanic Environment

(U) The waters of the North Pacific between the Hawaiian Islands and Alaska below a depth of 2500 to 3000 meters vary little in temperature or salinity and are probably a region of slow currents, 0.3 knot or less. Compared with water at shallower depths, little is known of them except these characteristics. At the shallower depths there are three water masses: Subarctic Pacific, North Pacific Central, and North Pacific Equatorial. The Subarctic Pacific water mass lies generally north of 45°N latitude and is characterized by cold water having a salinity of 33 $^{o}/_{oo}$ or less at the surface increasing to about 34.65 $^{o}/_{oo}$ at the bottom (Sverdrup, et al., 1942). A region of transition exists between the southern boundary of the Subarctic Pacific and the northern boundary of the North Pacific Central water masses. A region of transition between water masses of unlike properties can be termed a front (Uda, 1943). The North Pacific Central water mass is warm and has a salinity of 35 $^{o}/_{oo}$

or more. The North Pacific Equatorial water is also warm but has a salinity of 34 $^{o}/_{oo}$ or less (Sekel, 1962). In the summer months, the northern boundary of Equatorial water occasionally nearly reaches the Hawaiian Islands. During these periods the ocean around the islands becomes a transition region.

(U) The temperature structure of these water masses was observed repeatedly during PARKA I. Figure 4 is an example of two different observational methods employed, the aircraft-dropped AXBT's (4A) and the thermistor chain towed by MARYSVILLE and REXBURG (4B). The subarctic water mass is evident north of 45°N. The North Pacific Central water extends from roughly 38°N southward to 28°N where pronounced temperature and salinity gradients exist which apparently mark the northern boundary of the transition to the Equatorial water mass.

(U) Sverdrup, et al. (1942) distinguished Eastern North Pacific Central water from Western North Pacific Central water. Winter data (November to February) show only a single high salinity cell across the northern portion of the Pacific and give no evidence of a separate Eastern cell (McGary, 1956). However, summer surface salinity data (April to August) show two high salinity cells in the northern portion of the area. This is explained as a separation of the single winter cell caused by the deflecting effect of the Hawaiian Island chain on a westward setting current (Seckel, 1962).

(U) In summary, proceeding from the Hawaiian Islands north to the Aleutian Islands during the summer months (June-August), the following water types and masses will be encountered in sequence:

1. Occasionally, transition water between North Pacific Equatorial and North Pacific Central Water masses.
2. North Pacific Central Water mass.
3. Transition water between North Pacific Central and Subarctic Pacific water masses.
4. Subarctic Pacific water mass.

(U) A bibliography of scientific discussion of this portion of the North Pacific Ocean is given at the end of this chapter.

Oceanographic Results

(U) As previously pointed out, oceanographic data were collected at regular intervals during each day of the experiment at several key locations: the acoustic source, the receiver, and at one to three points in between. Every ship in the experiment was engaged in the collection of environmental data, including the four primarily occupied with acoustical measurements. The other five ships devoted full time to the collection of oceanographic data. These data comprise measurements of sound velocity or of temperature and salinity as functions of depth to points well below the axis of the permanent sound channel and to the deep ocean bottom in many cases. All ships took expendable bathythermograph (XBT) readings of temperature vs. depth to 2500 ft every six hours. Deep data were taken by five of the ships at intervals ranging from six to twenty-four hours. Sampling at a higher rate to observe more rapid variations in the near-surface structure was accomplished by having aircraft drop aircraft expendable bathythermographs (AXBT's) at 25-mile spacings along the acoustic path on alternate days. Another aircraft made two continuous recordings of sea-surface temperatures along the whole PARKA track, one on 22-23 August and the other on 28-29 August. Thus, the most

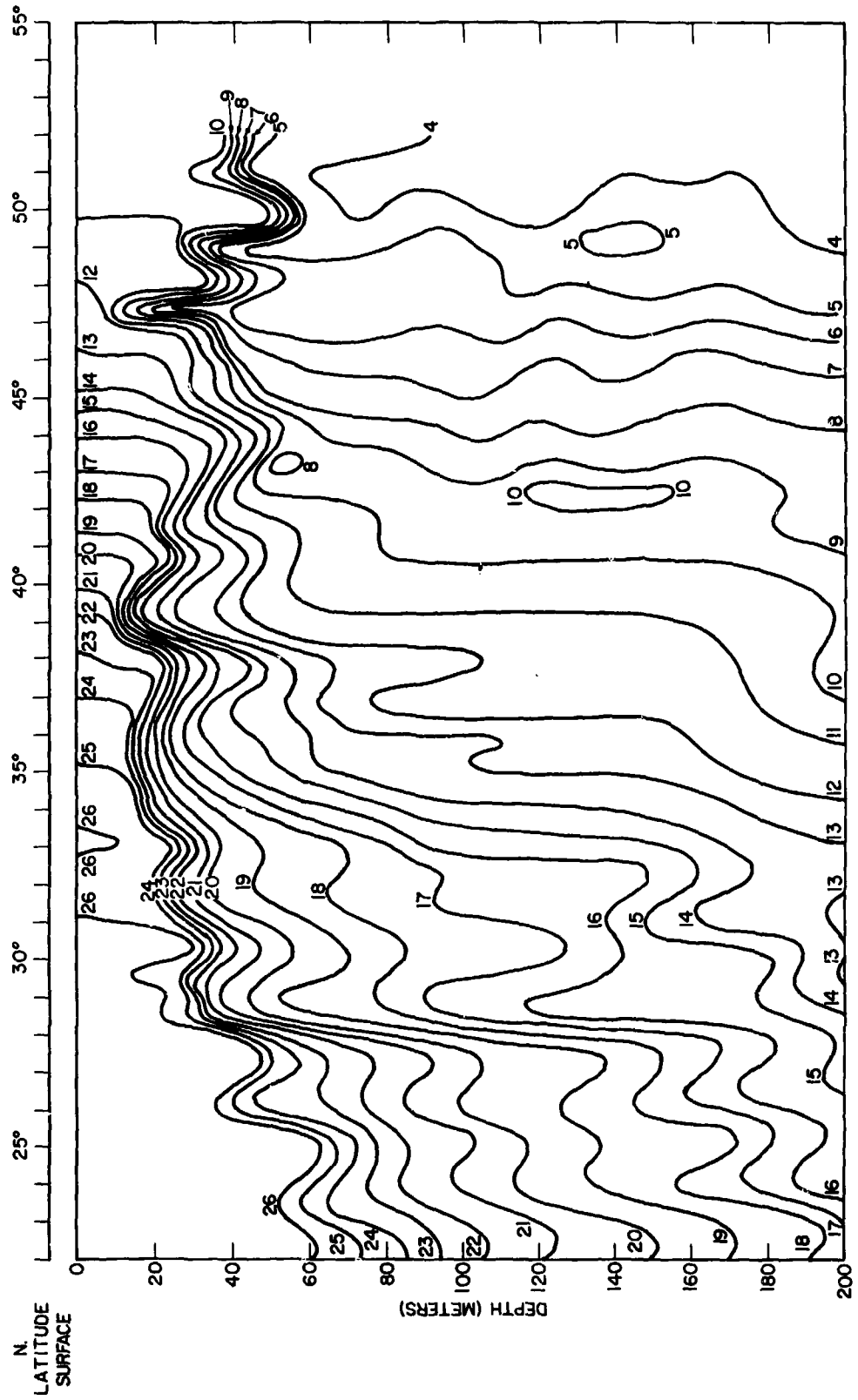

Fig. 4a – Isothermal contours in degrees Celcius along PARKA track (U)

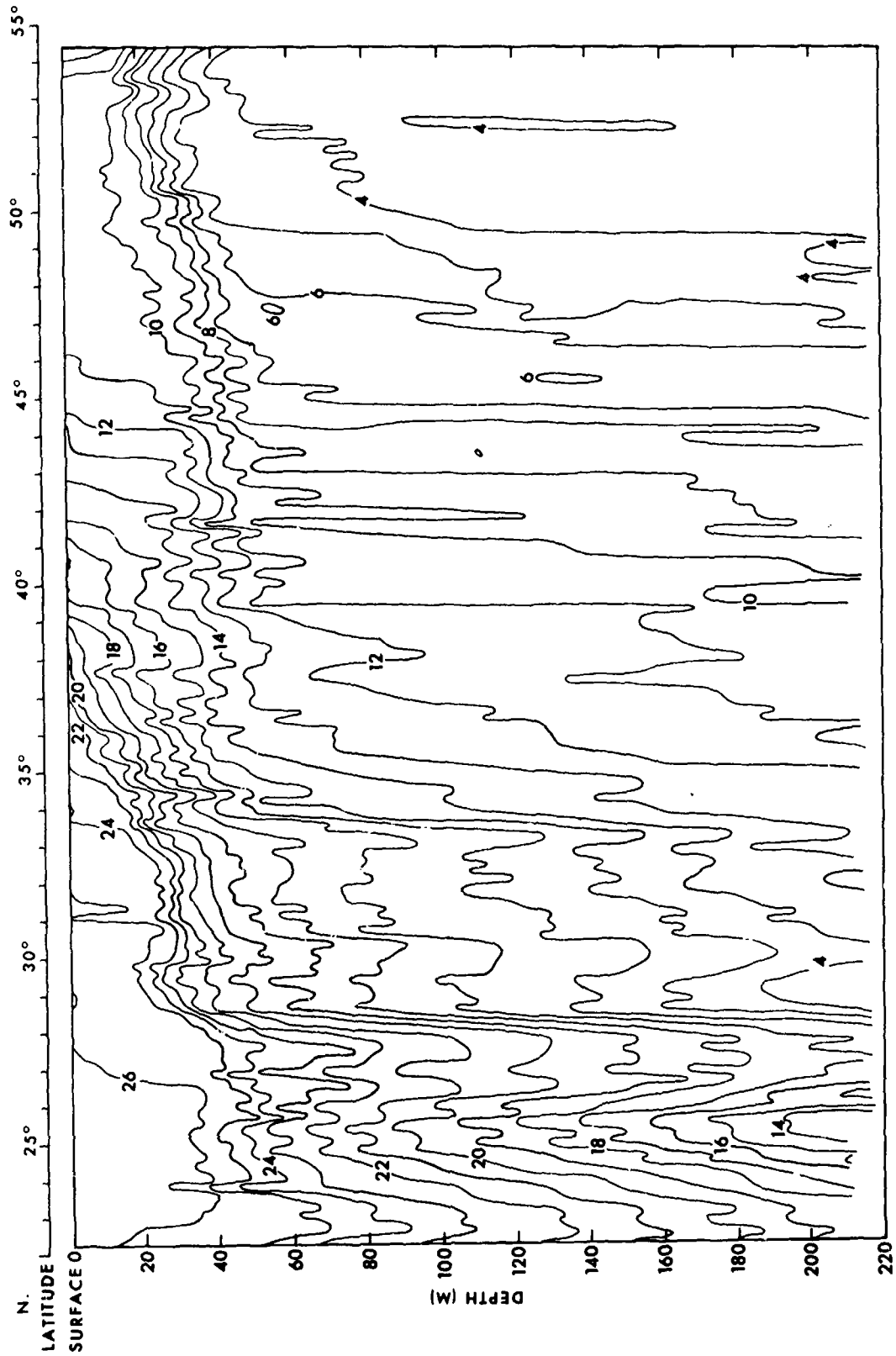

Fig. 4b — Temperature structure profile from hourly averages derived from continuous NUWC thermistor chain data along 157°50'W longitude during Phase Zero, 2000, 22 July to 2000, 5 August (increasing time north to south), temperatures in degrees Celcius (U)

complete picture possible of the oceanographic conditions existing in the area was sought, with the emphasis on describing this picture most thoroughly during the actual period when acoustic energy was being propagated along the PARKA I track.

(U) A total of about 500 AXBT's was dropped by aircraft in their nine runs along the track. All ships combined dropped a total of nearly 600 XBT's along various portions of the track. A thermistor chain tow produced a continuous temperature profile to 220 meters below the surface once along the entire track and several other times over selected portions of it. In addition there were 51 salinity-temperature-depth (STD) vertical profiles and 99 deep sound velocimeter vertical profiles taken during the PARKA I experiment. Continuous bathymetry and frequent weather and sea state observations were also collected by all ships equipped to do so.

(U) A Scripps-Convair Monster Buoy moored at 43°N on the track provided temperature data from the upper 500 m of water in the thermal boundary region, transmitting it to FNWC four times a day. Details of its instrumentation are given in Appendix F.

(U) In designing the oceanographic sampling program, the intent was to acquire much more information than was necessary for a test of the propagation loss model as programmed at present. This was accomplished. For example, Fig. 5 shows the sound velocity vs. depth profiles along the entire track that were collected during just one representative twenty-four hour period. An extensive bank of oceanographic data and associated acoustical data has thus been established, which can be used for further model development. Some representative samples of the environmental data are included in this report. The total data collection is stored on digital tape, as are all

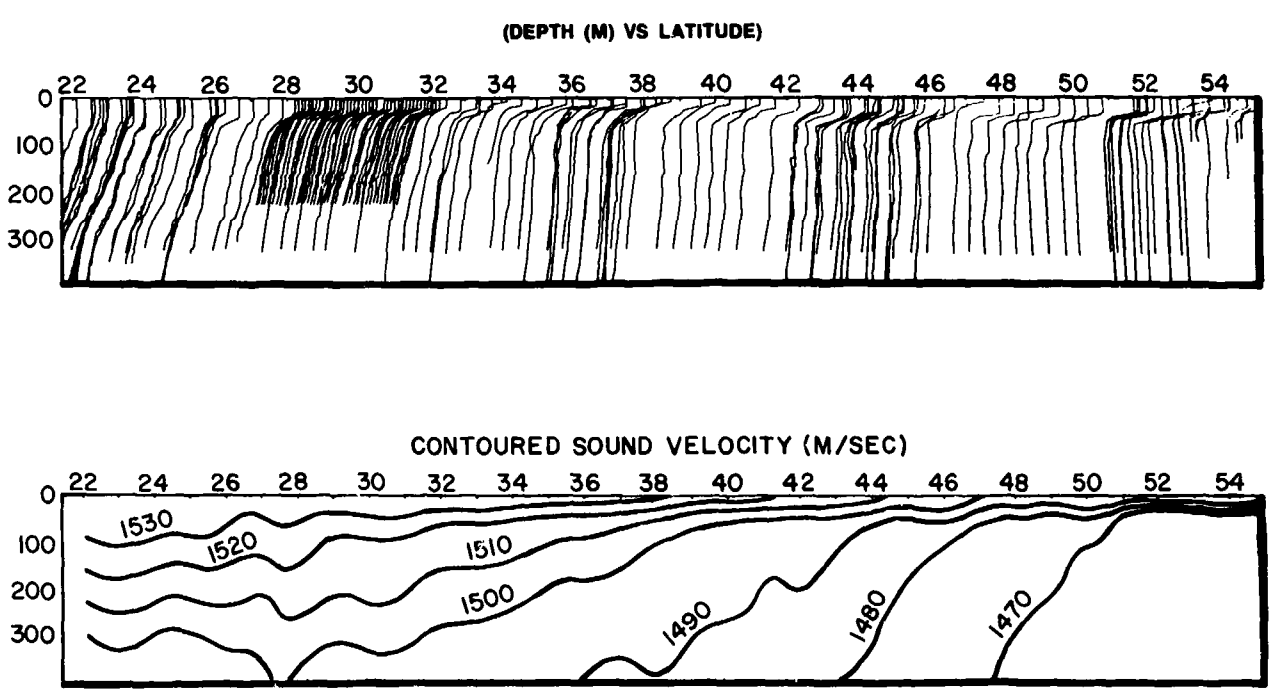

Fig. 5 — Sound velocity profiles — 2-3 September 1968 (U)

the acoustical measurements. Copies of these tapes are available to qualified agencies upon application to the Director, Maury Center, Code 102-OS, Office of Naval Research, Washington, D. C. 20360.

The Sampling Program

Phase 0

(U) Phase 0 consisted of all PARKA I observations carried out prior to the commencement of acoustic transmissions, and was completed by 5 August. R/V TERITU was the largest contributor to Phase 0, completing a series of STD stations to a depth of 1500 m between 22°N and 30°N once each month in May, June, and July. The July section is shown in Fig. 6 and illustrates the upper water column structure south of the front at 28°N. The entire Phase 0 program of R/V TERITU is discussed in Volume 2, Appendix B-10.

(U) In addition, during late July and early August, USS MARYSVILLE made a transit south along the entire PARKA track towing the Naval Undersea Warfare Research and Development Center (NURDC) thermistor chain, recording a continuous temperature profile to a depth of 220 m (Fig. 7). Also during this period, R/V CONRAD collected XBT and vertical STD profiles and a bathymetric and seismic reflection profile along the track while enroute to Hawaii from Alaska. The Phase 0 information was used to determine where to position the environmental data ships during the experiment itself. A plot of the time and location of each oceanographic data point in Phase 0 is shown in Fig. 8A.

Phase 1

(U) In order to obtain oceanographic information where it would be most useful, plans called for frequent 750-meter XBT drops from the source ship, particularly in areas where large changes of surface temperature were evident. Although it would have been useful to have data deeper than 750 meters available at the source location, stopping the source ship to collect it was not considered practicable. At the other end of the track, the FLIP/SANDS combination made several deep sound velocimeter measurements to the bottom, at their location in addition to numerous XBT drops.

(U) During most of Phase 1, M/V PACIFIC APOLLO collected deep velocimeter data and XBT's several times a day along the southern half of the track, maintaining an average speed of advance (SOA) of five knots. Since the source ship averaged about 10 knots, PACIFIC APOLLO remained approximately half way between the source and the receiver.

(U) R/V MIKIMIKI departed Honolulu several days before CONRAD, and collected one deep velocimeter station and several XBT's every day until she arrived at the water mass boundary at 43°N, where she was overtaken by CONRAD. MIKIMIKI's SOA was reduced to five knots, providing time for several deep stations a day in addition to XBT's. In this manner MIKIMIKI remained about midway between CONRAD and the water mass boundary.

(U) In addition, USS REXBURG towed the NURDC thermistor chain along the track from 37° to 45°N, then back to 41°N. This permitted a measurement of the position of the water mass boundary located in this region.

(U) Independent of other ship movements, TERITU collected STD data to 1500 m and XBT's between 22° and 30°N during part of Phase 1.

(U) Fig. 8B shows the time and location of each oceanographic data point in Phase 1.

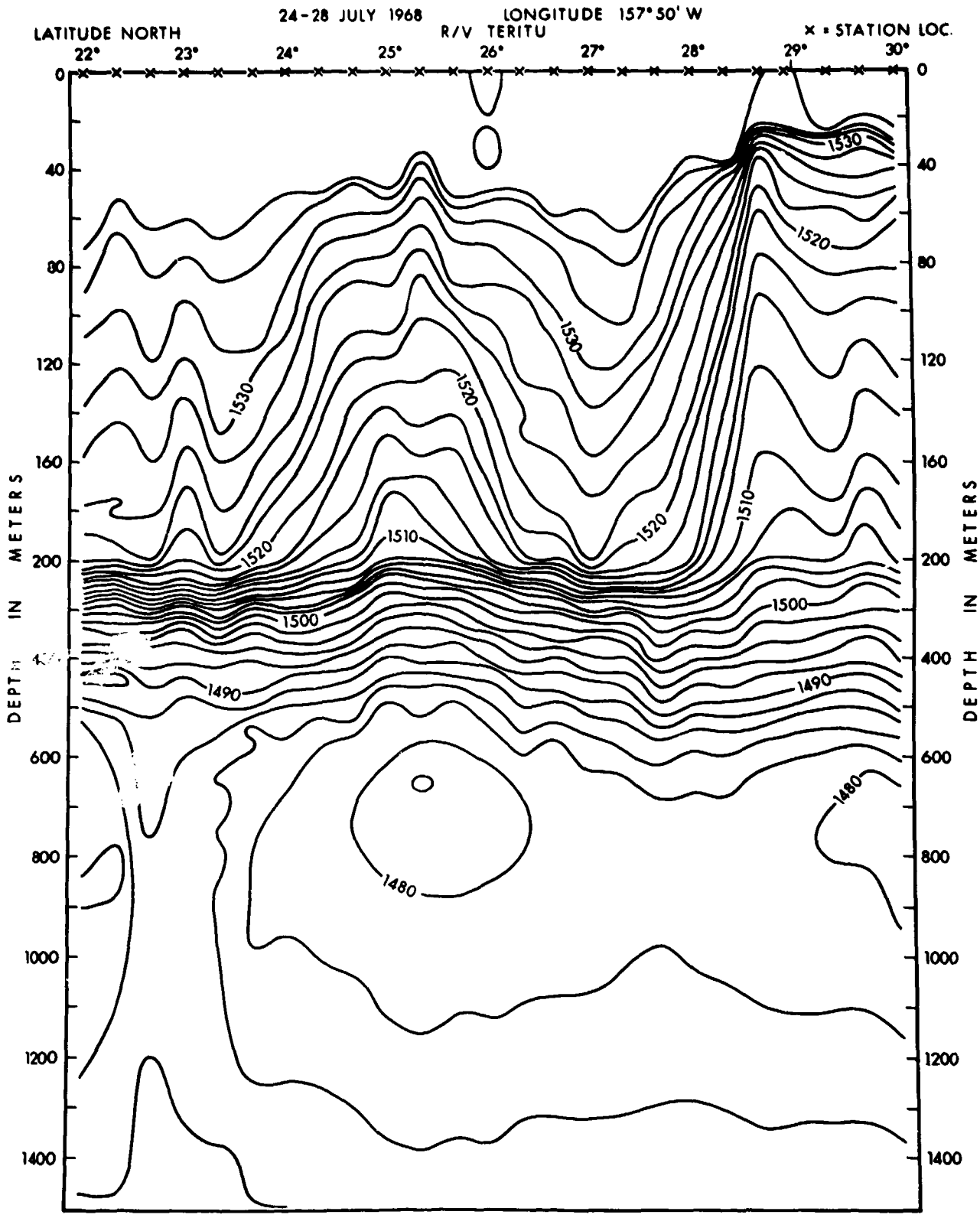

Fig. 6 – PARKA Phase 0, Run 3-R, sound speed – M/S (U)

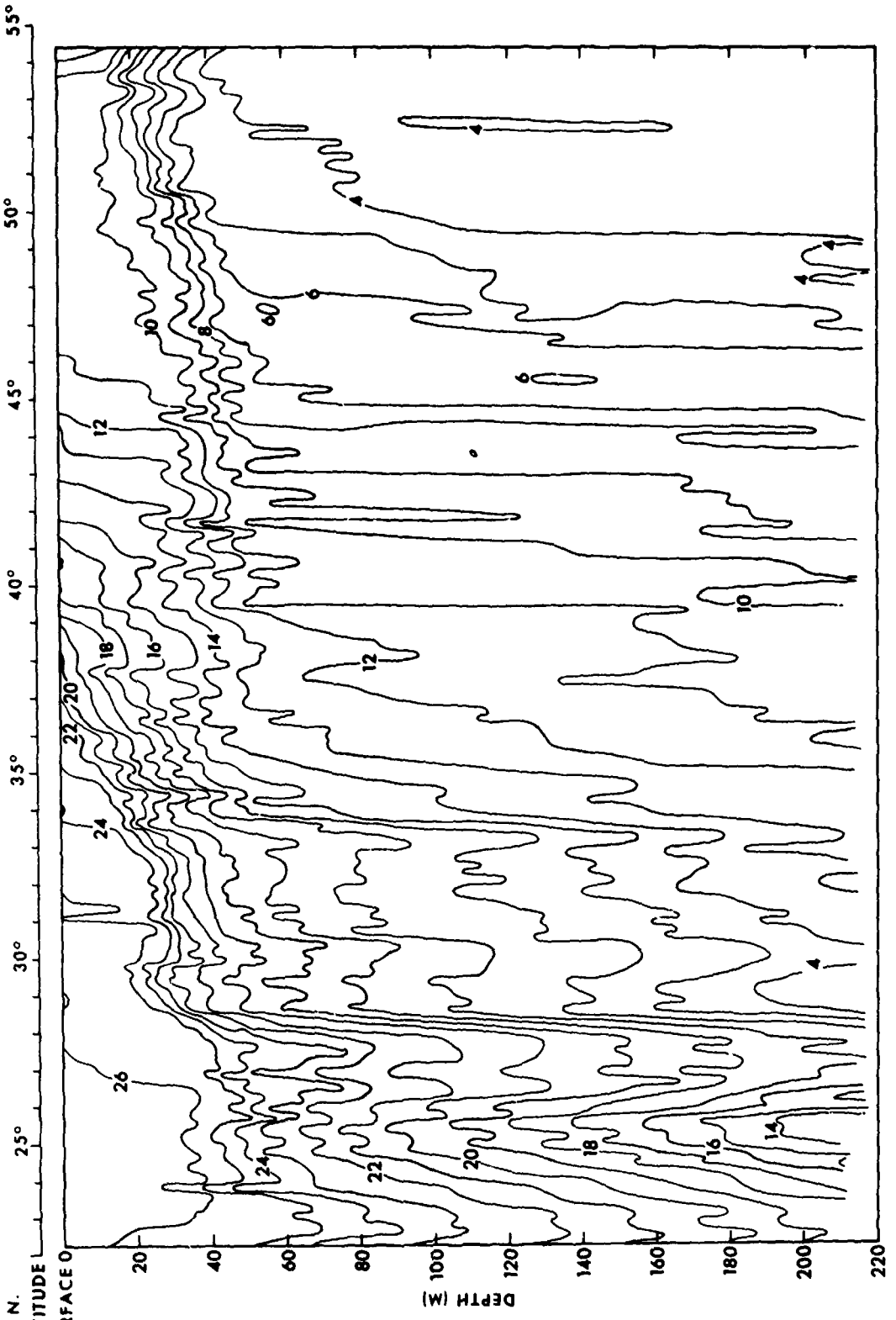

Fig. 7 – Temperature structure profile from hourly averages derived from continuous NUWC thermistor chain data along 157°50'W longitude during Phase Zero, 2000, 22 July to 2000, 5 August (increasing time north to south)

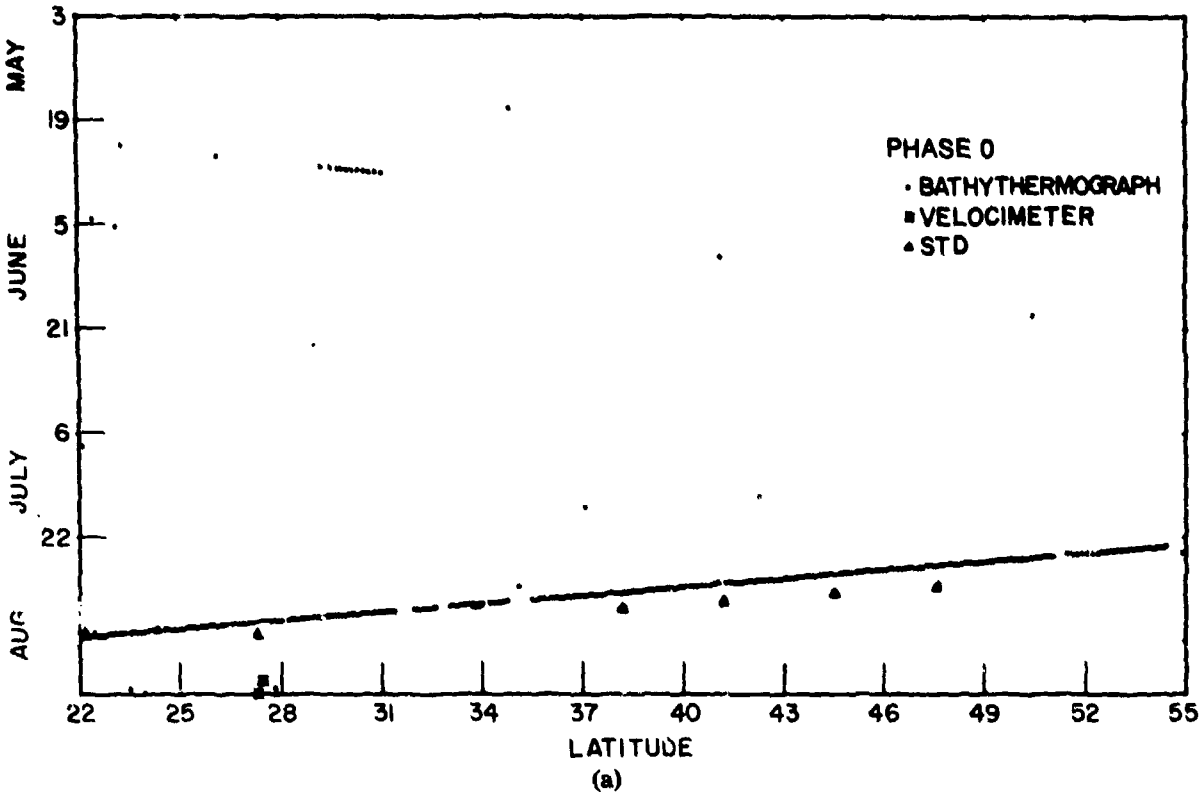

(a)

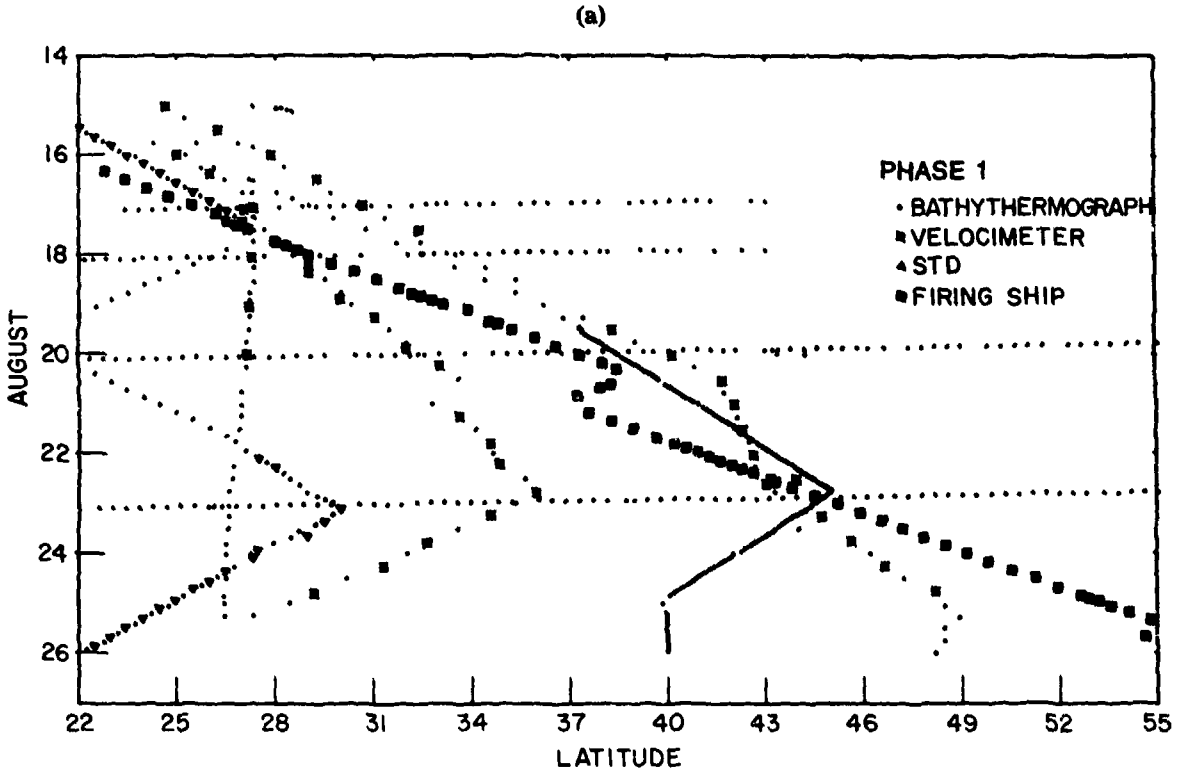

(b)

Fig. 8 — Time and location of oceanographic data points (U)

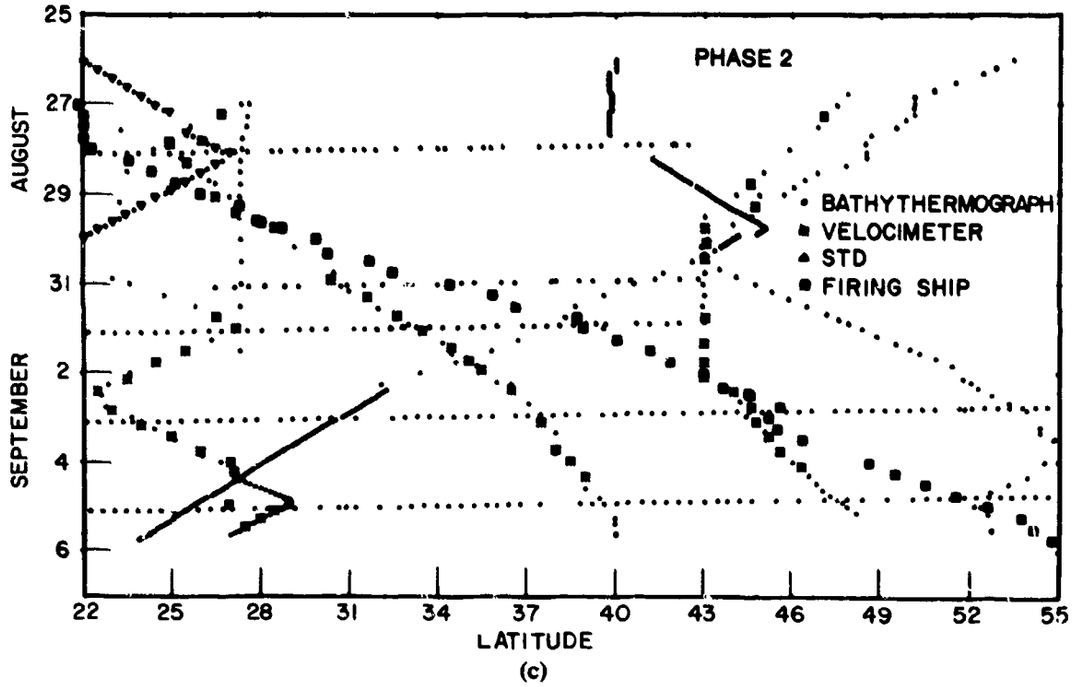

(c)

Fig. 8 (Continued) – Time and location of oceanographic data points (U)

Phase 2

(U) During Phase 2 USS RADFORD acted as source ship, and MARYSVILLE became the environmental data collector along the southern half of the track. MARYSVILLE's schedule was similar to that of PACIFIC APOLLO during Phase 1 – an average speed of five knots so that her position remained roughly halfway between RADFORD and the receiver. During the first half of Phase 2, MIKIMIKI steamed southward and met RADFORD at about 43°N, halfway through the Phase. During the second half of Phase 2, MIKIMIKI repeated her pattern of observations of Phase 1, taking stations at points halfway between the source ship and the watermass boundary at 43°N.

(U) CONRAD also collected local oceanographic data along the northern half of the track and TERITU continued observations between 22°N and 30°N. PACIFIC APOLLO had to return to Honolulu for minor repairs after repositioning FLIP prior to the commencement of Phase 2, but was able to collect several deep vertical sound velocity profiles between 22° and 30°N.

(U) During the first three days of Phase 2, REXBURG drifted to conserve fuel. Just before being reached by RADFORD, REXBURG resumed towing the thermistor chain through the water mass boundary from 41° to 44°30'N, then back south to 43°30'N. At this point, the thermistor chain was retrieved to allow REXBURG to proceed south at greater speed to investigate local conditions nearer to FLIP/SANDS. The thermistor chain tow was resumed from 32°N southward to 24°N giving a good temperature profile to a depth of 220 meters in the region of the large horizontal gradients previously found just north of FLIP/SANDS.

(U) All ships took XBT's every 6 hours. The times and locations of the oceanographic data points in Phase 2 are shown in Fig. 8C.

Phase 3

(U) Phase 3 comprises programs of bottom reflectivity and coherence measurements. They are to be reported separately.

Data Quality and Reliability

(U) Appendix B-3 contains a review of the steps taken to intercompare the quality of oceanographic measurements on the different ships. The aircraft-dropped AXBT results were not compared in detail with other results. They appear, however, to exhibit satisfying internal consistency both within individual profiles. Tests by FNWC prior to Phase 0 suggest an uncertainty of about 0.2°C in their temperature recordings. The results from PARKA I are consistent with this estimate. The XBT records, however, were more variable in quality, particularly at greater depths. This variability is discussed in Appendix B-3. The STD and sound velocimeter results have been intercompared with great care. A depth measurement problem was identified in two instances where pressure sensors were employed. One could be corrected but the other was variable in some unknown pattern and could not be corrected. Nevertheless, nearly all velocimeter data appear to have been accurate to within 0.2 meters/sec for a given arbitrary depth.

Oceanographic Results

(U) As mentioned earlier, the results are discussed in some detail in the Appendices, and they are available to qualified users in complete detail by application to Code 102-OS, Office of Naval Research. Nevertheless, the construction of a sound velocity profile along the PARKA I track was the primary objective of the oceanographic measurements program. By employing a combination of the results of Phase 0 with archival data, a predicted profile was constructed by FNWC for Phase 1. Also, based on an analysis of the data of Phases 1 and 2, profiles were produced to represent actual conditions during Phases 1 and 2. These three sound velocity structures are shown in Fig. 9. It was not considered necessary to construct more than one profile for each phase even though some change in the structure had taken place during each phase. These profiles as introduced into the computer at FNWC are to be regarded as the oceanographic results of PARKA for use in testing the propagation model. Columnar listings of the vertical profiles used to construct these contoured sections are given in Appendix B-11.

Geophysical Results

(U) The bathymetric profile along the PARKA I track used in the calculations of propagation loss in this report is based on a single echo-sounding profile made by CONRAD. Her position was carefully controlled by means of Transit satellite navigation. Digitized soundings (one sounding per mile) were prepared aboard CONRAD and furnished to FNWC immediately after Phase 0. Bathymetry for the short length of track from the end of the CONRAD profile to the Kaneohe MILS hydrophone was taken from the detailed site survey for that hydrophone. For detailed analysis of PARKA I results at short ranges, this profile is not adequate because of the lateral drifting of FLIP. A strip chart of topography of the sea floor (Appendix B-13) was prepared by combining all CONRAD PARKA I data, a set of profiles collected by ESSA between Hawaii and Alaska for Project SEAMAP, and a detailed survey of an area just north of Oahu completed by NAVOCEANO during the previous year from R/V HUNT and USNS SILAS

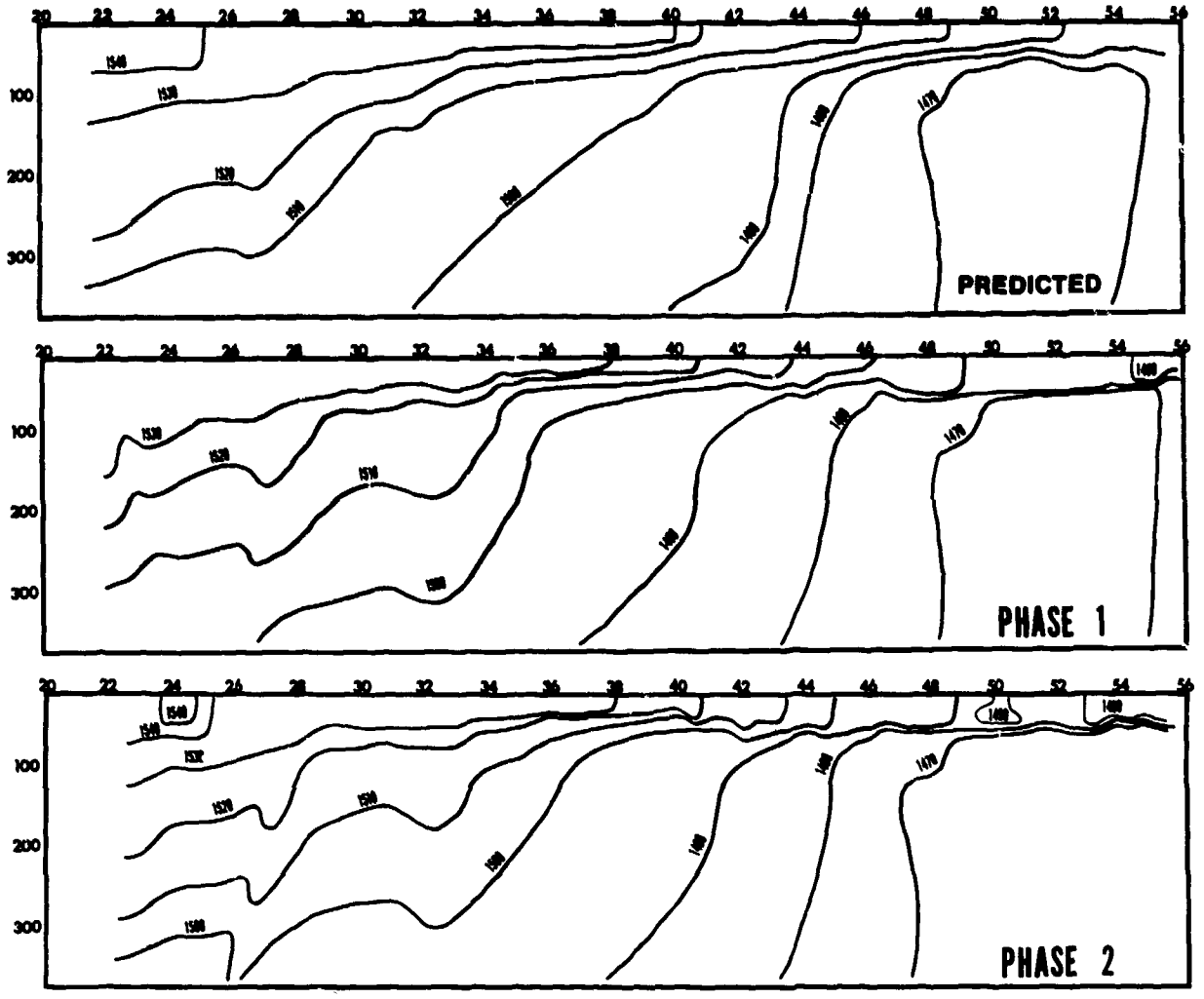

Fig. 9 – PARKA I isovelocity contours (M/S) (U)

BENT. Topography within 20 miles of FLIP, was provided by a detailed survey carried out by the Coast and Geodetic Survey and NAVOCEANO in support of preparations for the implantation of SEA SPIDER for PARKA II.

(U) The general geological description and analysis of bottom loss of the PARKA I track is given in Appendix B-14. The three regimes of bottom loss are postulated, but without clear identification of the areas as to MGS bottom loss classes. This failure is part of our present lack of quantification of the relationship between bottom loss and shape as provided by echo sounders. As a result, bottom loss classes 3 and 4 have been used in the long range calculations thus far. The results suggest that class 4 is too lossy. Continuing short range analysis suggests that either class 2 or class 3 is more appropriate within 125 miles of FLIP.

Sound Velocity Along the PARKA I Track

(U) The principal characteristics of the sound velocity structure of the water along the PARKA I track are described here beginning with the deepest water (where the structure is least variable) and proceeding to the surface. Figure 10 summarizes the entire acoustic structure and identifies the axis and the bottom of the sound channel as it was during August and September 1968.

(U) At depths greater than 2500 m sampled by the PARKA ships, the sound velocity was nearly constant both in time and geographic location at a given depth. The measurements of CONRAD (STD) and PACIFIC APOLLO (SV) from 25°N to 48°N show that the sound velocity profile at depths below 2500 m was independent of location to within 0.2 m/sec. The gradient is everywhere positive with sound velocity increasing slowly with depth from about 1497 m/sec at 2500 m to 1523 m/sec at 4000 m.

(U) The sound channel was limited by the sea floor south of FLIP where the bottom of the sound channel was at a depth of 4800 m. North of 34°N the bottom of the sound channel shoaled rapidly to the northern end of the track, where it intersected the continental slope of the Alaska Peninsula at a depth of about 1700 meters. Over the entire section of the track north of 27°N only a very few small topographic features extended 100 m or less into the deep sound channel.

(U) Going upward toward the axis of the channel at depths shallower than 2500 m the sound velocity gradient is diminished because of the gradually increasing temperature. This axis maintained a rather uniform depth of some 750 m northward from Hawaii to 31°N latitude, shoaled slightly in the vicinity of 36°N to 700 m, and again deepened to about 800 m at about 39°N. Beyond this point the axis shoaled gradually to the north, reaching a depth of about 100 m in the vicinity of 49°N. The minimum sound velocity at the axis decreased from 1483 m/sec in the south to 1472 m/sec in the vicinity of 45°N. At the northern terminus the minimum sound speed was 1470 m/sec, or slightly less.

(U) The velocity structure above the axis of the sound channel is portrayed as a series of vertical profiles in Fig. 11 and as a vertical section of isopleths of sound velocity (isovels) in Fig. 12. These data are taken from velocimeter measurements on MARYSVILLE during Phase 2 (see Appendix D of Volume 2) and from STD

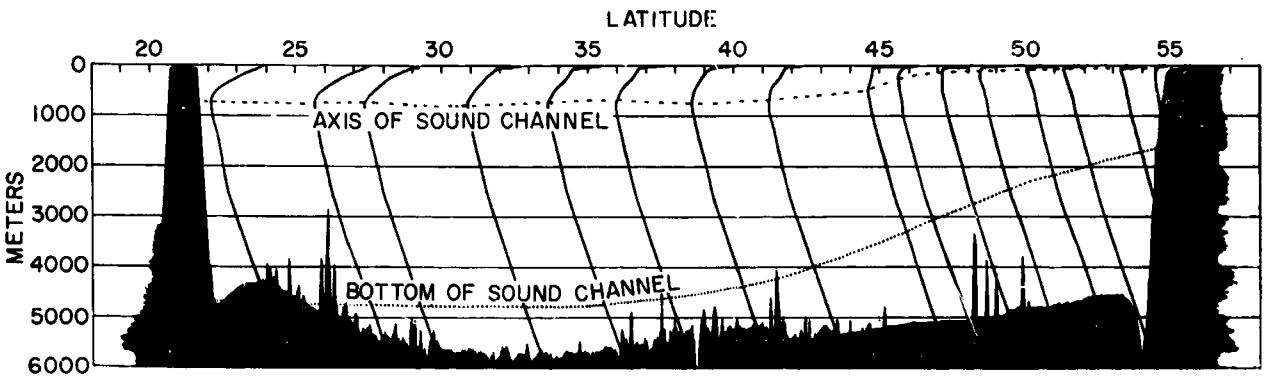

Fig. 10 – Acoustic environment along PARKA I track (U)

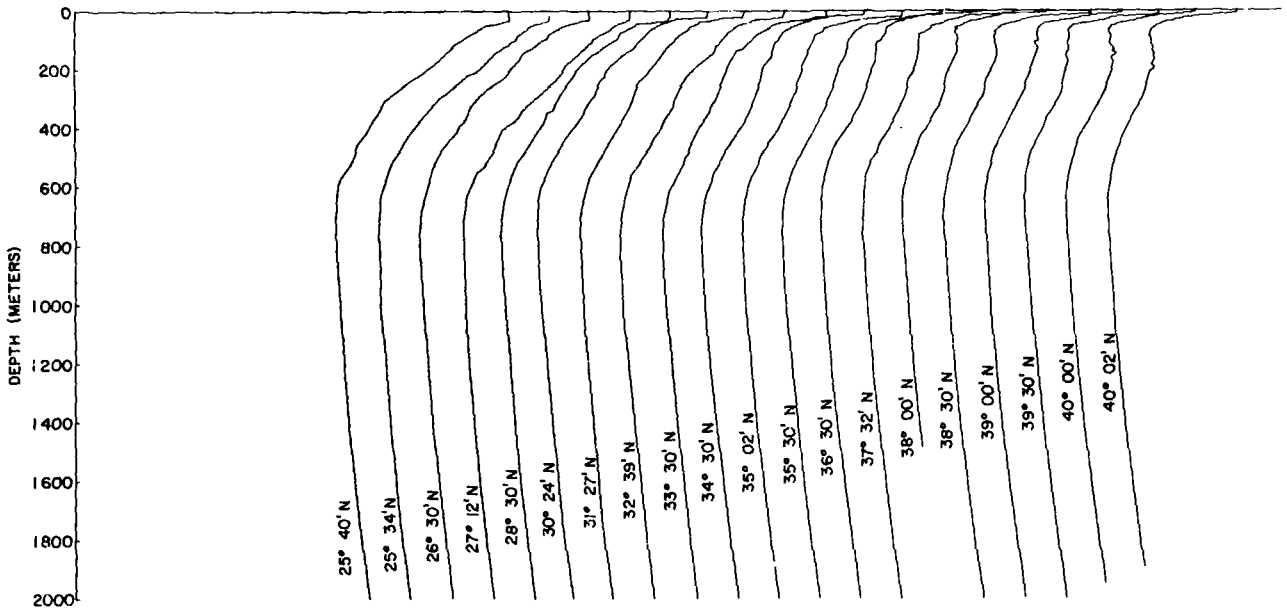

Fig. 11 — Velocity profiles along track (Phase II) (U)

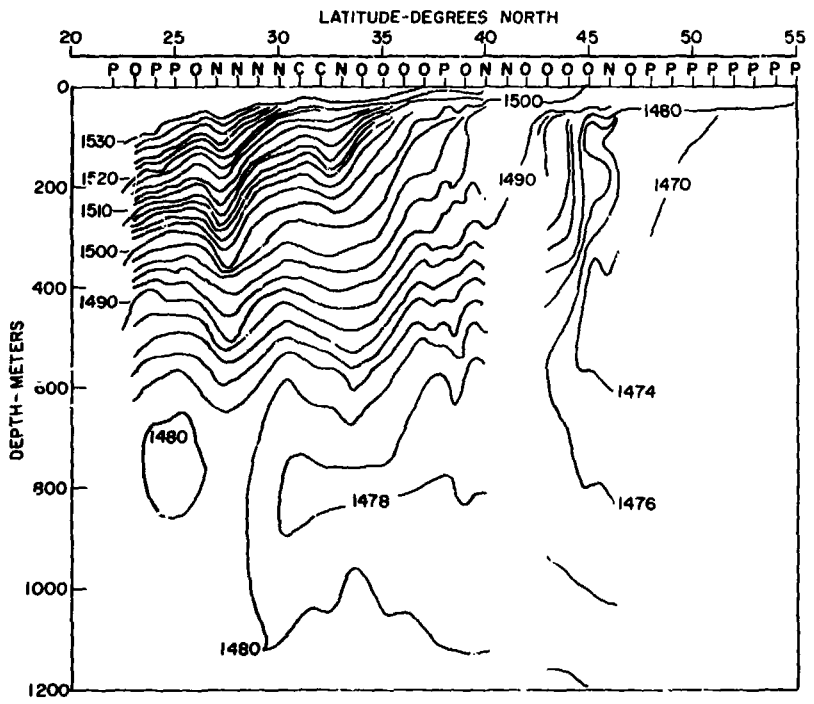

Fig. 12 — Sound velocity cross-section (M/S). Letters indicate nature of near surface gradient: P = positive; O = neutral; N = negative; and C = confused. (U)

data by MIKIMIKI, also in Phase 2. The data were taken over several days and, hence, cannot be regarded as synoptic. Nevertheless, they are used here as though they portray the instantaneous sound structure along the PARKA I track.

(U) The sound velocity gradient increases somewhat irregularly from the axis of the channel to the base of the mixed layer for all profiles south of 34°N (Fig. 11). Beginning with the profile at 34°30′N the gradient increases above the axis for a few hundred meters, then decreases over a variable depth interval to a depth of about 100 m where the gradient increases sharply to the base of the mixed layer. North of 37°30′N the gradient decreases to zero, reverses, and then reverses again before increasing to the base of the mixed layer. Thus a secondary sound channel is formed having its axis at about 100 m. This sigmoid shape of the velocity vs. depth curve persists northward from 37°30′N to the northern part of the transition zone from the North Pacific Central water mass to the Subarctic water mass at 45°N. At this point the deep and shallow sound channels merge. North of 45°N the axis of the sound channel remains at depths of 50 to 100 m. The axis does not rise to the surface because there is a layer of mixed water from about 30 to 60 m thick everywhere north of 45°N.

(U) The mixed layer is readily recognizable on the majority of recordings during PARKA I. For example see the 24-hour sampling of shallow velocity structure shown in Fig. 5. The layer is seen to be thickest (about 60 m) at the southern end of the PARKA I track, thins to less than 10 m (in places, zero) near 34°N and thickens again to 40 to 60 m north of 43°N. There are areas of positive, zero, and negative gradient along the track, plus some areas where the gradient is confused. The positive gradients occur mostly at the ends, up to 26°N and from 47°N to 55°N. The intervening part is a mixture of types, suggesting that surface ducting would be difficult to predict except at the ends of the track.

(U) The most prominent horizontal gradient is associated with the subarctic front at 45°N. However, the largest horizontal gradients of sound velocity are to be found in a short distance near 28°N and a second somewhat lesser gradient near 35°N. Other lesser gradients are evident in the region between 22°N and 28°N. They are discussed in detail in Appendices B7, B8, and B10 of Volume 2. At the surface the region of highest horizontal gradient is the transition zone between 34°N and 45°N.

Sound Velocity Structure as Input to the Propagation Loss Model

(U) The velocity structures illustrated in Figs. 4A and 4B were used for calculation of propagation loss for Phases 1 and 2 respectively.

Calculated Propagation Loss

(C) At this writing, examples of the calculated propagation loss are available from Phase 1 (60 ft source, 100, 200, 400 Hz) and from Phase 2 (500 ft source, 178 Hz) for the 2500 ft and 10,800 ft receivers at FLIP and for the receiver at Kaneohe. These results are shown in Figs. 13 to 16. The most striking feature of all calculations is the variability evident in the short range loss compared with that at long range. The sawtooth pattern evident at short range in Figs. 13, 15, and 16 is a manifestation of the familiar convergence zones, here spaced about 30 miles apart. The large increases in

loss between the zones at short range results from dependence on the comparatively inefficient bottom bounce propagation there. The convergence zones broaden with range and eventually fill these zones so that large increases in loss are not predicted for ranges greater than 200 to 300 n.m. (Fig. 15). For the 10,800 ft receiver and the 60 ft source (Fig. 14) the 30-mile convergence zone is modified to a much shorter separation.

(C) It is worth noting that predictions of the sort shown here are not produced automatically by exercise of the computer model. The programming for horizontal gradients in the water and arbitrary bottom profiles causes focusing and defocusing of ray bundles so that ray spacings can be made close enough for convergent intensity computations only after detailed inspection of an initial set of computations (see discussion, p. 12). Without such detailed attention, the results exhibit very large increases in loss (e.g., 220 dB) which are artificial results of the choice of ray spacing.

Bibliography

(U) McGary, J. W. and E. D. Stroup, Mid-Pacific Oceanography, Part VIII, Middle Latitude Waters, January-March 1954, U.S. Fish and Wildlife Service, SSR-Fisheries No. 180, 1956.

(U) Seckel, G. R.,. Atlas of the Oceanographic Climate of the Hawaiian Islands Region, U.S. Fish and Wildlife Service, SSR-Fisheries No. 193, 1962.

(U) Sverdrup, H. U., M. W. Johnson and R. H. Fleming, The Oceans; Their Physics, Chemistry and General Biology, Prentice-Hall New York, 1942, 1087 p.

(U) Thorp, W. H., Analytic Description of the Low-Frequency Attenuation Coefficient, Journal of the Acoustical Society of America, 42(1), p. 270, 1967.

(U) Uda, M., On the Structure of the Boundary of Water Masses, Journal of the Oceanographic Society of Japan, 2(4), 1943.

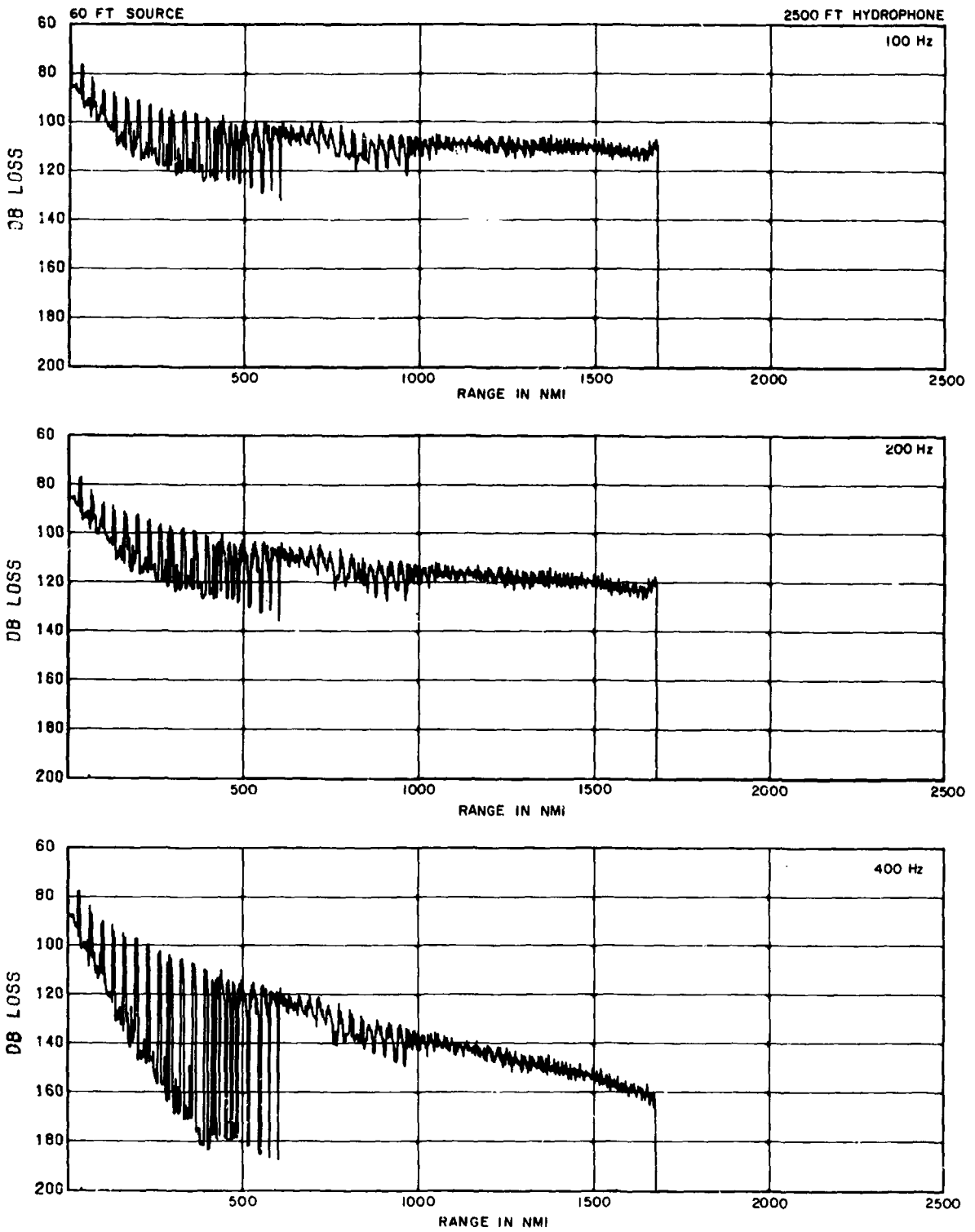

Fig. 13 – Computed transmission loss (C)

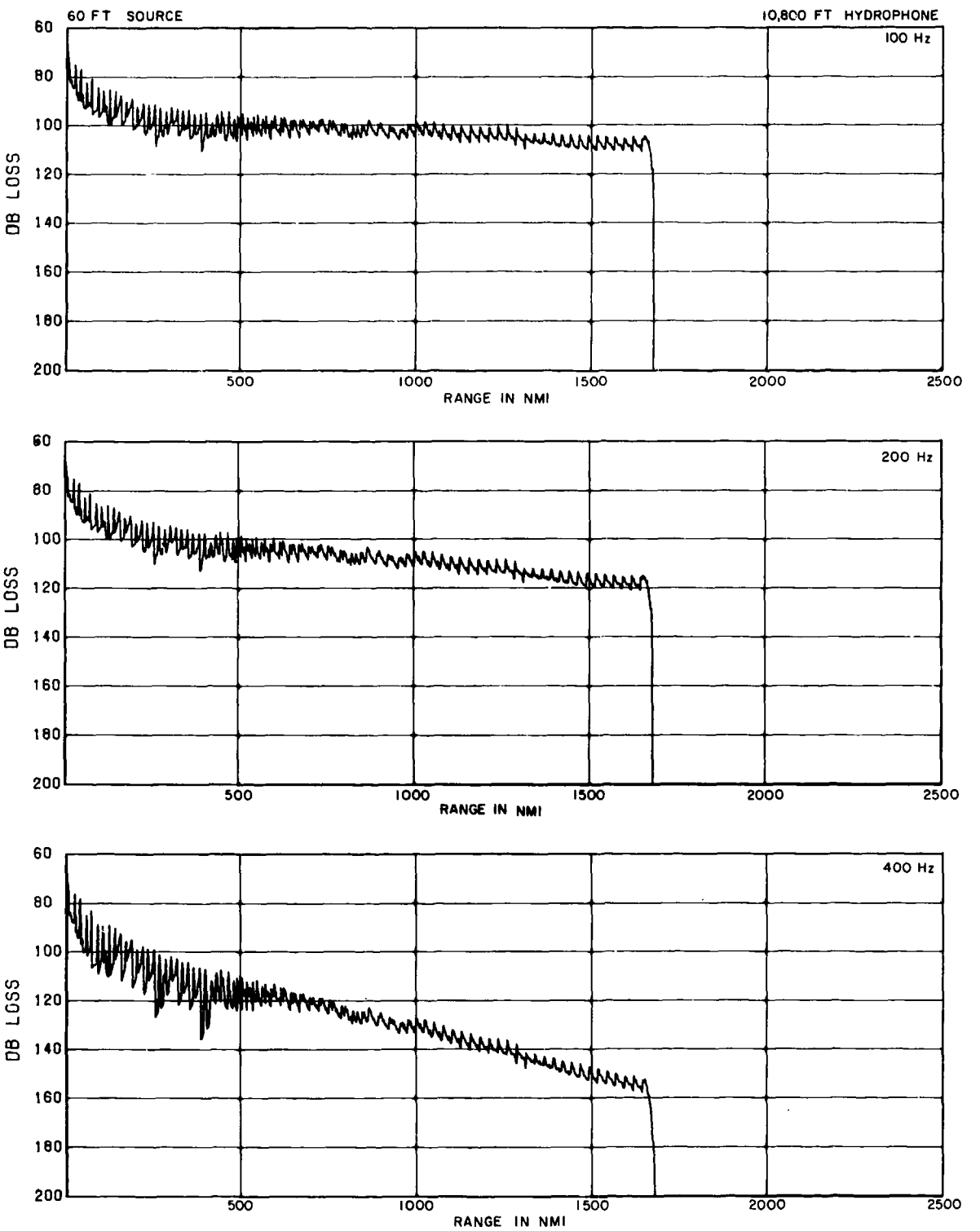

Fig. 14 – Computed transmission loss (C)

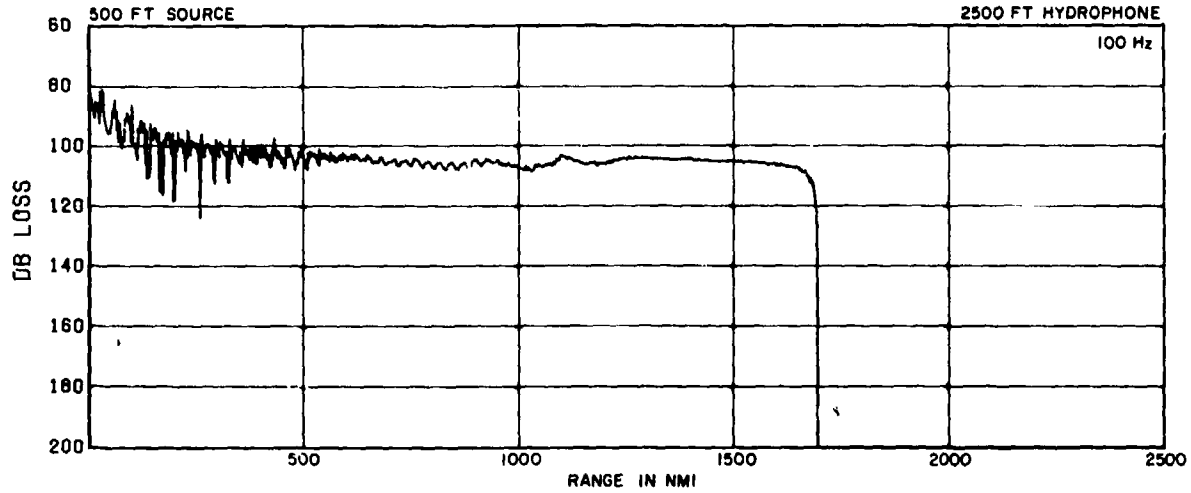

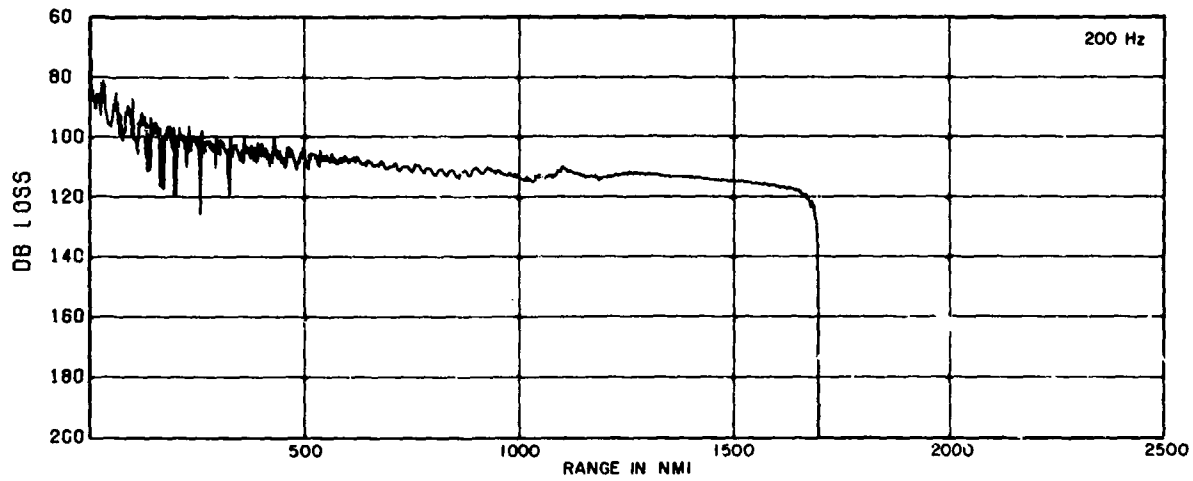

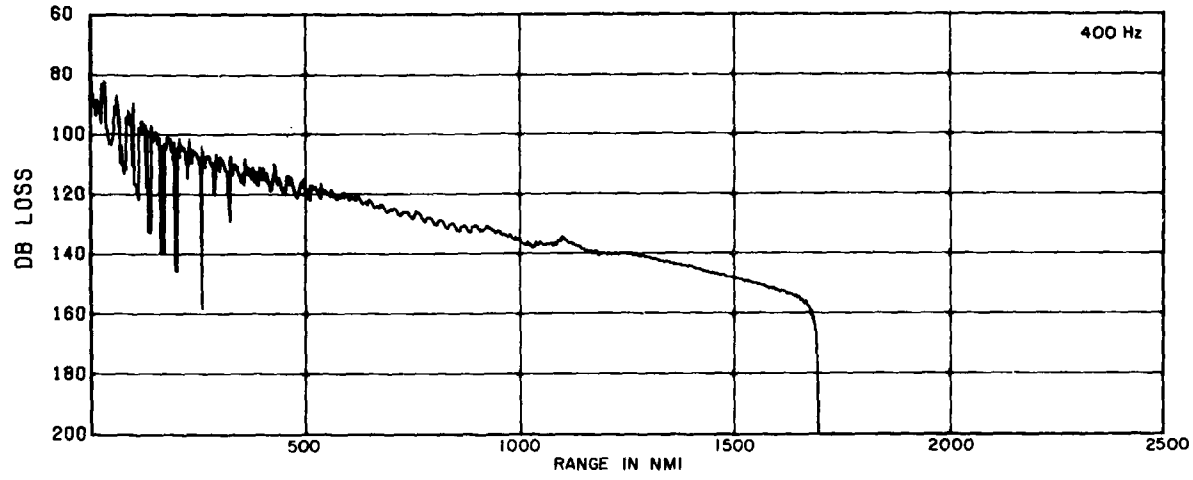

Fig. 15 – Computed transmission loss (C)

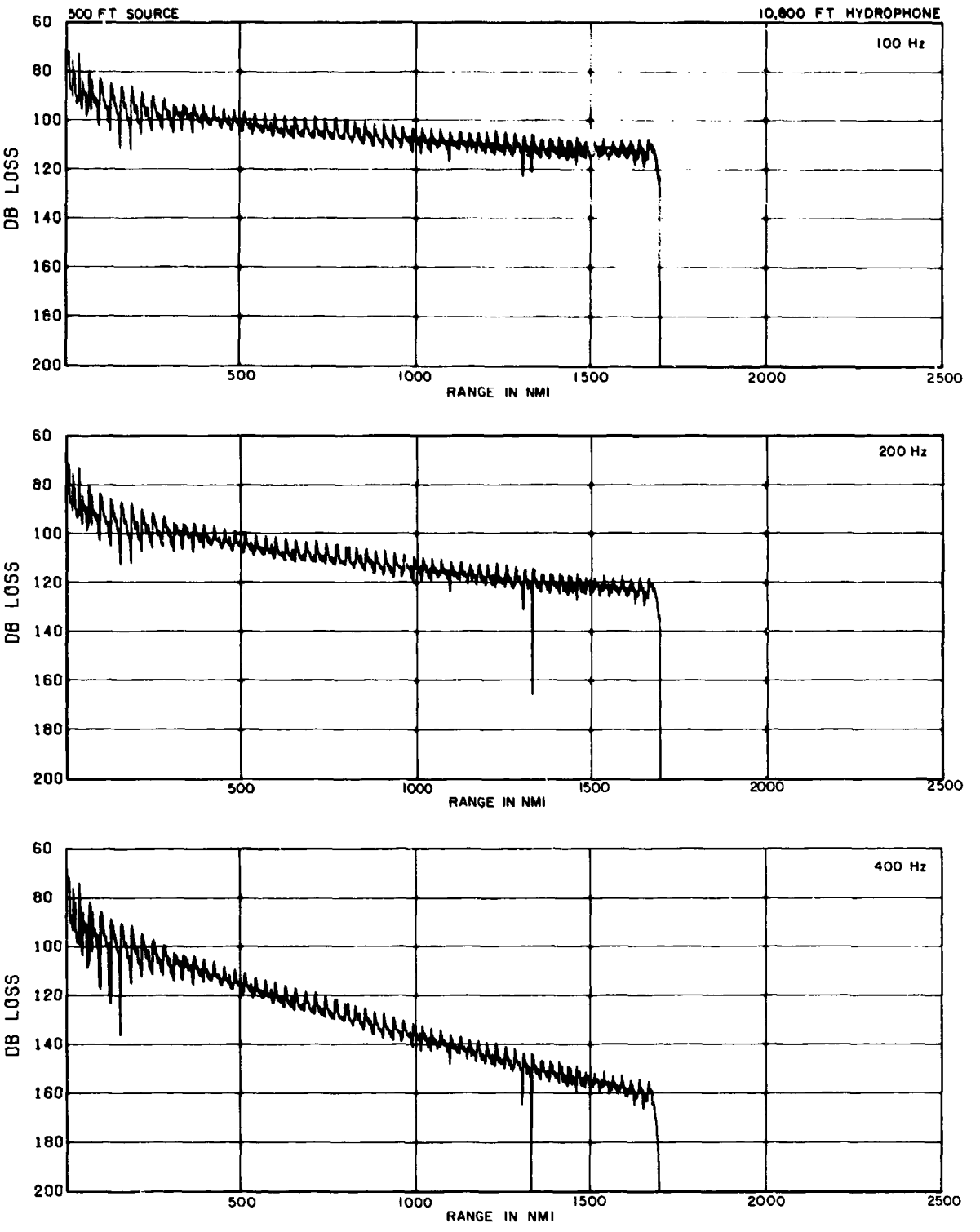

Fig. 16 – Computed transmission loss (C)

Introduction

(C) The acoustic results from PARKA I required for testing the long range sound propagation model are the propagation loss characteristics. This report presents the acoustic propagation loss values that were computed aboard SANDS in real time from the measured data taken on the FLIP hydrophones. Data recorded at Kaneohe that were subsequently processed aboard SANDS and at USL, are also given. Noise measurements made from the several receiving hydrophones are presented and discussed. The determination of source level for the various sources is included as background for the appraisal of the propagation loss results.

Source Levels

(C) The determination of absolute propagation loss requires a knowledge of source level. In May 1968 a number of charges of the type used for PARKA I were calibrated in deep water off Bermuda so as to determine the necessary source levels for calculating propagation loss.

(C) The charges used at the 60 and 500 ft depths consisted of six one-half pound blocks of TNT packed in a faired, plastic container and weighted so the descent rate was the same for all charges. Detonation was by lighted fuse cut to the appropriate length for the depth desired. The charge used at the 2500 ft source depth was a SUS MK 59 Mod 4, a cyclotol-filled, 4-pound TNT-equivalent charge, hydrostatically detonated.

(C) During the measurements off Bermuda, R/V SIR HORACE LAMB occupied stations at various ranges within a radius of 10 n.m. from the bottom-moored TRIDENT vertical array and detonated charges at the desired depths. These shot signals were received by the top hydrophone of the vertical array and by a hydrophone suspended over the side of SIR HORACE LAMB at a depth of 4200 ft. They were recorded at the Tudor Hill Laboratory at Bermuda on a MINCOM C-100 seven-channel tape recorder operated at 60 ips in the FM mode. The recordings were processed through an Ambilog 200, a hybrid analog-digital computer, in 1/3 octave bands from 10 to 2000 Hz. Received energy was calculated referenced to a calibrated signal and corrected for range in accordance with acoustic ray geometry to obtain the energy flux density in contiguous 1/3 octave bands one yard from the source. The data set used to obtain the 60 ft source level curve consisted of spectra from 23 charges obtained when the source ship was directly over the TRIDENT Vertical Array. The data for the 500 ft source level curve came from 6 shots detonated directly over the TRIDENT vertical array, 12 shots detonated at a horizontal range of 5 n.m., 5 shots detonated at a range of 10 n.m. and 6 shots recorded aboard SIR HORACE LAMB, making a total of 29 shot receptions for determining the shot spectrum for this depth.

(C) The source level curves used for determining propagation loss are shown in Figs. 17 and 18. The vertical lines indicate the total range of values obtained from the family of shots used. Incorporated with these curves are other pertinent data for comparison (Christian, Weston, Western Electric Co.). It is apparent that at 100 Hz and higher frequencies, the uniformity of results by different observers suggests a high degree of confidence in the knowledge of source level. When considering frequencies as low as 31 Hz, there is a significant disparity among observers in source levels for the 60 ft depth. These differences are currently under study. Until this study is completed, the source level at 31 Hz must be assumed to be more uncertain than the source

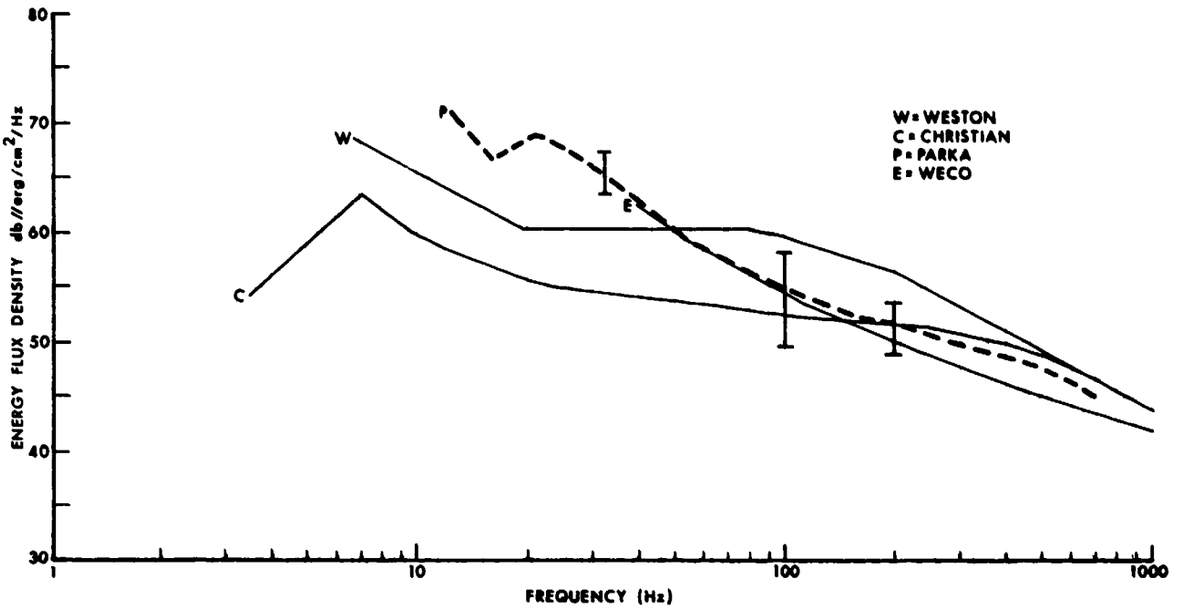

Fig. 17 – Source spectrum level – 3 lb TNT at 60 ft (U)

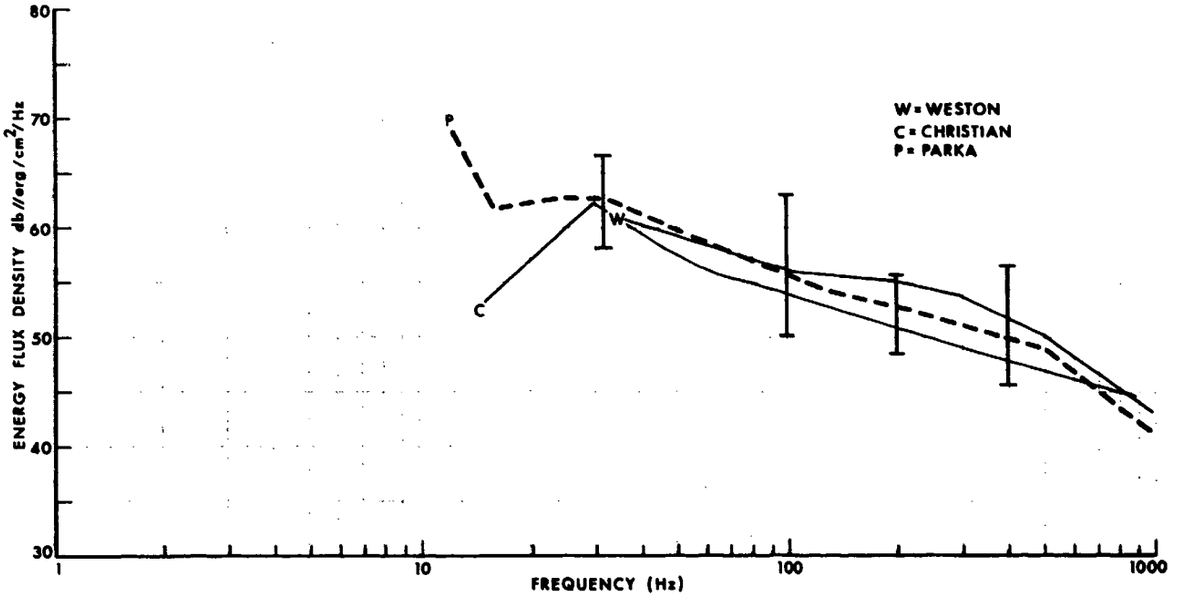

Fig. 18 – Source spectrum level – 3 lb TNT at 500 ft (U)

levels at the other frequencies covered in this report. However, it should be noted that *differences* of propagation loss resulting from the same shots are valid, e.g., receiver position comparisons, loss vs. range comparisons, etc.

(C) At the lower frequencies, source level becomes more sensitive to depth change as the bubble pulse interval approaches the reciprocal of the analysis frequency. In addition, at the lower frequencies and shallower depths, the water surface has a significant effect on the source level pattern. Figure 19 is a plot of apparent source level as a function of angle for a frequency band centered at 31 Hz and at 100 Hz and for two source depths, 60 and 500 ft. The curves in this figure result from considering an impulse function exciting a linear system having an ideal band-limited frequency characteristic. The ocean surface is assumed to cause a 180° phase change in the incident signal. The acoustic source pattern is determined by integrating the composite signal resulting from the direct and surface reflected paths.

(U) Each of the patterns in Fig. 19 has a null at 0° relative to the ocean surface due to

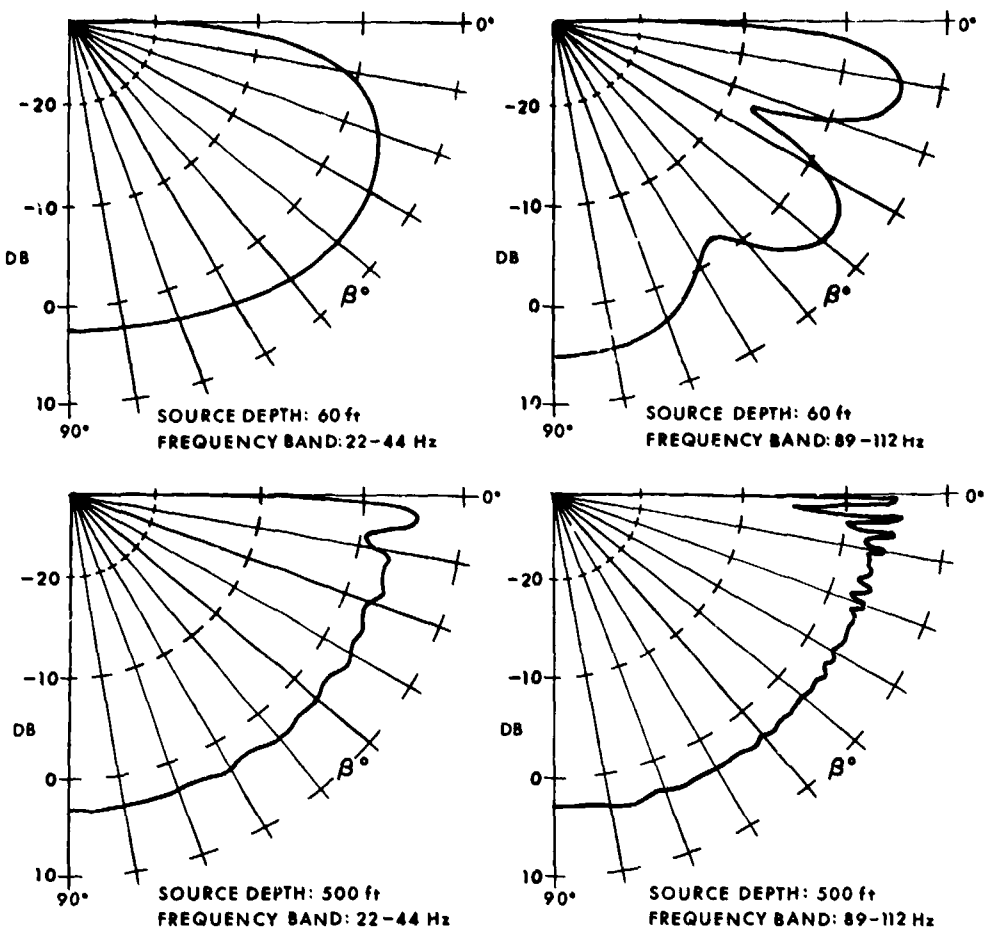

Fig. 19 – Radiated power patterns of sources detonated near ocean surface (angles measured from ocean surface) (U)

the 180° phase shift occurring at surface reflection. Each plot is relative to the free-field source level computed through the same filter. Peaks in the patterns of approximately 6 dB occur, corresponding to in-phase addition to direct and surface reflected signals.

(C) To explain propagation results at long ranges, the patterns shown in Fig. 19 are integrated over the angular aperture visible to a distant receiver. The lower limit of this aperture is assumed as 0° and the upper limit the angle of the limiting ray at the receiver. For geometries of significance in PARKA I, this upper limit is generally less than 20°. With 0° as a lower limit, the patterns were integrated to $\beta°$ and the results averaged by dividing by the angle. Ratios of the integrals were then taken and plotted in Fig. 20. Assuming that all source energy radiated between 0° and 15° was received at a given range, the propagation loss for the 60 ft shots would need to be corrected by about 7 dB at 31 Hz compared with

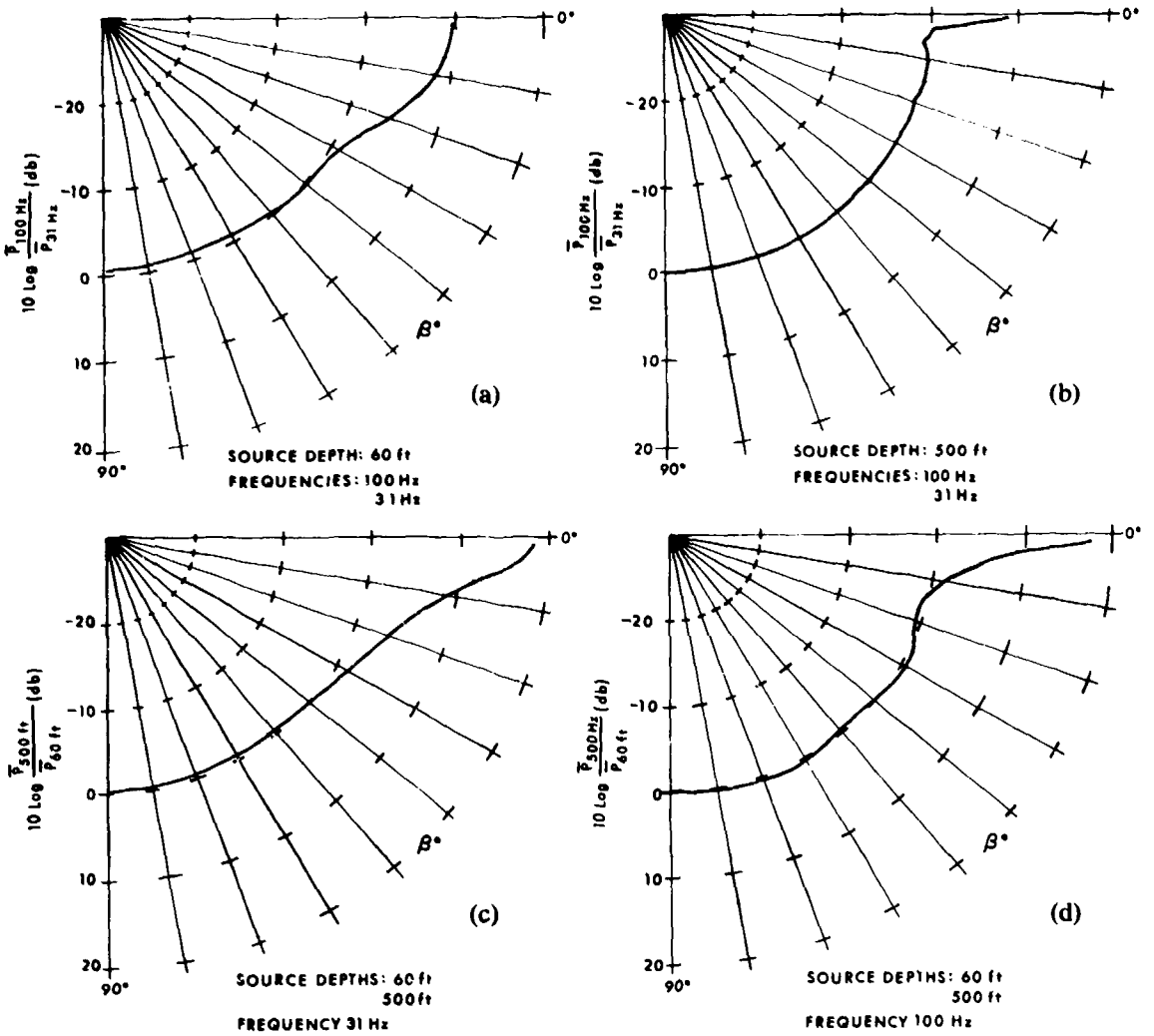

Fig. 20 — Ratio of normalized radiated powers averaged over angular aperature 0° to $\beta°$: (a) and (b) show ratios in dB of radiated power in 1/3 octave bands at 100 Hz to that at 31 Hz for two depths; (c) and (d) show ratios in dB of radiated power in 1/3 octave bands for source depth of 500 feet to that at 60 feet at two frequencies (U)

100 Hz to allow for effective source directivity, while there would be negligible difference between these two frequencies for the 500 ft shot. Similarly, the results for the 31 Hz analysis using 60 and 500 ft shots indicate a 6 dB greater loss fro... the shallow source. A slight difference would also be expected for a 100 Hz analysis of 60 and 500 ft sources.

The Drift of FLIP

(C) As discussed in the Experimental Procedures section of this report, FLIP served as the platform for the receiving hydrophones located nominally at Point ALPHA with coordinates 27°30'N, 157°50'W. FLIP was tethered to SANDS which maneuvered to hold FLIP at a particular location for the duration of the exercise. Although the drift rate of FLIP was materially reduced, there were significant changes in the bottom topography near FLIP during the period of the acoustic measurements, due to drift. Figure 21 shows the drift patterns of FLIP/SANDS for Phases 1 and 2.

Propagation Loss Results

(C) The summary in Table I presents the combinations of source and receiver depths

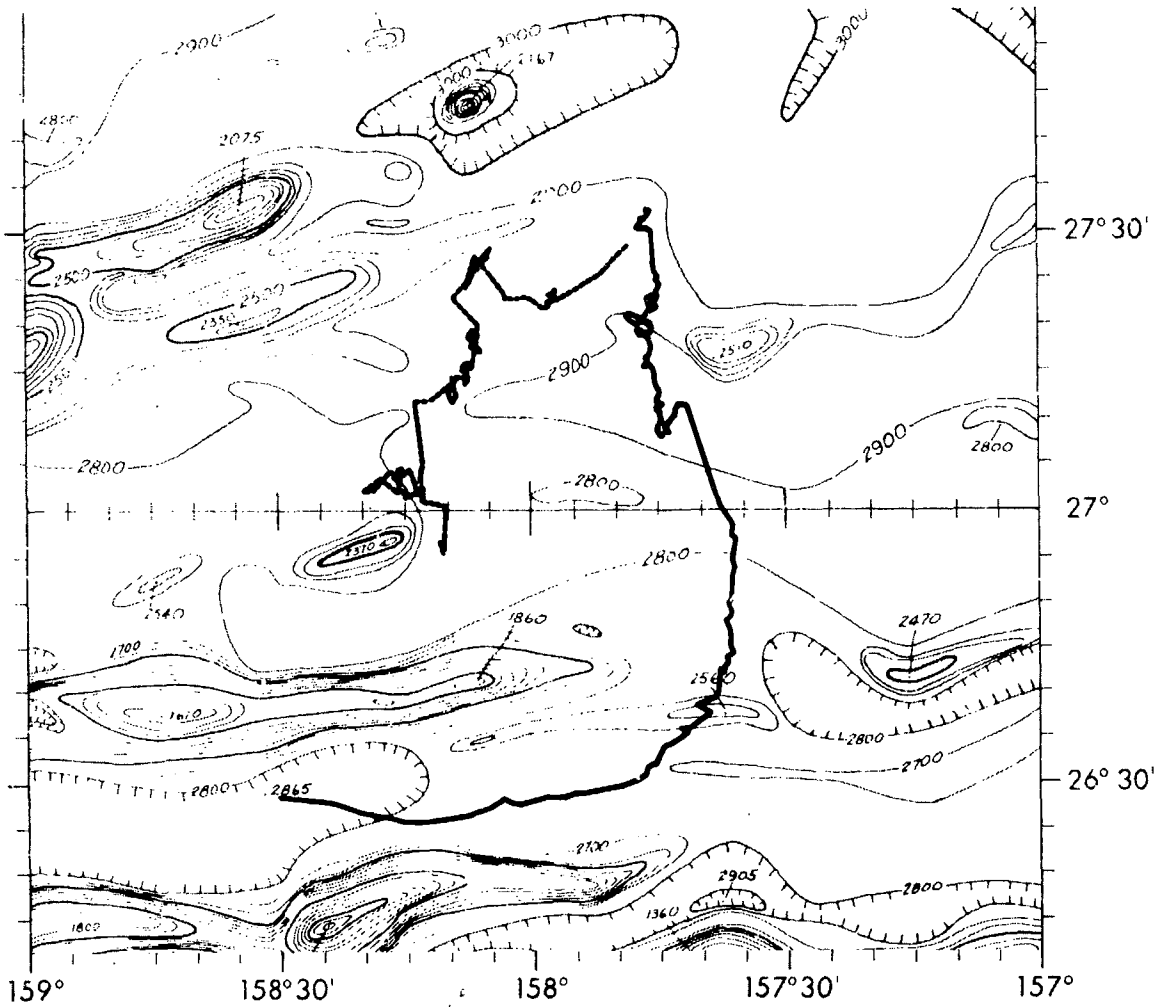

Fig. 21 — SANDS/FLIP track (U)

Table I
PARKA -- Source depth, receiver depth, and frequency analysis bands

Source Depths (ft)	Receiver Depths (ft)	Frequencies (Hz)	Bandwidths (Octave)
PHASE 1			
60 500	300 2,070 (Kaneohe) 2,500 10,800	31 100 200 400	1 1/3 1/3 1/3
PHASE 2			
60 500 2,500	300 2,070 (Kaneohe) 2,500 10,800	31 100 200 400	1 1/3 1/3 1/3
500	300 2,070 (Kaneohe) 2,500 10,800	178 (CW)	1 Hz

and frequency bands available in the results from SANDS that were computed on-line and from Kaneohe that were computed during the return journey of SANDS. A few of these are not available because of channel limitations in the computer program. An exception to real time data reduction was the FLIP/SANDS data south of FLIP during Phase 1. Because the computer was off-line during this period, the Phase 1 "FLIP-South" data were processed from analog magnetic tape. Figures 22 through 60 present the processed propagation loss data received at FLIP and Kaneohe during the PARKA I Experiment. A special analysis was made of the data received from the 500-ft shots of Phase 1 at Kaneohe in order to study frequency-dependent effects in some detail. These results are shown in Fig. 61.

(U) It is helpful when studying these propagation loss curves to refer to the PARKA Event Log shown in Fig. 62. In this figure the status of the instrumentation and operating modes of FLIP, SANDS and the source ship are keyed to the latitude of the source ship for both phases of the experiment. An arrow notes the latitude of Kaneohe and a bracket represents the range of latitudes occupied by FLIP and SANDS during each phase of the experiment. Gaps in the propagation loss curves can generally be explained by referring to this log. For example, gaps in the Phase 1 data near 27°N, 36.5°N and 43°N are explained by *B*, *D* and *G* respectively of the Phase 1 log. *A* of the Phase 1 log indicates that the digital system was off line. These data were later processed on the SANDS' computer from recorded magnetic tape and are presented as part of the propagation loss curves. While this log applies specifically to the data processed on FLIP, it also is applicable to the Kaneohe results when the status of the source vessel is involved.

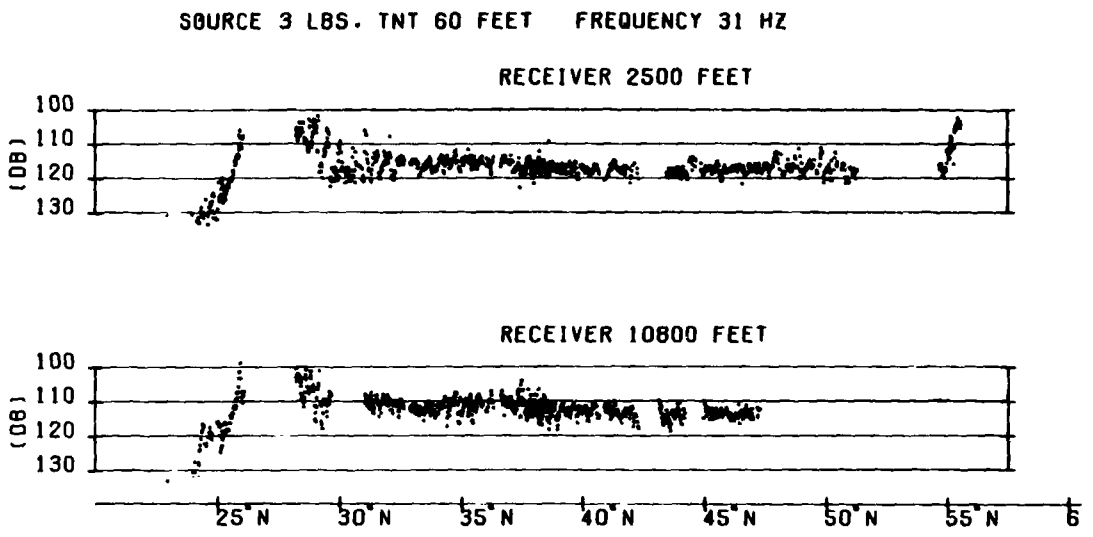

Fig. 22 – PARKA Phase 1 Propagation Loss (C)

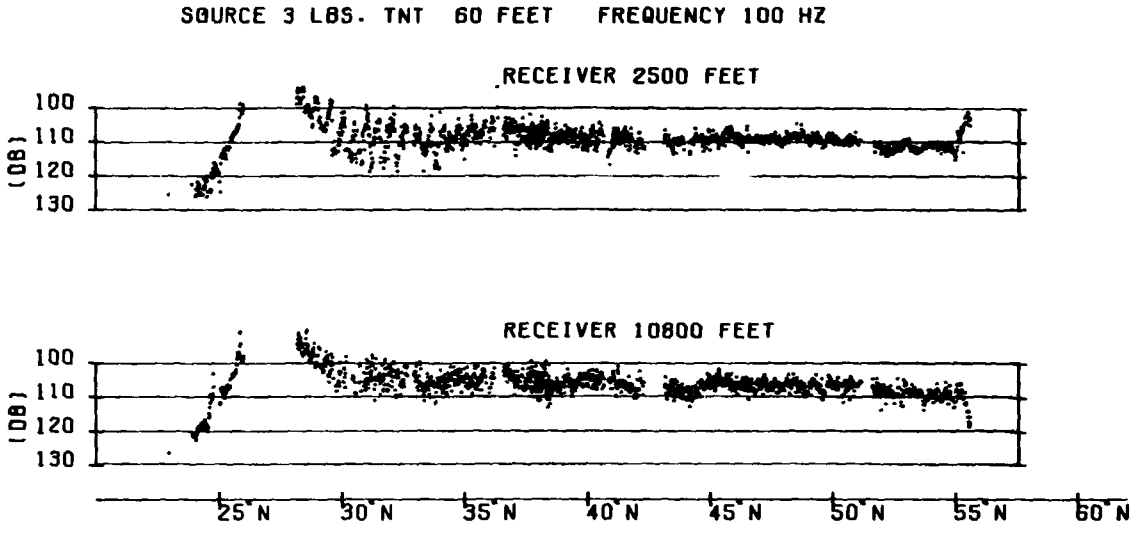

Fig. 23 – PARKA Phase 1 Propagation Loss (C)

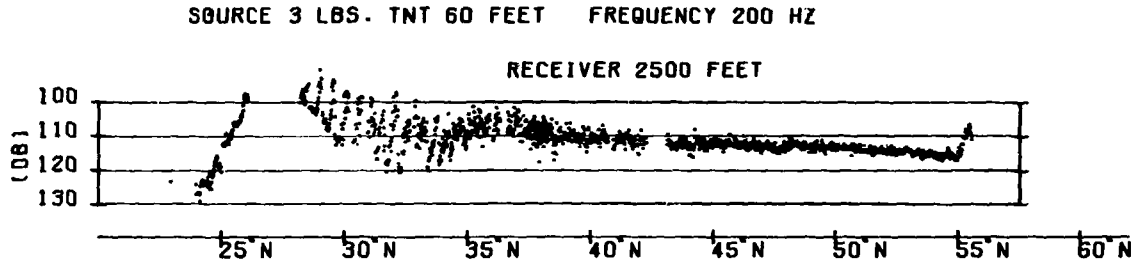

Fig. 24 – PARKA Phase 1 Propagation Loss (C)

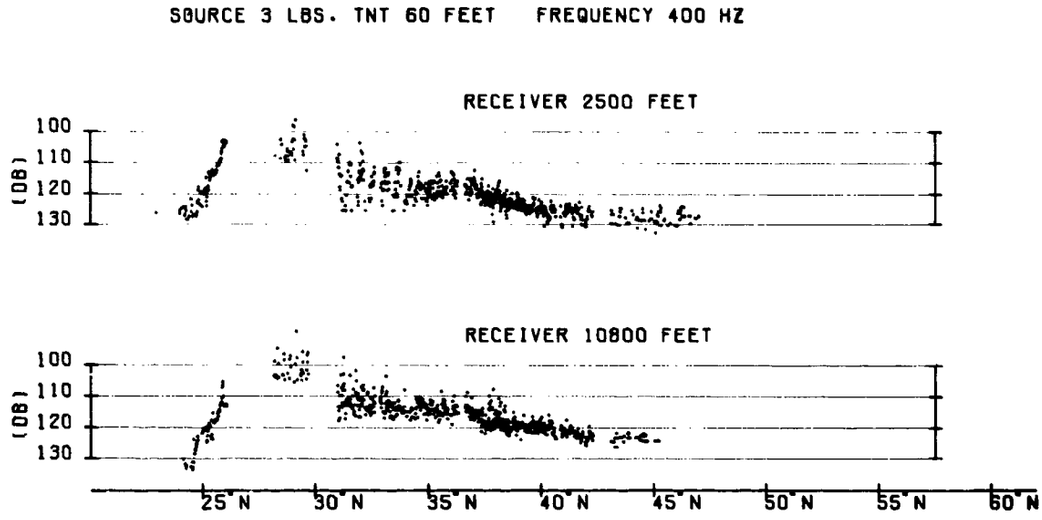

Fig. 25 – PARKA Phase 1 Propagation Loss (C)

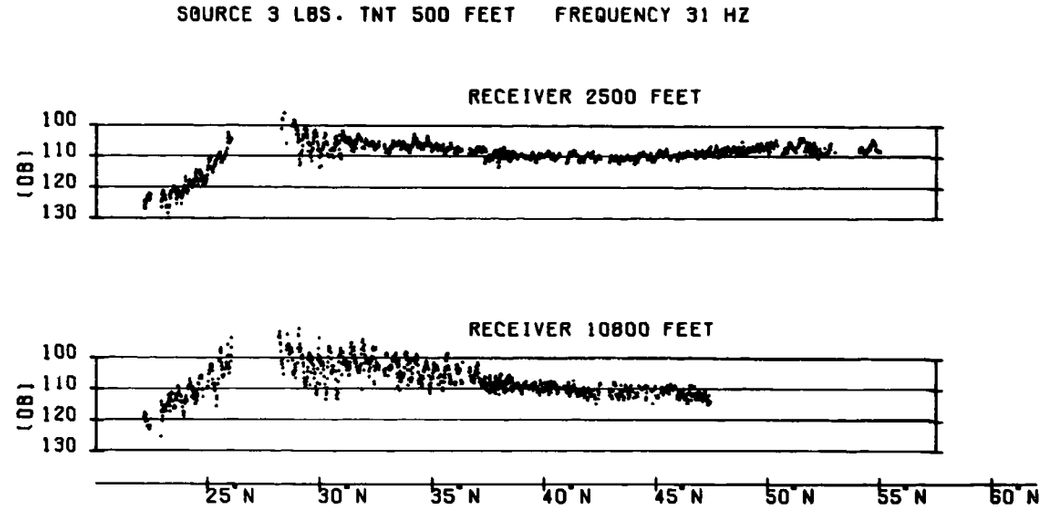

Fig. 26 – PARKA Phase 1 Propagation Loss (C)

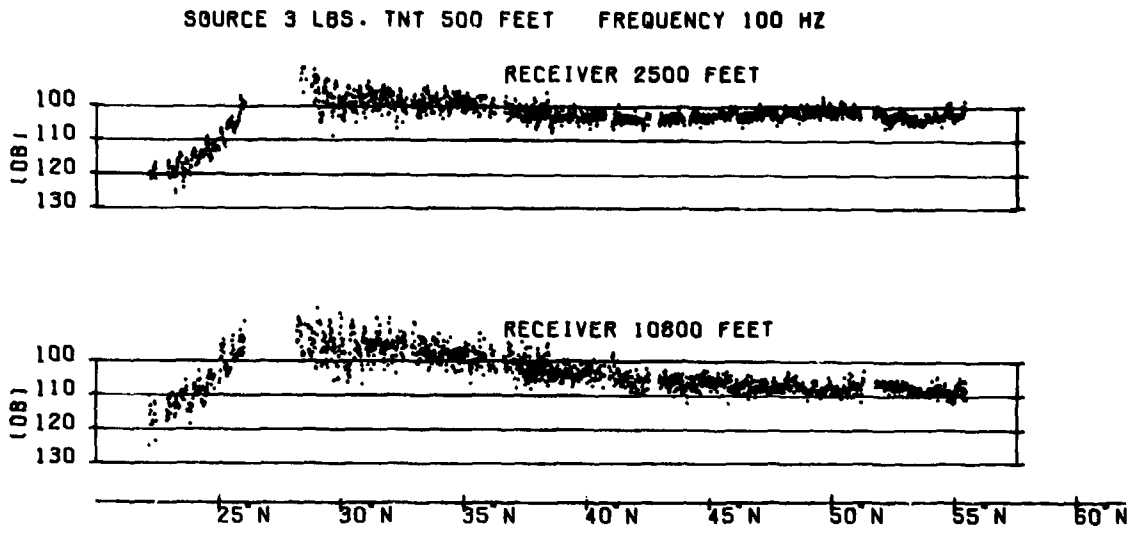

Fig. 27 – PARKA Phase 1 Propagation Loss (C)

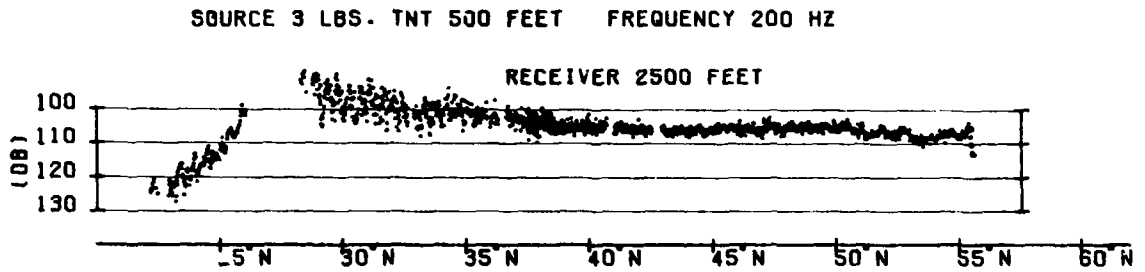

Fig. 28 – PARKA Phase 1 Propagation Loss (C)

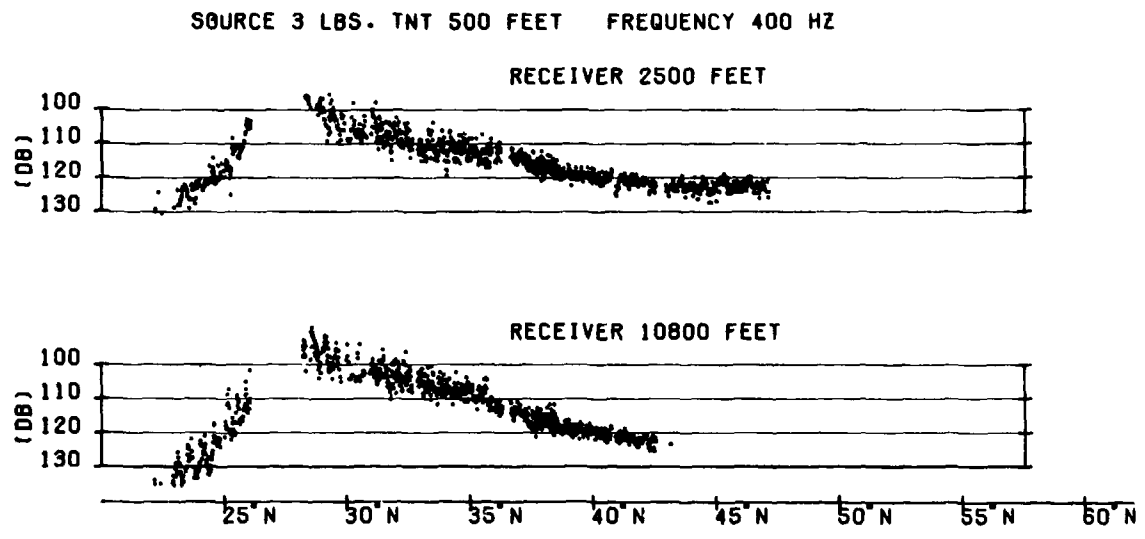

Fig. 29 – PARKA Phase 1 Propagation Loss (C)

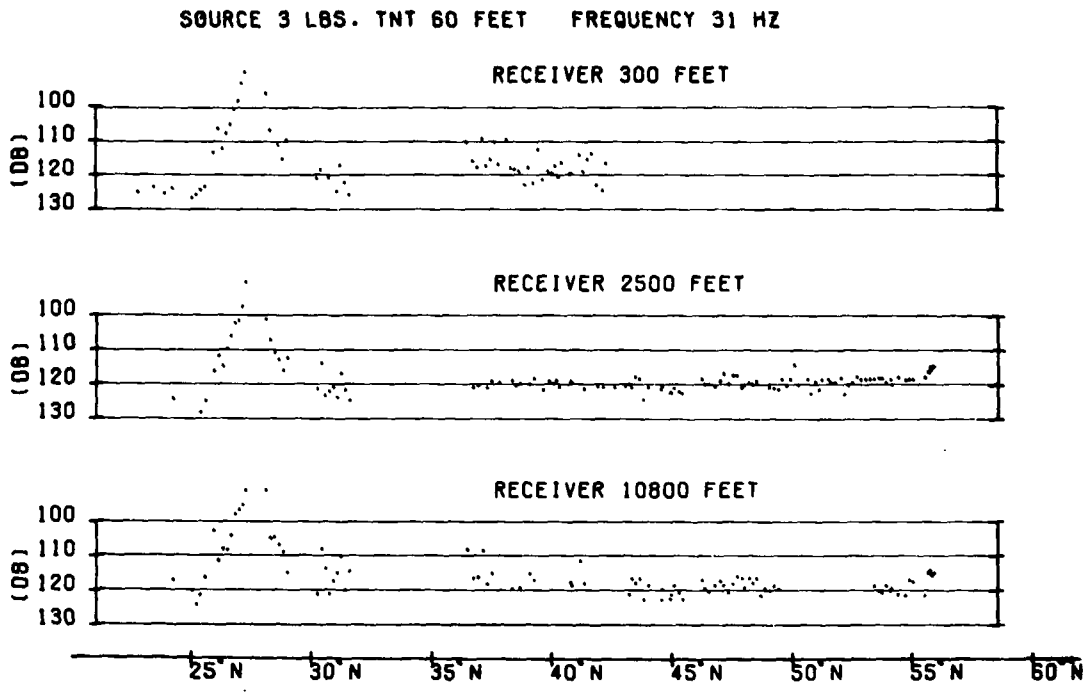

Fig. 30 – PARKA Phase 2 Propagation Loss (C)

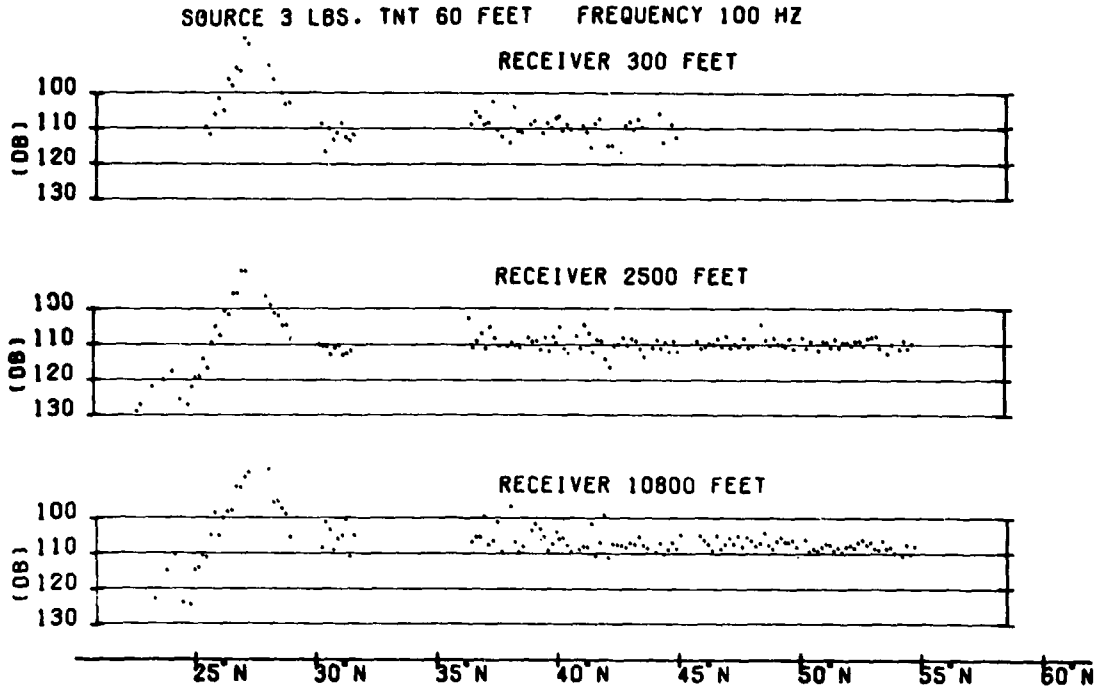

Fig. 31 – PARKA Phase 2 Propagation Loss (C)

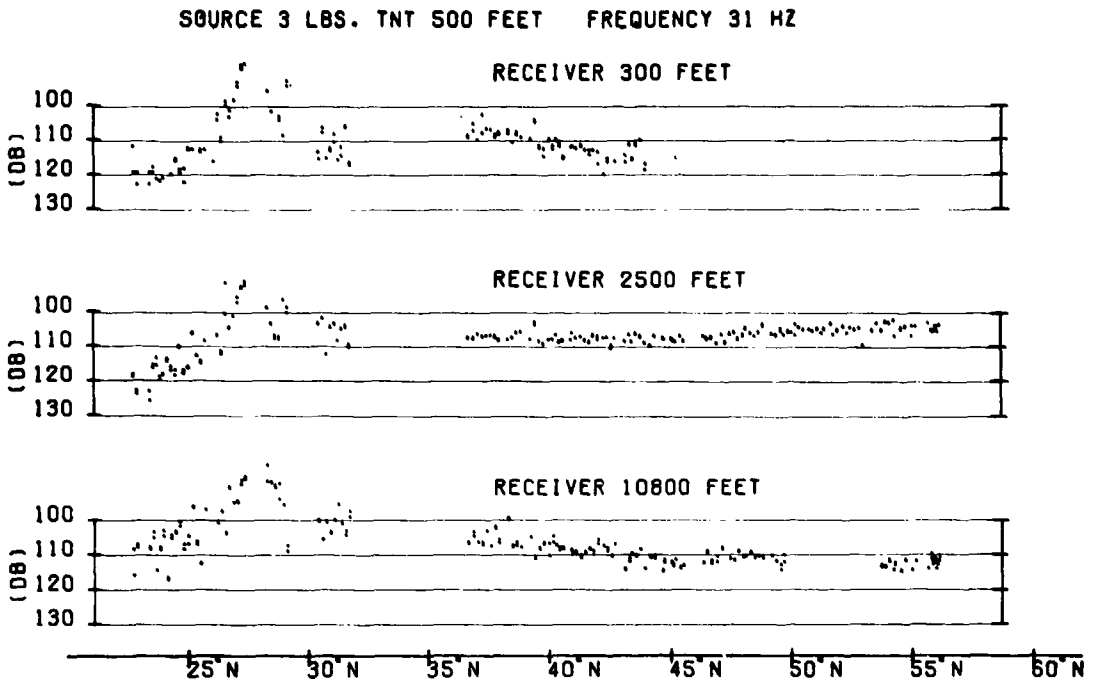

Fig. 32 – PARKA Phase 2 Propagation Loss (C)

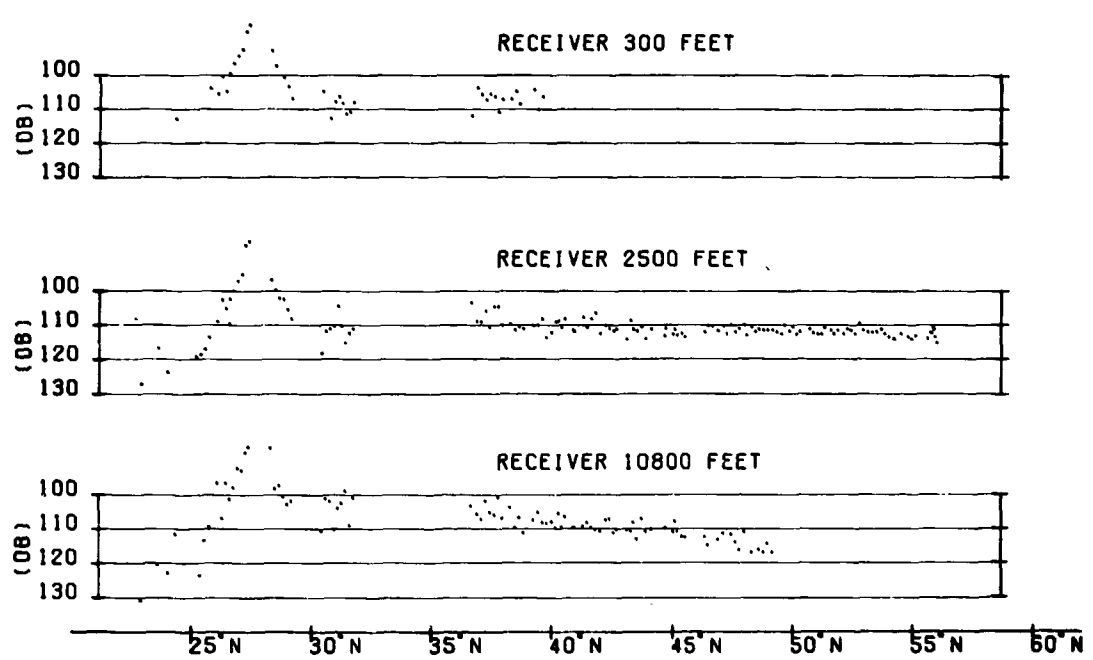

Fig. 33 – PARKA Phase 2 Propagation Loss (C)

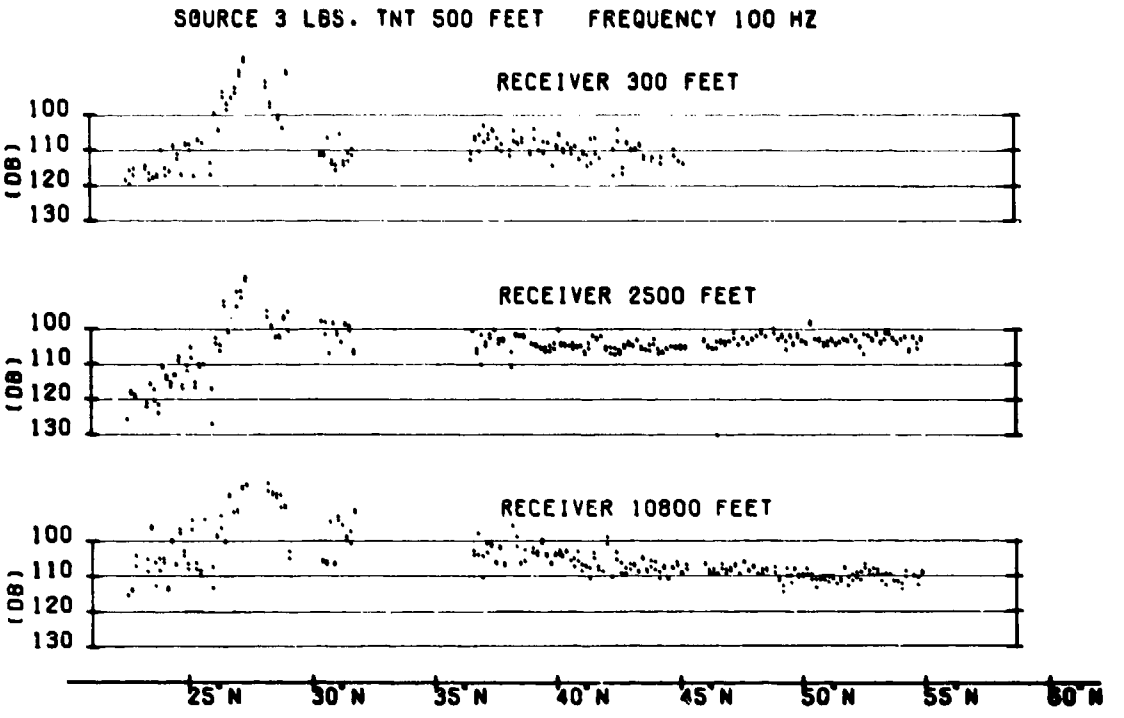

Fig. 34 – PARKA Phase 2 Propagation Loss (C)

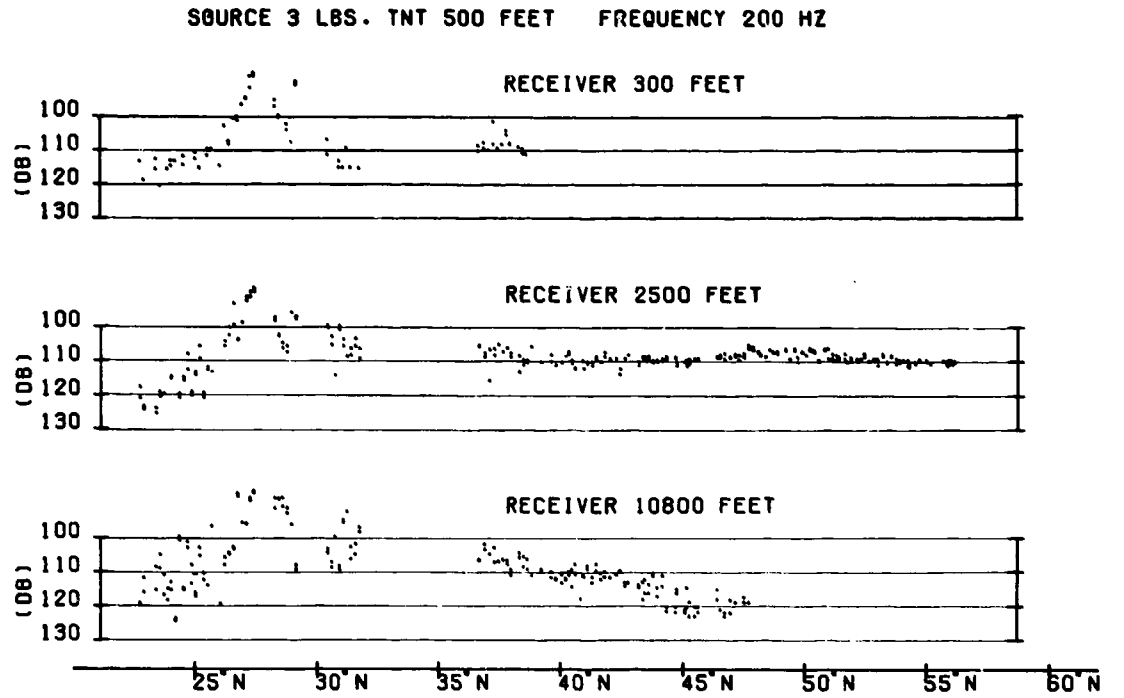

Fig. 35 – PARKA Phase 2 Propagation Loss (C)

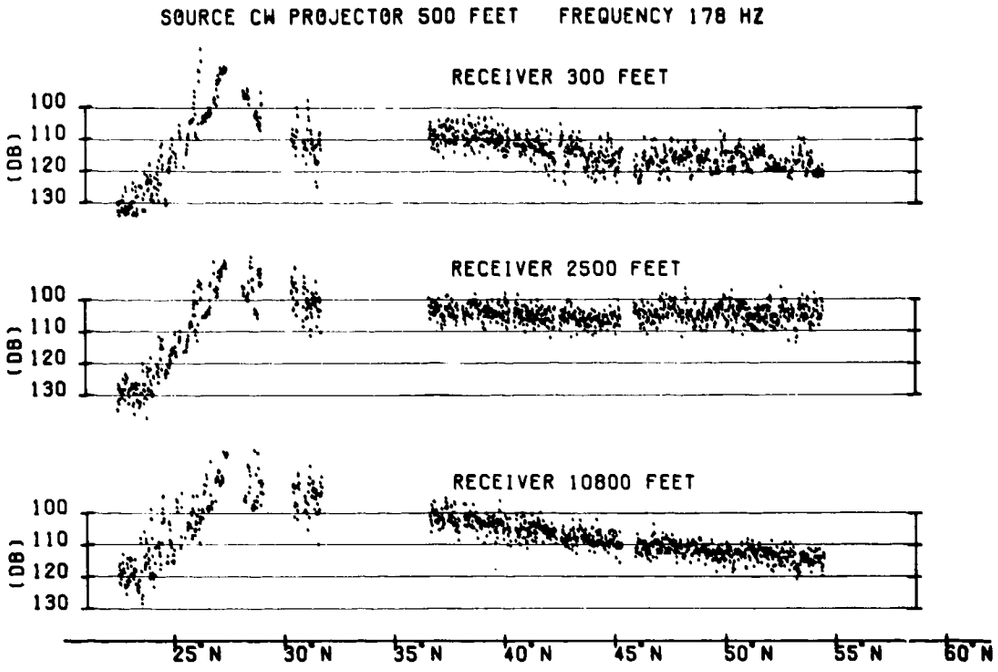

Fig. 36 – PARKA Phase 2 Propagation Loss (C)

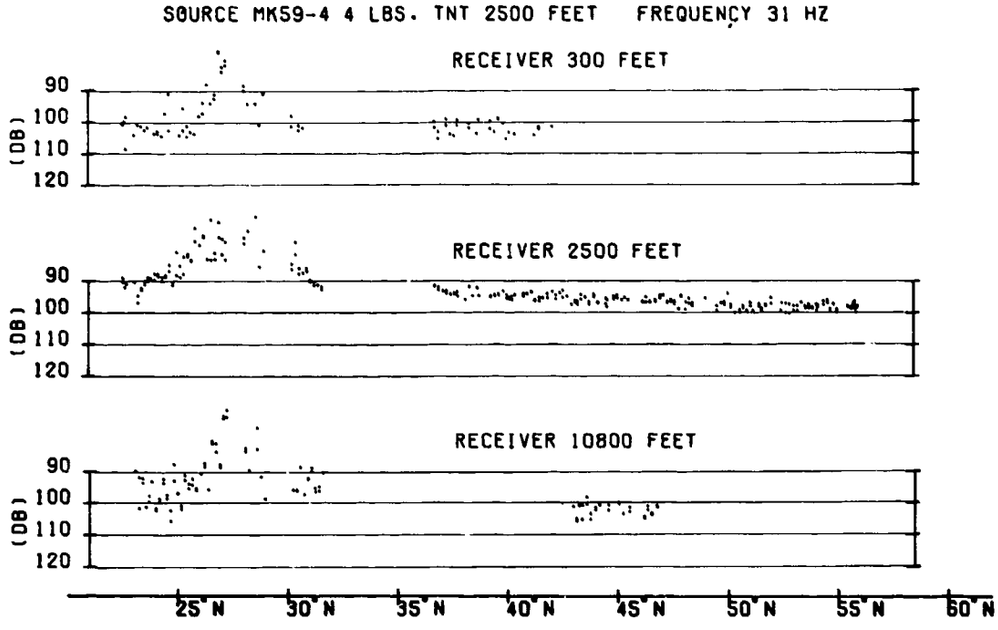

Fig. 37 – PARKA Phase 2 Propagation Loss (C)

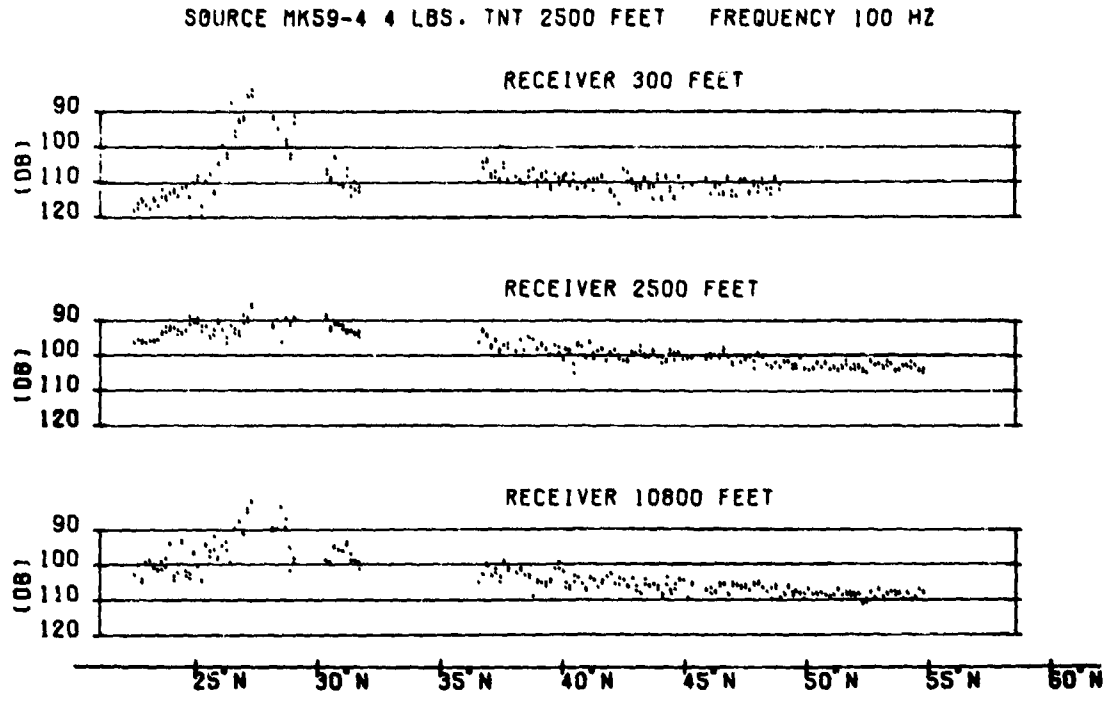

Fig. 38 – PARKA Phase 2 Propagation Loss (C)

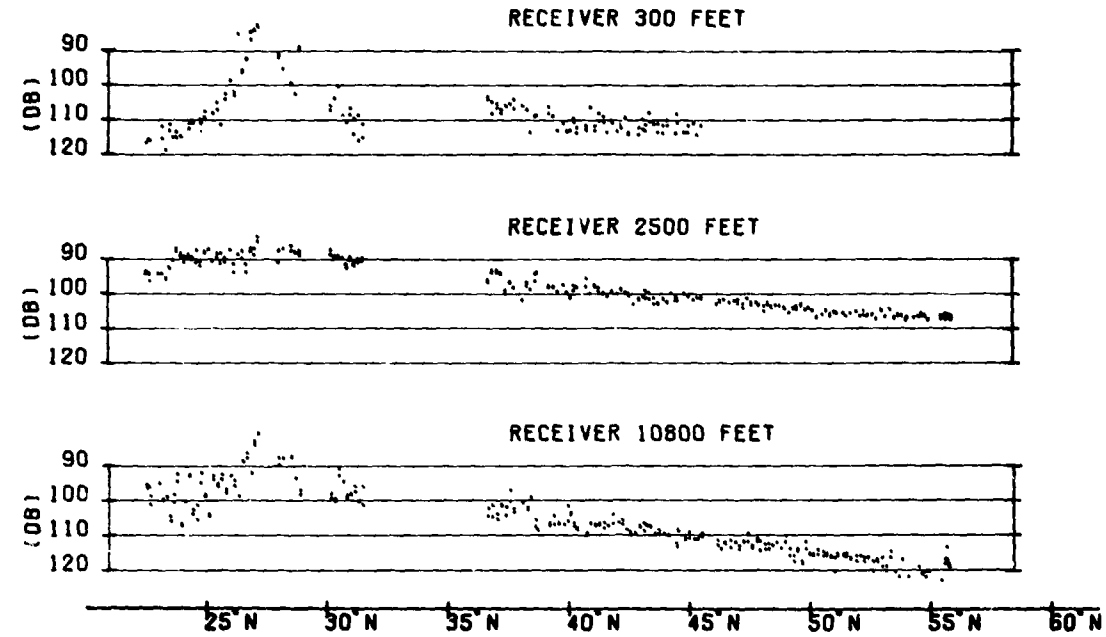

Fig. 39 – PARKA Phase 2 Propagation Loss (C)

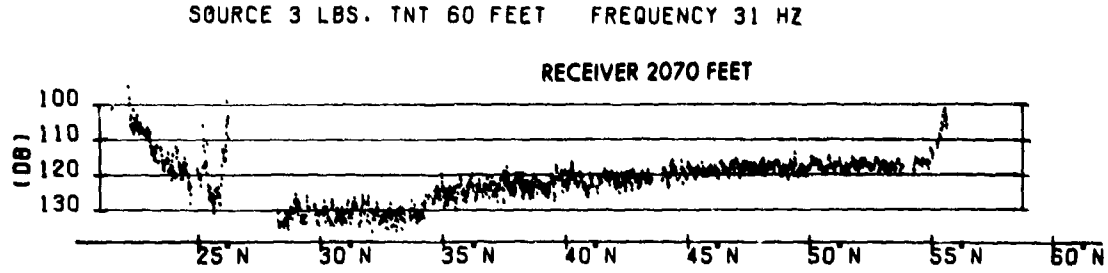

Fig. 40 – PARKA Phase 1 Propagation Loss Kaneohe (C)

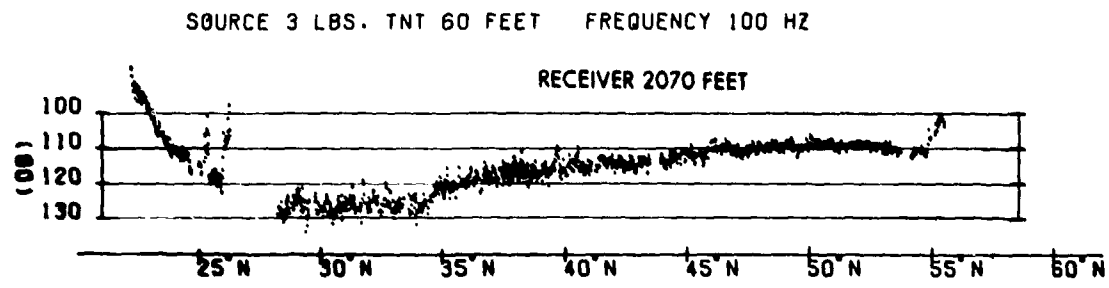

Fig. 41 – PARKA Phase 1 Propagation Loss Kaneohe (C)

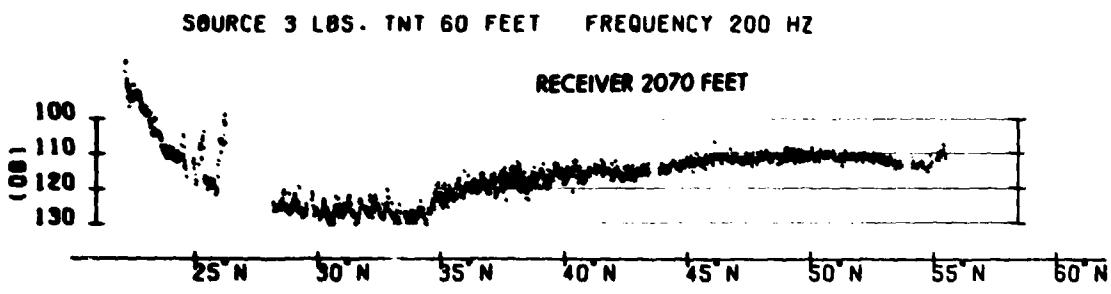

Fig. 42 – PARKA Phase 1 Propagation Loss Kaneohe (C)

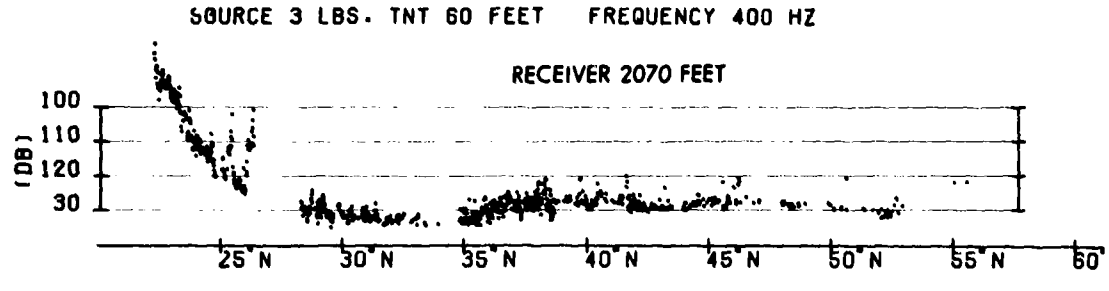

Fig. 43 – PARKA Phase 1 Propagation Loss Kaneohe (C)

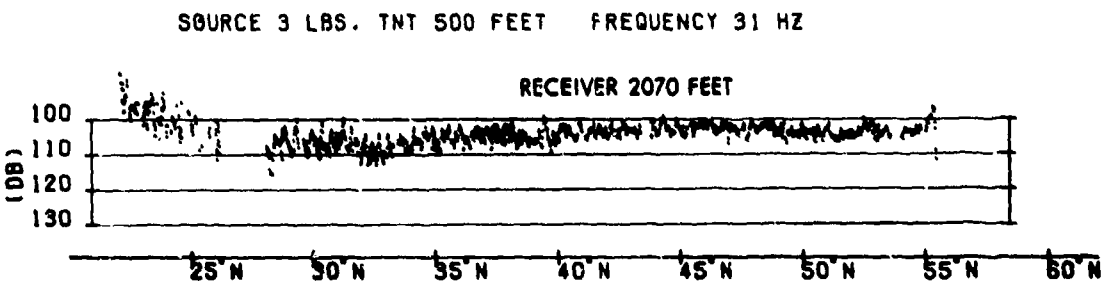

Fig. 44 – PARKA Phase 1 Propagation Loss Kaneohe (C)

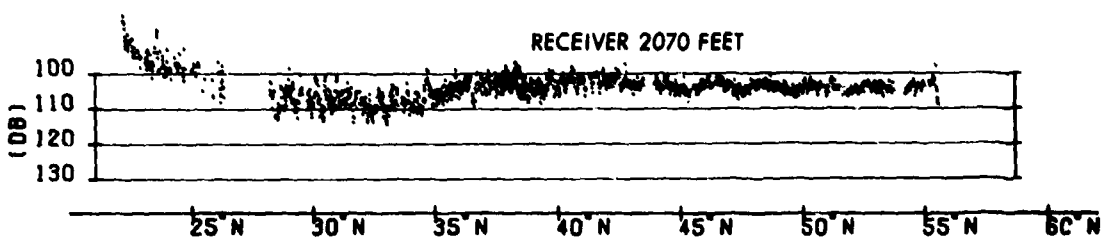

Fig. 45 – PARKA Phase 1 Propagation Loss Kaneohe (C)

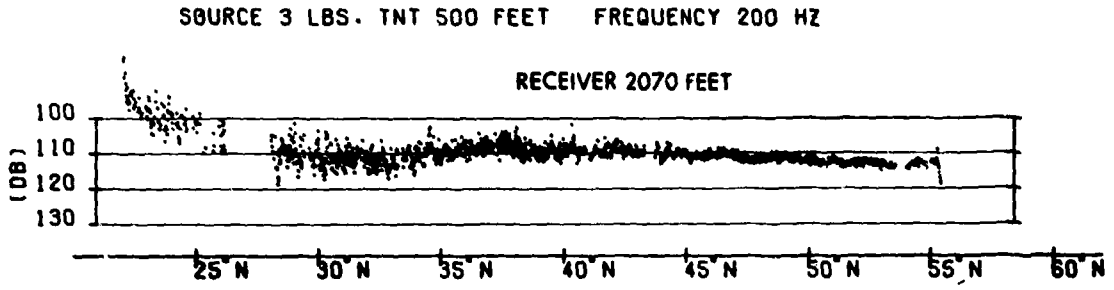

Fig. 46 – PARKA Phase 1 Propagation Loss Kaneohe (C)

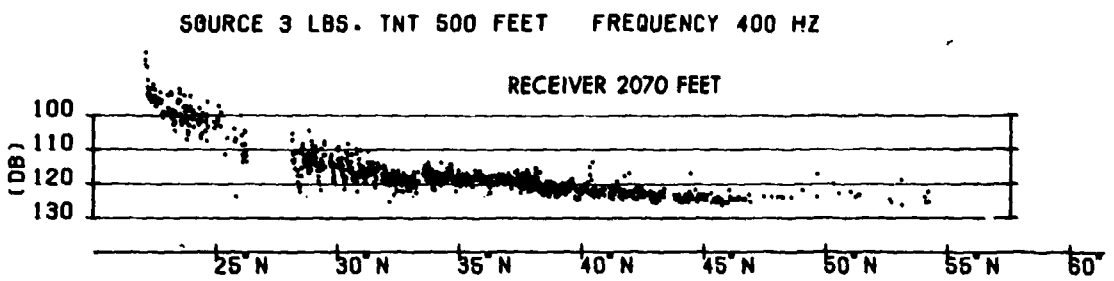

Fig. 47 – PARKA Phase 1 Propagation Loss Kaneohe (C)

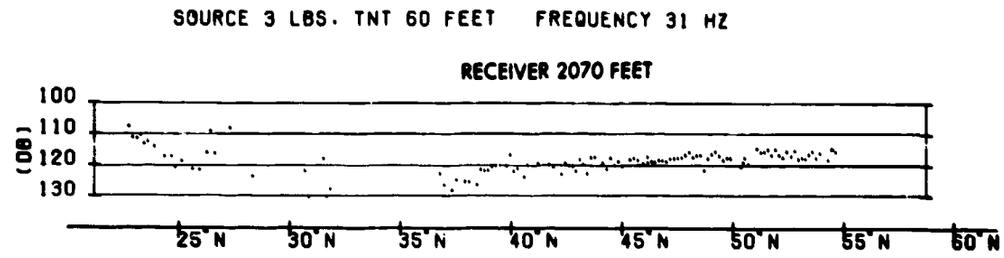

Fig. 48 – PARKA Phase 2 Propagation Loss Kaneohe (C)

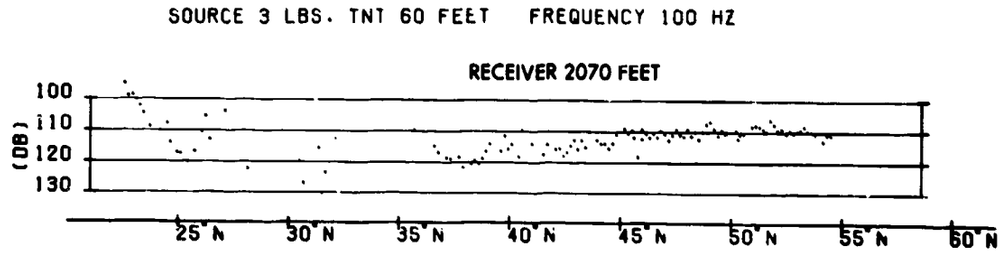

Fig. 49 – PARKA Phase 2 Propagation Loss Kaneohe (C)

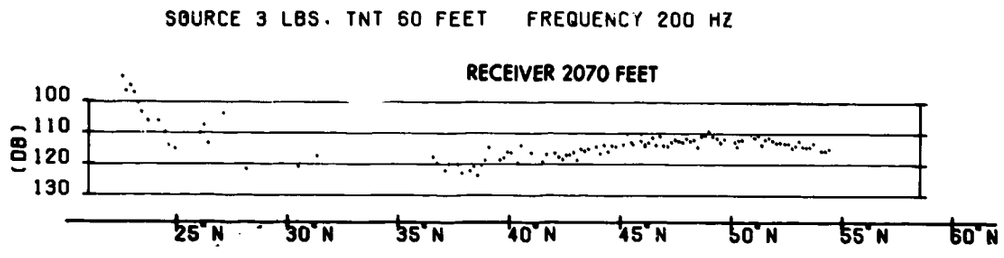

Fig. 50 – PARKA Phase 2 Propagation Loss Kaneohe (C)

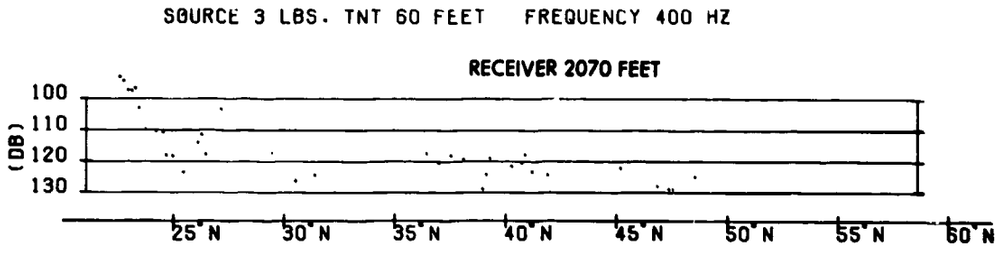

Fig. 51 – PARKA Phase 2 Propagation Loss Kaneohe (C)

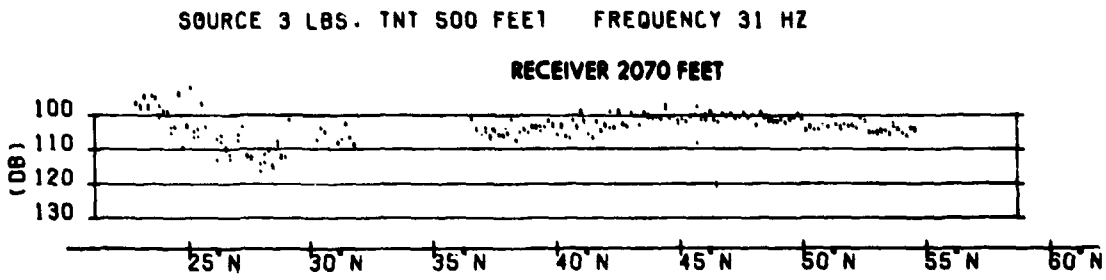

Fig. 52 – PARKA Phase 2 Propagation Loss Kaneohe (C)

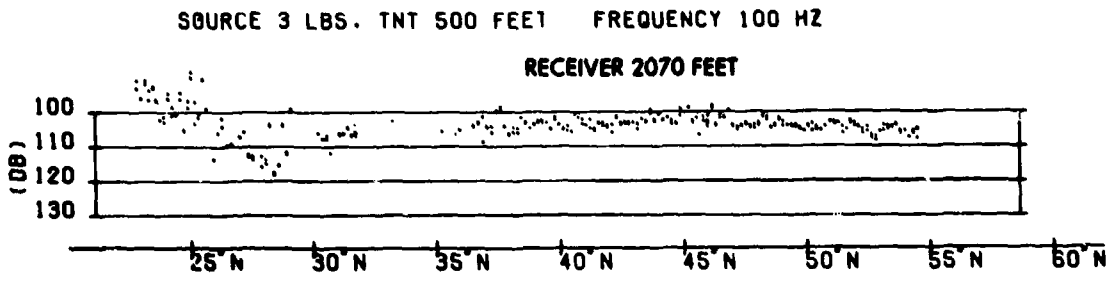

Fig. 53 – PARKA Phase 2 Propagation Loss Kaneohe (C)

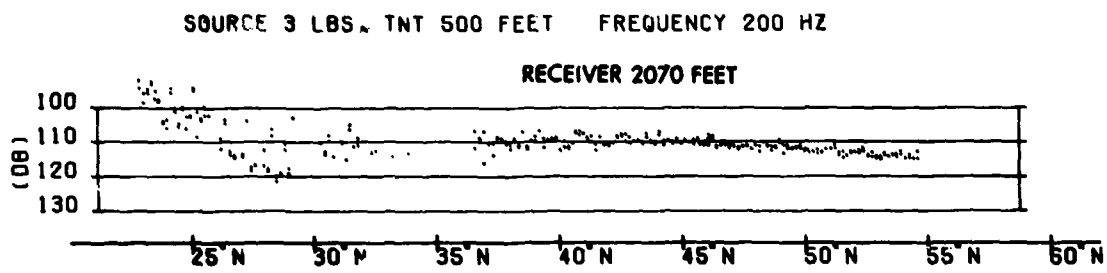

Fig. 54 – PARKA Phase 2 Propagation Loss Kaneohe (C)

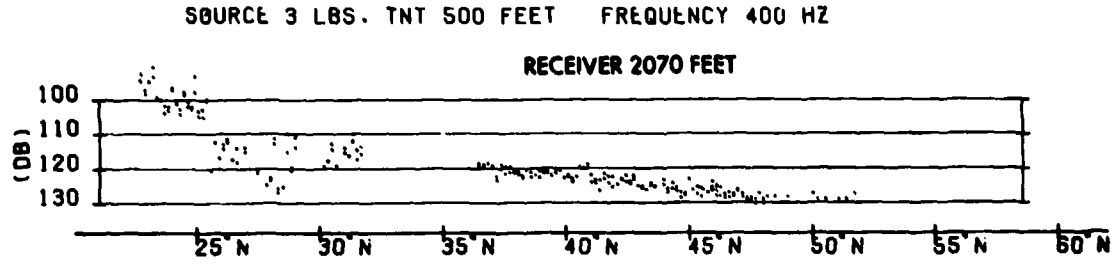

Fig. 55 – PARKA Phase 2 Propagation Loss Kaneohe (C)

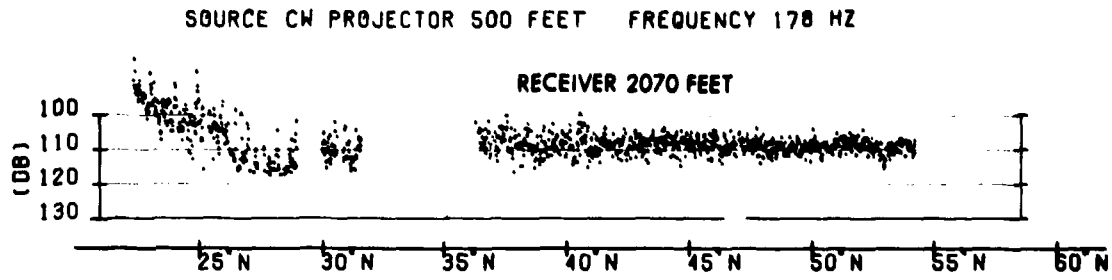

Fig. 56 – PARKA Phase 2 Propagation Loss Kaneohe (C)

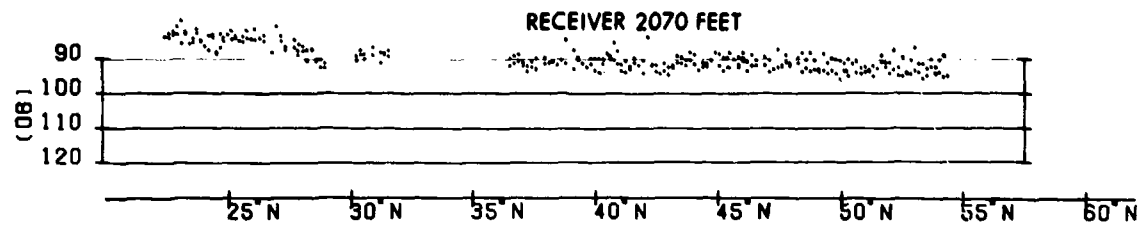

Fig. 57 – PARKA Phase 2 Propagation Loss Kaneohe (C)

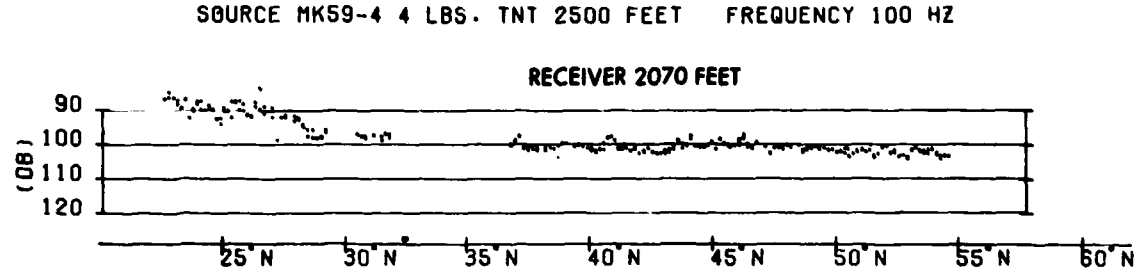

Fig. 58 – PARKA Phase 2 Propagation Loss Kaneohe (C)

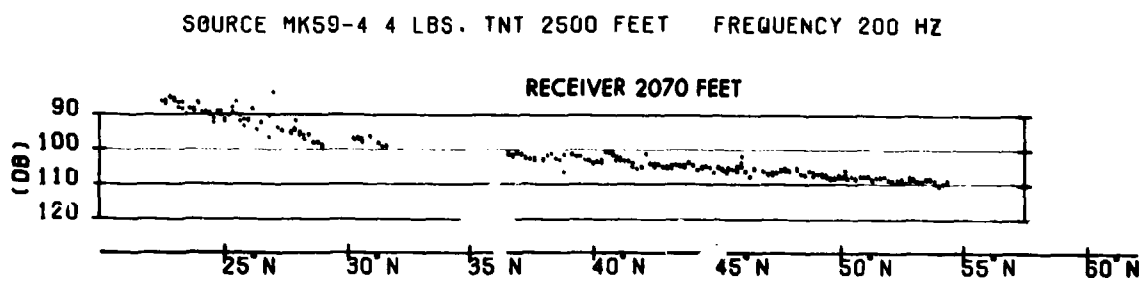

Fig. 59 – PARKA Phase 2 Propagation Loss Kaneohe (C)

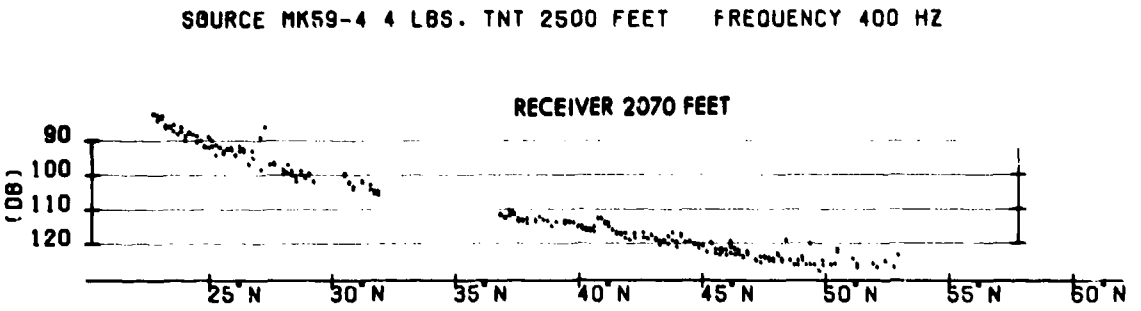

Fig. 60 – PARKA Phase 2 Propagation Loss Kaneohe (C)

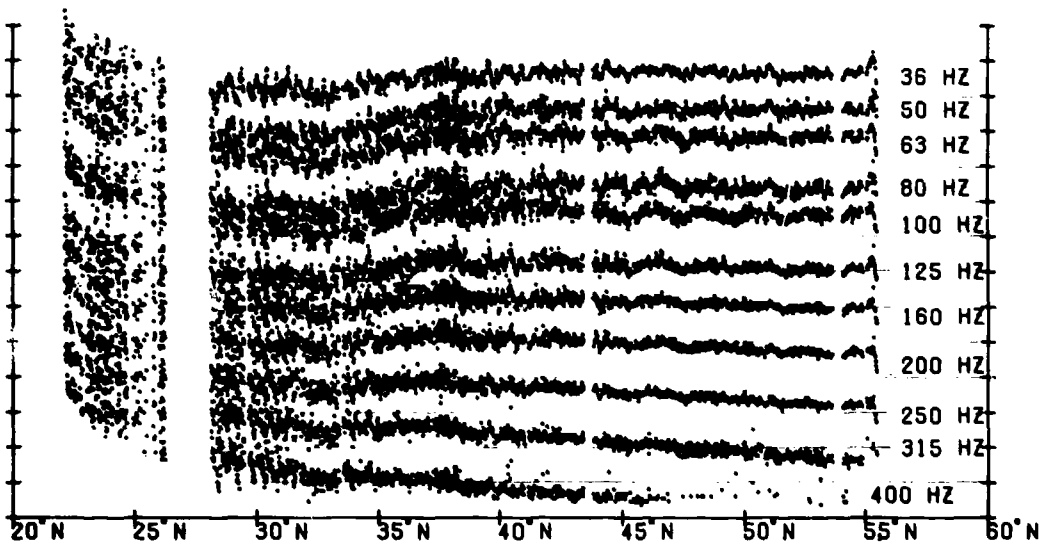

Fig. 61 – Propagation loss relative to 100 dB (1 division = 10 dB) (C)

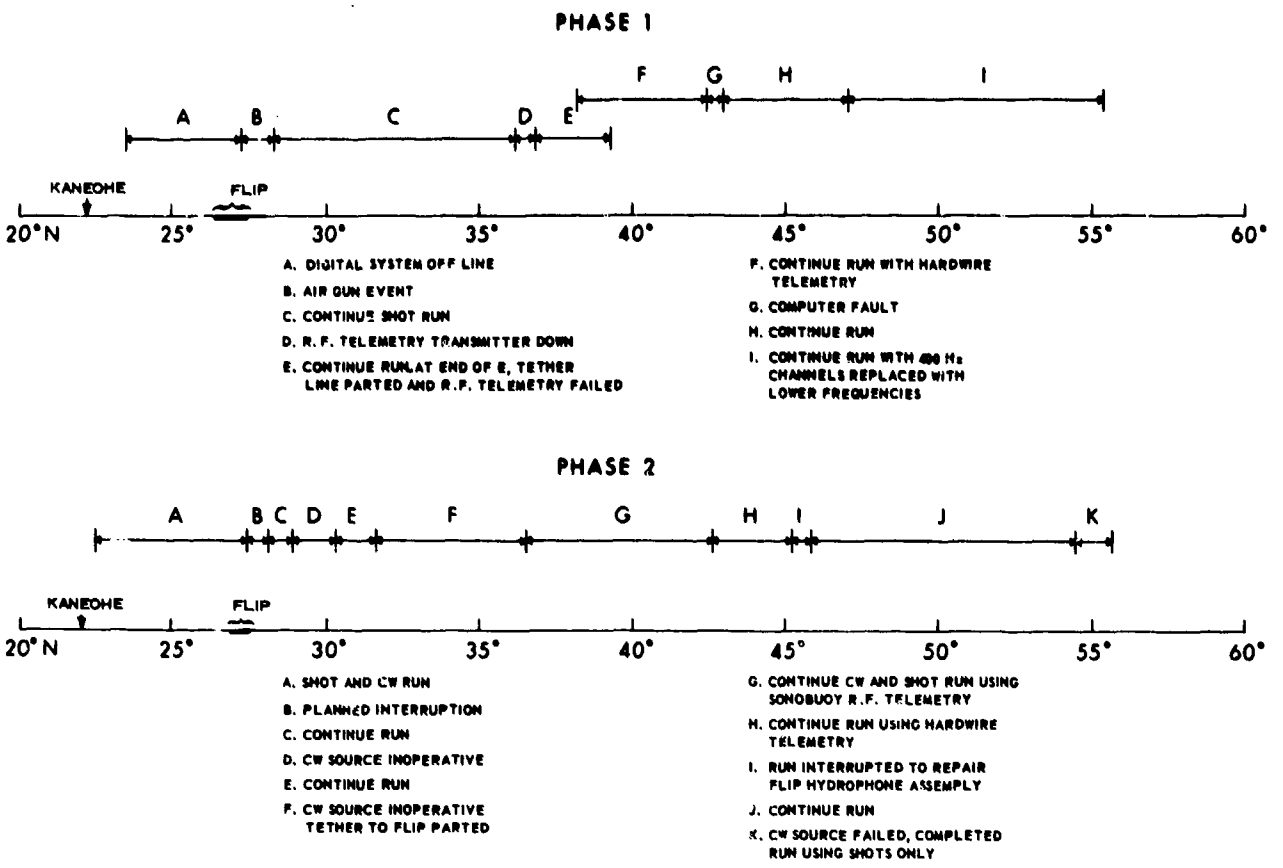

Fig. 62 – PARKA event log (C)

Discussion of Propagation Loss Results

(S) Certain salient features of the acoustic data which are of particular interest from the standpoint of surveillance systems design can be demonstrated by comparing propagation loss versus range in various combinations, as follows.

Effects of Hydrophone Depth and Location

(C) The effect of hydrophone depth depends on the source depth and on the environmental conditions along the acoustic path, as might be expected:

60 ft Source and FLIP

(C) Propagation from the shallow source was essentially identical, to the 300 ft and 2500 ft FLIP hydrophones, as seen in Fig. 63.

(C) Propagation from the shallow source is better to the deep (10,800 ft) FLIP hydrophone than to the one at the sound channel axis (2500 ft) by 3 to 5 dB over nearly the entire track, as shown in Fig. 64.

(C) The propagation loss to the deep hydrophone at 100 Hz is nearly constant over much of the range, increasing only about 4 dB (from 105 dB to 109 dB) between 200 and 1700 n.m.

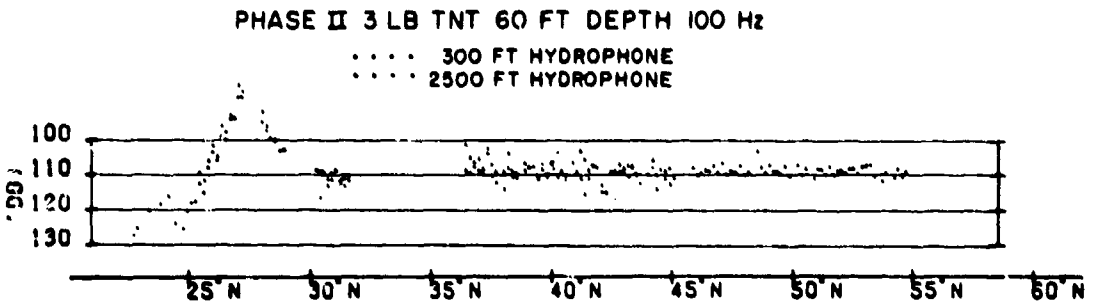

Figure 63 (C)

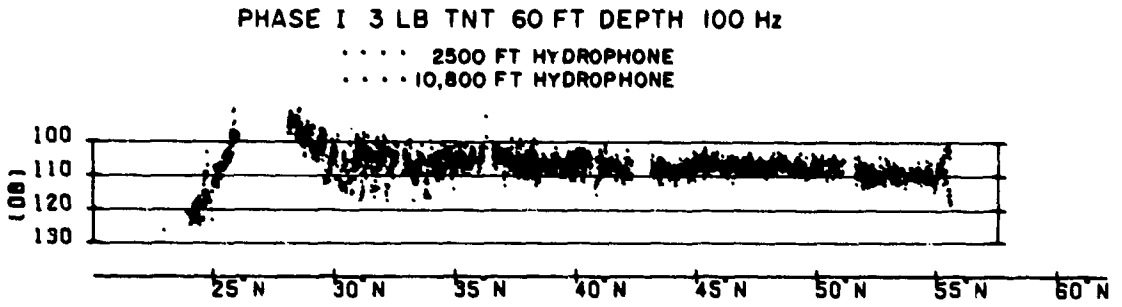

Figure 64 (C)

500 ft Source and FLIP

(C) With a 500 ft source, propagation to the 300 ft receiver was much poorer (by 5 dB) than to either the 2500 ft or 10,800 ft receiver over nearly all the range measured, Figs. 65 and 66.

(C) A comparison of propagation from the 500 ft source to the 2500 ft and 10,800 ft receivers, Fig. 67, shows a cross-over, the deeper unit having better reception at ranges out to about 500 n.m., and the shallower one having better reception at longer ranges, from 500 to 1700 n.m.

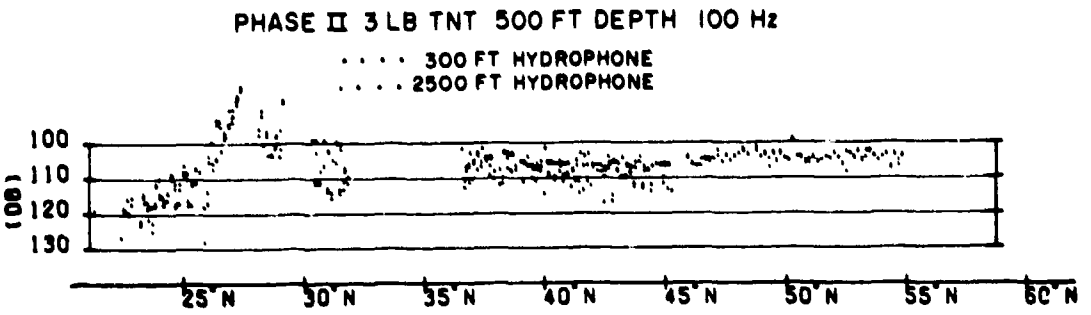

Figure 65 (C)

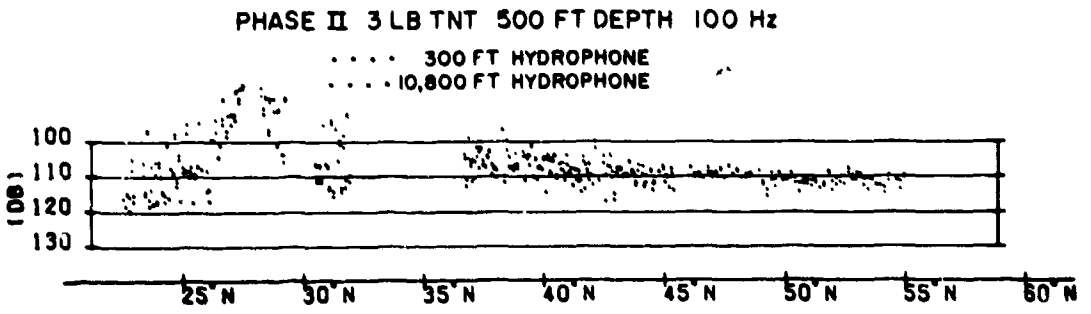

Figure 66 (C)

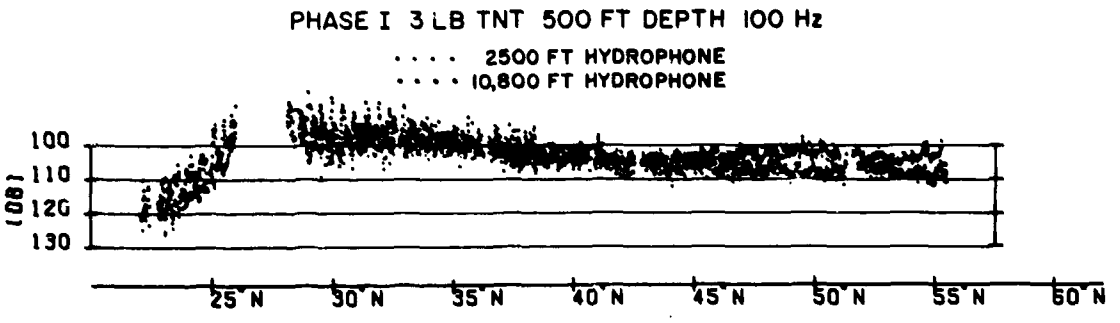

Figure 67 (C)

Kaneohe vs. FLIP, Long Range

(C) A comparison of propagation to one of the MILS units at Kaneohe with propagation to the 2500 ft FLIP hydrophone is shown in Fig. 68. Because of severe bottom-limiting close by, propagation to Kaneohe is much poorer than to FLIP at shorter ranges, i.e., to 45°N for the 60 ft source and to 37°N for the 500 ft source. However, at longer ranges to the end of the track at 55°N, the reception at Kaneohe is essentially identical to that at FLIP.

Kaneohe vs. FLIP, Inshore Track

(C) It is of interest to compare the reception at Kaneohe and at FLIP for sources on the portion of the track that lies between the two locations as shown in Fig. 69. For both depths of source, reception at the 2070 ft Kaneohe receiver and the 10,800 ft FLIP receiver is about the same, on the average, although the scatter is very large. Reception at the Kaneohe hydrophone and the 2500 ft FLIP hydrophone at about the same depth is quite different, on the average, the loss being greater at FLIP for a given propagation path length. This complicated behavior of propagation loss is undoubtedly due to the complicated bottom profile which lies completely above the bottom of the sound channel, and contains high obstructions. A change of a few miles in the position of FLIP relative to these features could change the propagation loss patterns markedly, and no other generalization should be drawn.

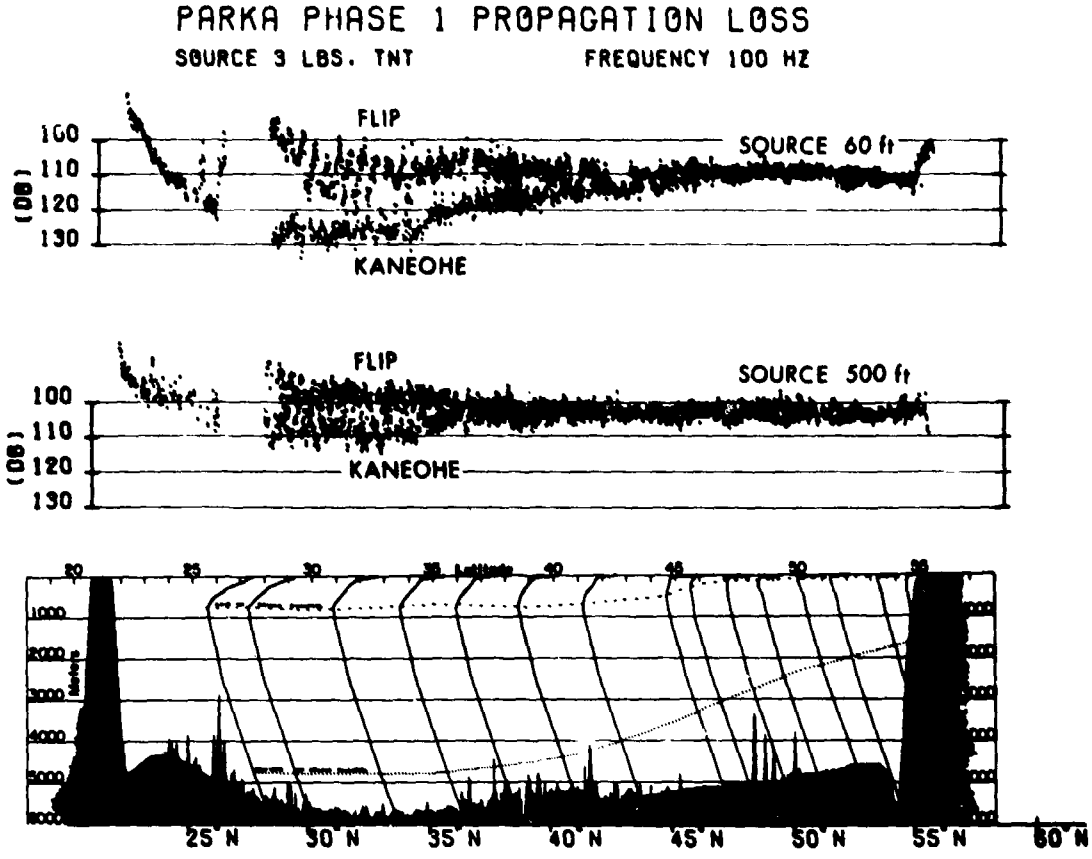

Fig. 68 — Comparison of FLIP and Kaneohe data with associated bathymetry (C)

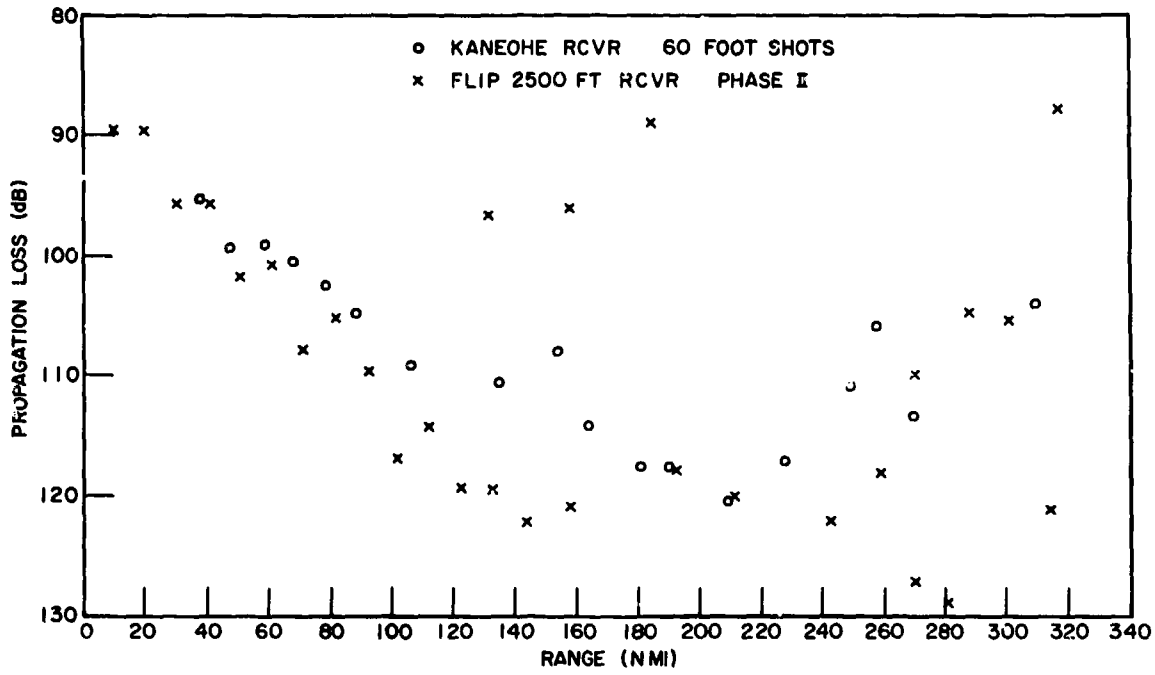

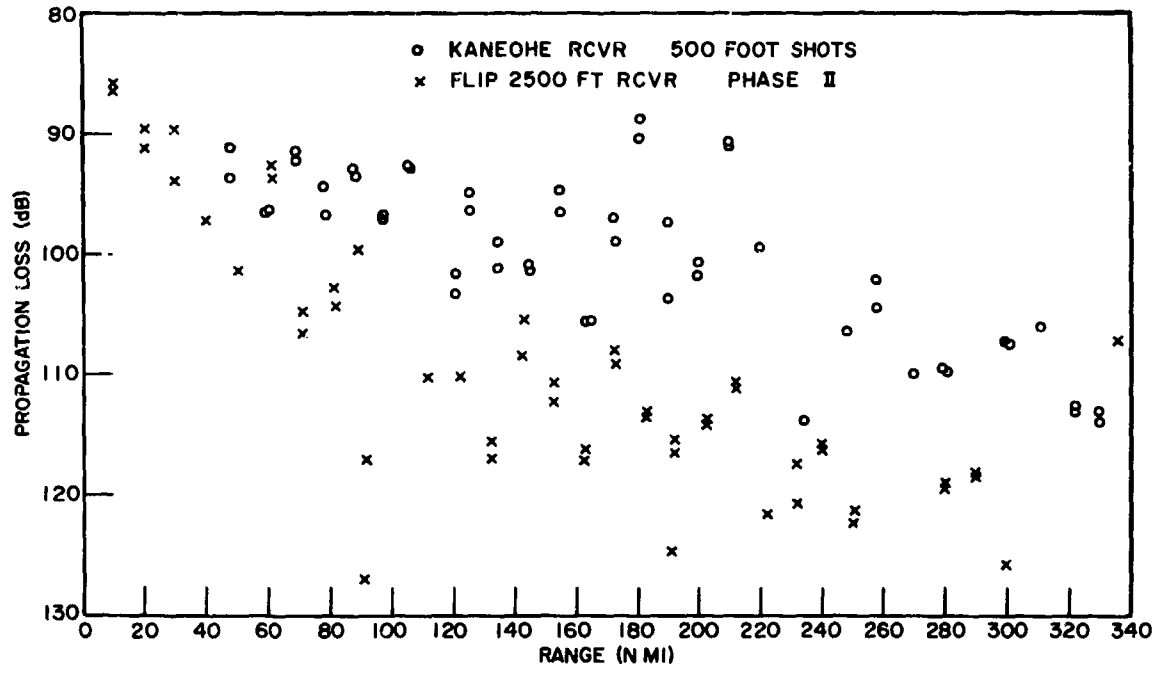

Fig. 69 — Comparison of propagation loss to FLIP and Kaneohe for source locations between the two (C)

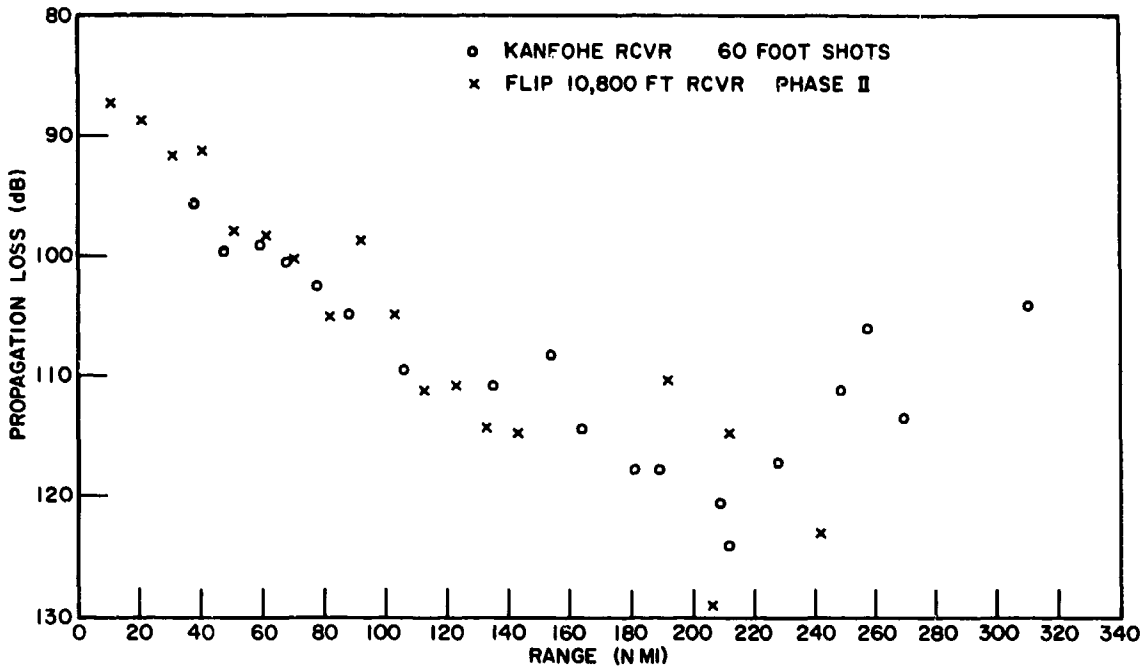

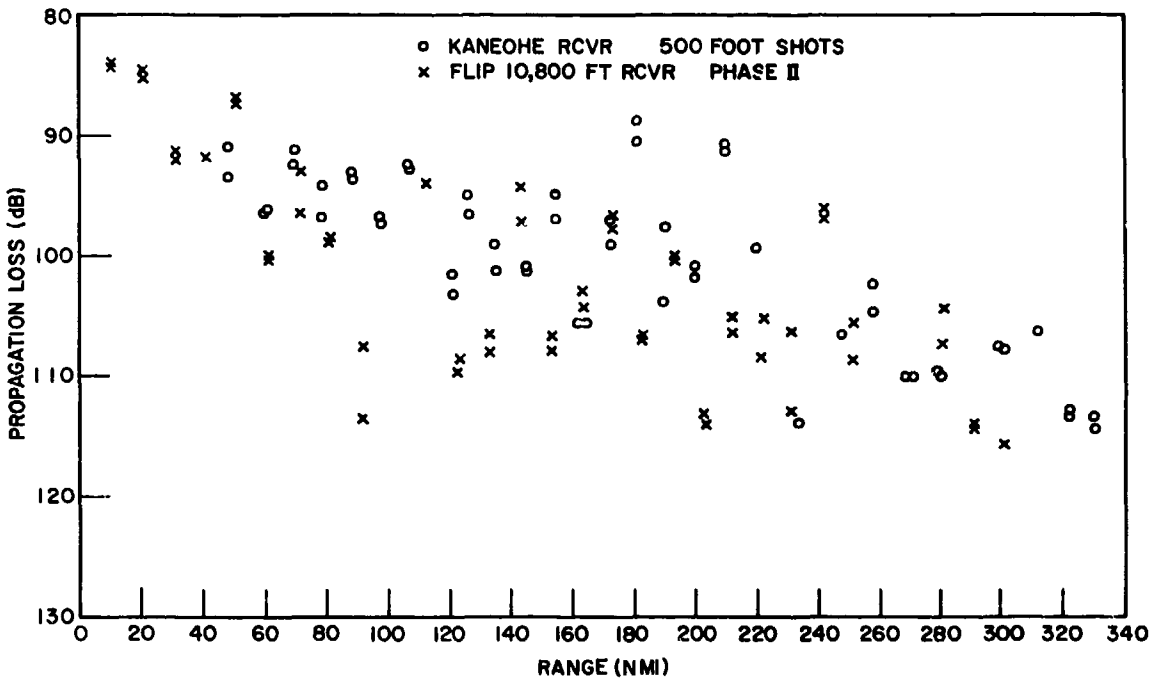

Fig. 69 (Continued) — Comparison of propagation loss to FLIP and Kaneohe for source locations between the two (C)

Effect of Source Depth

(C) Charges were detonated at each of three depths during the Phase 2 runs: 60 ft, 500 ft and 2500 ft. The first two are simulated target depths, and the third is sound-channel-axis depth in the region of FLIP and the southern end of the track. The 2500 ft charges were intended primarily for attenuation measurements.

60 ft vs. 500 ft Sources

(C) At the 300 ft FLIP hydrophone, the loss is the same for the 60 ft source and the 500 ft source; this is shown in Fig. 70.

(C) A comparison of propagation loss from the 60 ft and 500 ft sources to the 2500 ft and 10,800 ft FLIP hydrophones is seen in Fig. 71. At the 2500 ft receiver, the loss for a 60 ft source is 5 to 10 dB greater than for a 500 ft source over nearly all of the track (except within perhaps 50 miles of FLIP). At the 10,800 ft receiver, the loss for the 60 ft source is also 5 to 10 dB greater at ranges out to about 600 n.m., and then becomes identical for the two sources at the longer ranges.

(C) For all three receiver depths, then, reception from the shallow source was generally much inferior to that from the deep one, and at best was equal.

(C) The difference due to source depth is even more pronounced at the Kaneohe hydrophones as seen in Fig. 72. There the reception from the shallow source was as much as 20 dB poorer over the bottom-limited propagation range from about 200 n.m. to 700 n.m. The difference then decreased gradually with increasing range as the rising sound channel axis and decreasing surface temperature acted to reduce the interaction of the propagation energy with the bottom. For the last 600 n.m., the difference in propagation loss for the two source depths at 200 Hz was insignificant. At 100 Hz there was a difference of approximately 5 dB between the two source depths which could be attributed to the effect of the surface on the source pattern at this frequency.

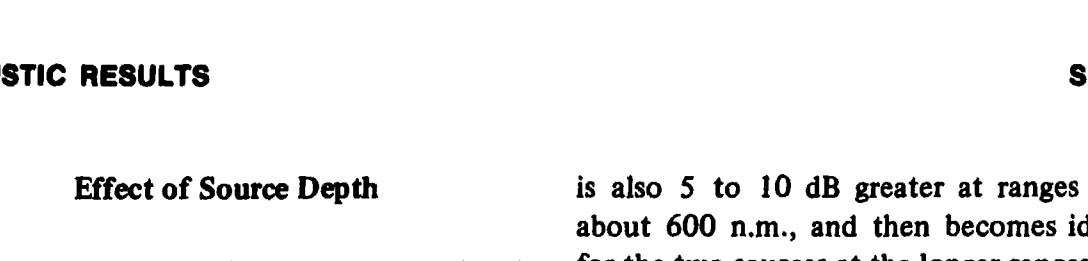

Figure 70 (C)

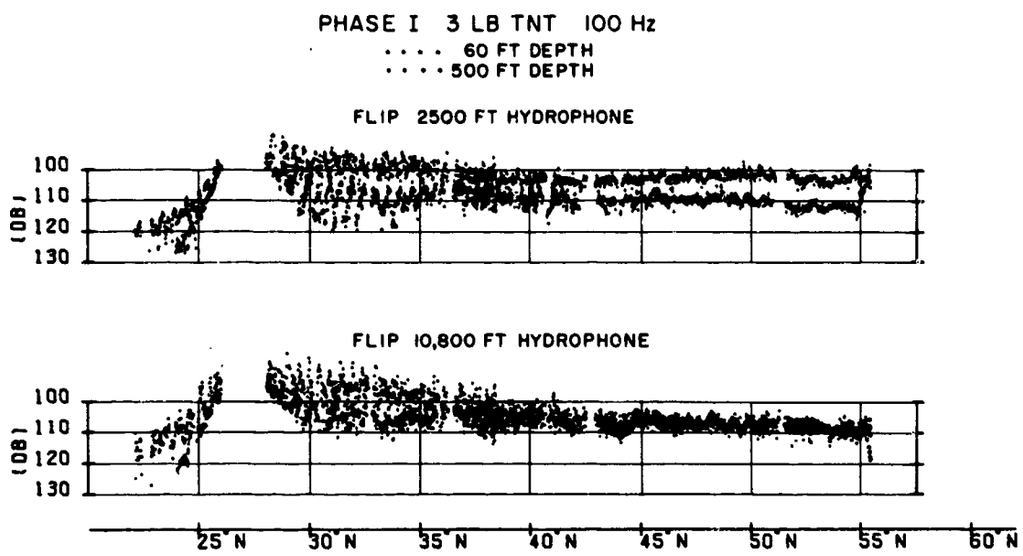

Figure 71 (C)

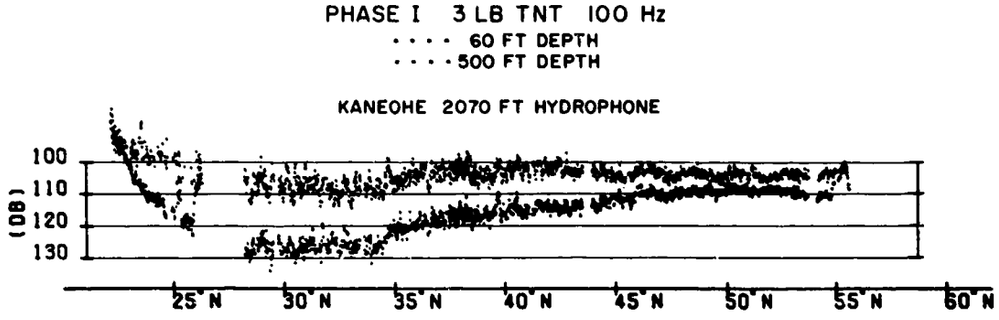

Figure 72 (C)

2500 ft Source vs. 60 ft and 500 ft Sources

(C) For the track north of FLIP, the results at the 300 ft hydrophone were essentially the same for all three depths of source charge (60, 500 and 2500 ft) as may be seen in Figs. 70 and 73. The same is generally true of the 10,800 ft hydrophone (Figs. 71 and 73).

(C) At the 2500 ft sound-channel axis receiver, however, propagation was generally best from the 2500 ft charge, as would be expected. It ranged from 20 dB to 7 dB better than from the 60 ft source over the range 200-1700 n.m., and from 10 to 0 dB better than the 500 ft source over the same range. The differences decrease with increasing range as the sound-channel axis rises above the depth of the 2500 ft charge and its source coupling to the sound channel becomes weaker.

(C) Propagation from the 2500 ft source to the 2500 ft FLIP receiver decreased only slightly with range over the part of the track from FLIP to 22°N, since it is primarily sound channel propagation for this configuration.

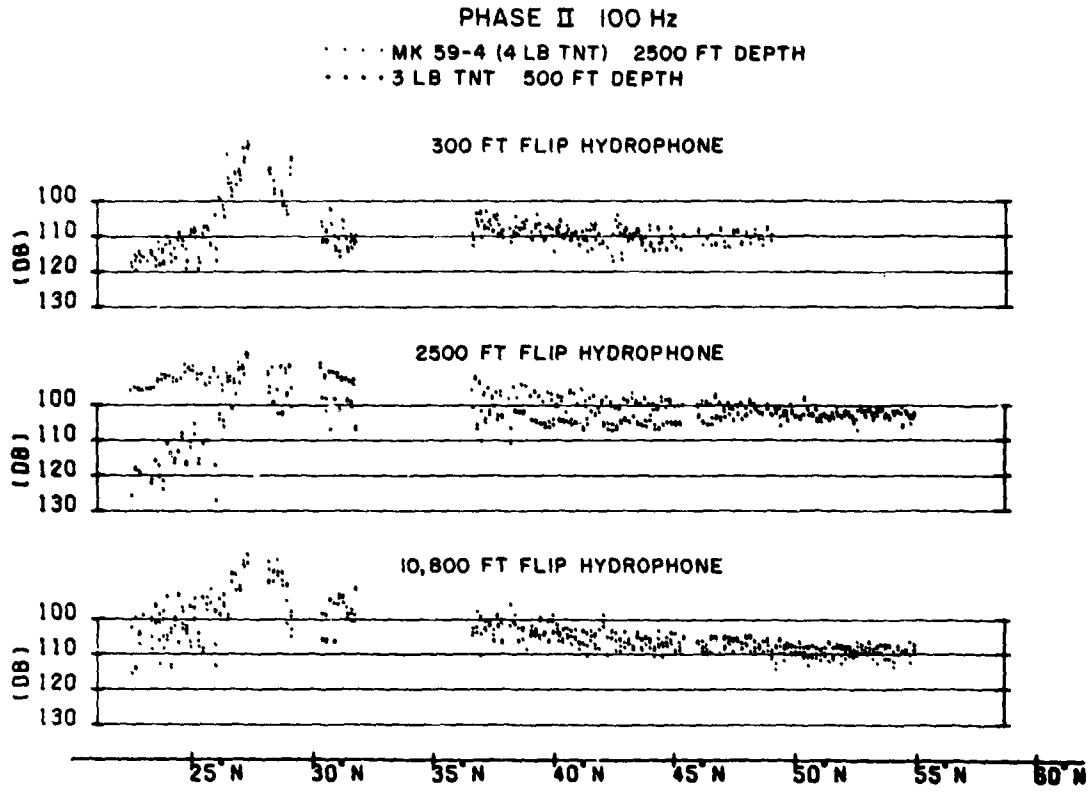

Figure 73 (C)

Comparison of Phase 1 and Phase 2 Results

(C) The results of the Phase 1 and Phase 2 measurements of propagation loss vs. range were identical within differences which might have been due to drift of FLIP during the two Phases. An example of the repeatability is seen in Fig. 74, in which the 100 Hz results of the 60 ft charge tests on two FLIP hydrophones for each Phase can be compared. Another example is given in Fig. 75 which shows the results of the 500 ft charge tests on the same hydrophones.

(C) While the data from Phase 2 are too sparse to allow highly detailed comparisons, the fact that the averages agree so well in general implies that the changes occurring in the ocean over a period of two or three weeks (the amount and nature of which may be seen in Fig. 76), did not greatly affect the acoustic results.

(C) The Kaneohe hydrophone, unlike the FLIP/SANDS receivers, remained fixed in location for the total duration of PARKA I. Comparison of the Phase 1 and 2 data indicate a much better detailed agreement at the Kaneohe location for the two phases than at FLIP/SANDS. Table II summarizes the comparison of Phase 1 and 2 data at Kaneohe.

Effects of Frequency

(C) In general, data received at FLIP exhibited increased propagation loss with increase in frequency. For example, the 200 Hz data show slightly greater propagation loss than the 100 Hz results, exhibiting about 3-5 dB more loss for a range of about 1600 n.m. For both the 60 and 500 ft sources, the propagation loss

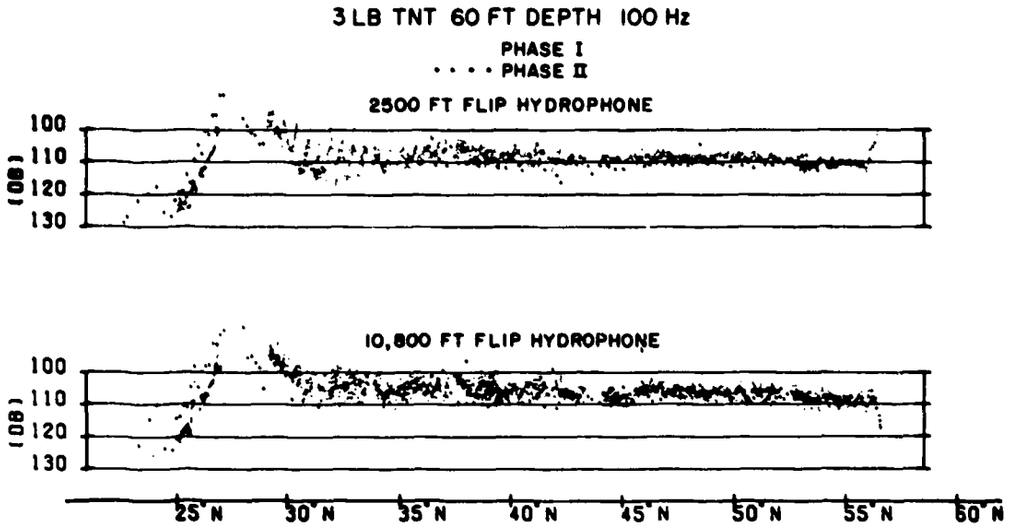

Figure 74 (C)

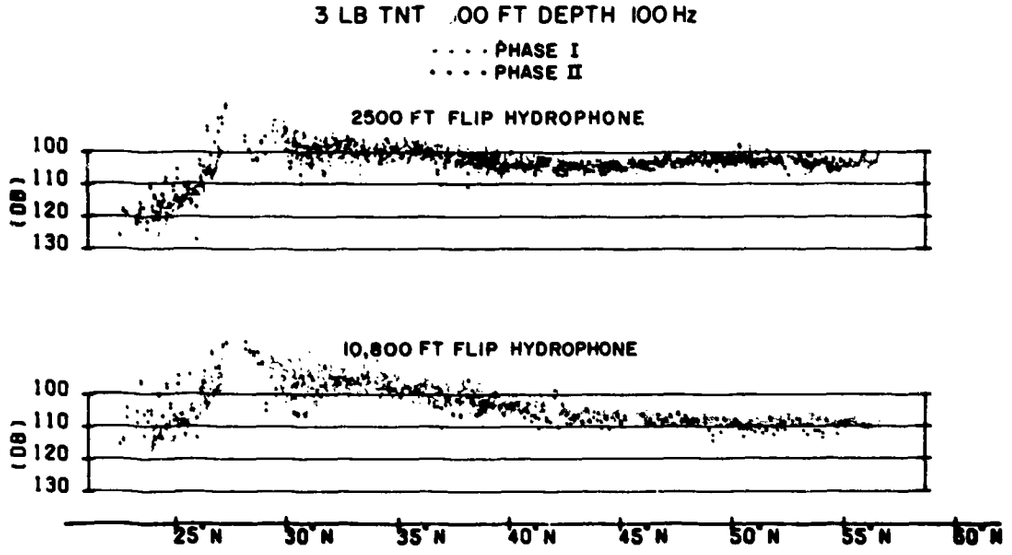

Figure 75 (C)

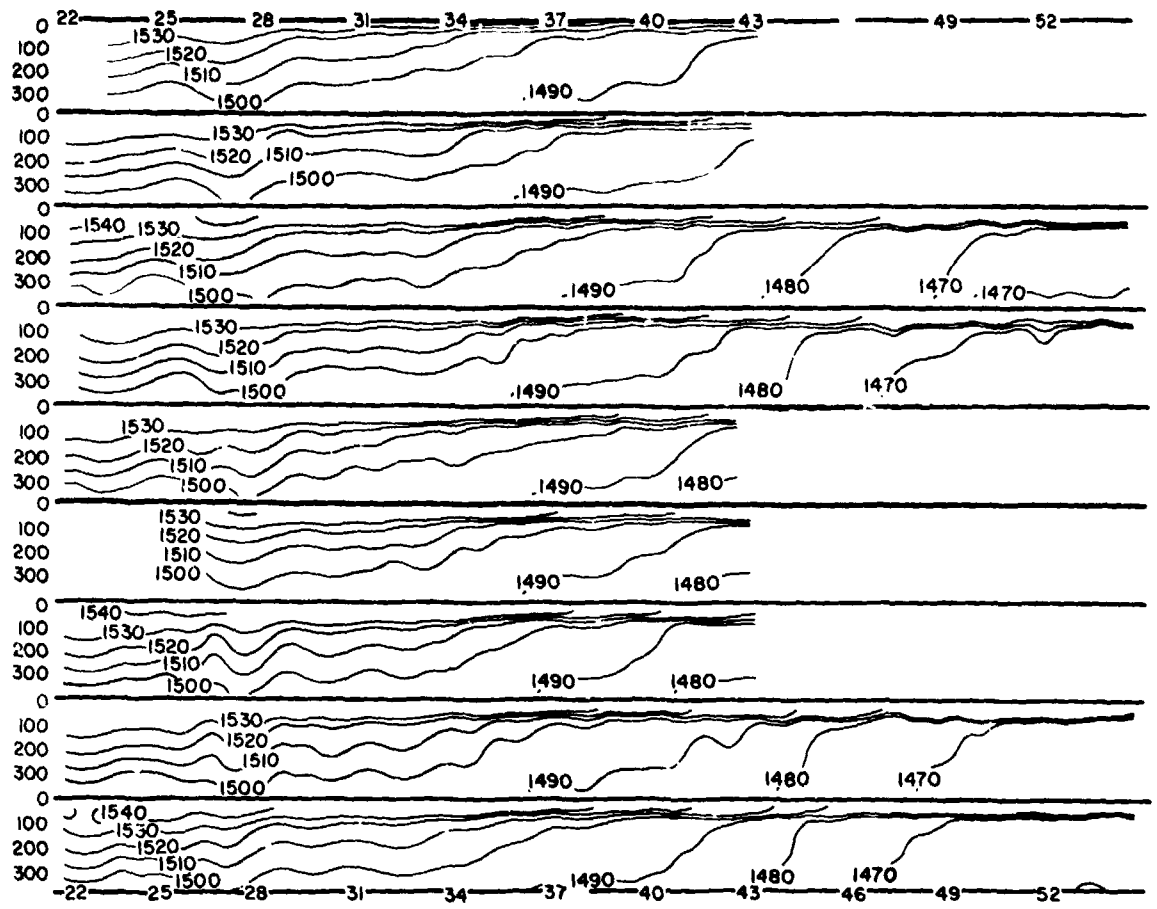

Fig. 76 – Sound velocity (m/sec) time series of synoptic AXBT sections (depth (m) vs latitude) (C)

at 45°N was about 15 dB more at 400 Hz than at 100 Hz at both the 2500 and 10,800 ft hydrophones.

(C) An exception is the 31 Hz data which displayed more propagation loss than the 100 Hz data. For any given source depth, the propagation loss difference is essentially constant with range. The difference for the 500 ft source is about 4 dB and the difference for the 60 ft source is about 9 dB. These differences are typical of both phases and all hydrophone depths. This apparent anomalous behavior agrees very well with what could result from a dipole radiation pattern from the source as discussed in the section on source levels (p. 34).

(C) Propagation loss as a function of frequency was obtained for the Kaneohe site in contiguous 1/3 octave bands centered at frequencies from 36 Hz to 400 Hz and in an octave band centered at 36 Hz. These data are shown in Fig. 61 for the 500 ft explosive source plotted versus latitude of the source ship.

(C) At 100 Hz and below, there are no apparent differences between the curves. Above 100 Hz, the curves diverge and exhibit prominent slopes at the longer range. Assuming a ray propagation model above 100 Hz that is invariant with frequency, and assuming that the energy is not bottom-limited at long range nor suffers any frequency dependent surface

Table II
Propagation Loss Summary Comparison – Phases 1 and 2

Frequency (Hz)	Source Depth (ft)	Comparison Phase 1 vs. Phase 2
31	60	identical
100	60	identical
200	60	identical
400	60	identical to 27°. Phase 2 data has about 3 db less loss at greater ranges, however, data are sparse.
31	500	identical
100	500	identical
200	500	identical
400	500	identical except at long range where Phase 1 S/N editing biases data slightly.

loss, one can interpret the divergence in the curves as attenuation in the medium. Table III shows the difference in the propagation loss between 100 Hz and higher frequencies measured at the greatest range and compared with expected differences calculated using published attenuation coefficients (Thorp 1967). The 400 Hz differential was measured at 44°N and corrected to 55°N. Such assumptions result in an attenuation curve in this frequency range having a slope significantly less than previously reported.

Table III
Attenuation Differential Between 100 Hz and the Frequency Indicated

Frequency (Hz)	Differential Loss at 55°N (db)	Expected Differential db (Thorp)
125	5	2.4
150	6	7.0
200	9	12.8
250	13	22.0
315	20	35.6
400	28	57.6

SUS Charge Studies

(C) In addition to charges detonated at 60 and 500 ft, SUS MK 59 Mod 4 charges were used during Phase 2 and were detonated at 2500 ft over the total length of the PARKA track. The principal purpose for using the SUS charges was to obtain information for studying attenuation by the method of Thorp (1967). These studies are underway and will be reported later. Nevertheless, some cursory observations can be made.

Propagation Loss

(C) Following the general trend with depth exhibited by the 60- and 500-ft charges, the propagation loss from the 2500-ft SUS charges to the hydrophones at Kaneohe and FLIP are essentially identical.

(C) For approximately the first half of the run, the SUS charge detonates on the axis of the SOFAR channel and there was less propagation loss to the 2500-ft hydrophone at FLIP than that experienced by the 500-ft charge. At the higher latitudes, the minimum sound velocity axis rises, and losses from the 2500- and 500-ft charges become comparable.

Signal Characteristics

(U) The oscillograms of Fig. 77 and graphical recordings of Fig. 78 illustrate received signal characteristics as a function of range from FLIP; the latitudes of the shots are keyed on the oceanographic chart at the bottom of the figure. Note the increase in the multipaths with distance from FLIP and the gradual metamorphosis to a fully developed SOFAR arrival as shown resulting from the sound channel axis rising up to the source depth as the ship proceeded north.

Comparison of Projector and Charge Results

(C) It is of particular interest to compare the results of measurements made with the two very different types of sound sources that were used, the explosive charges and the towed CW projector. While a direct comparison at the same frequency is not possible, since no suitable 178 Hz filter was provided for the charge measurements, comparison can be made between the projector tests at 178 Hz and the charge tests at 100 Hz and 200 Hz. One example is shown in Fig. 79. The average for the projector data at 178 Hz lies below that for the charges at 100 Hz, and lies above and close to that for the charges at 200 Hz. This would be expected on the basis of the increase in attenuation with increasing frequency, and indicates a satisfactory agreement between results of the two types of sources.

(C) A noteworthy point is the wider scatter of data with the projector than with the charges. This is presumably due to the influence of changing multipath phasing interferences on the instantaneous levels of the CW signals received as the source moves and as the characteristics of the water path fluctuate with time.

Ambient Noise

Results

(C) Figure 80 presents representative values of ambient noise level obtained at Kaneohe and FLIP during Phases 1 and 2. Figs. 81-85 present data representative of effects which will be discussed below. Noise data were obtained during PARKA I at each frequency that was investigated for propagation loss. On SANDS, samples were obtained from FLIP once an hour at each frequency and hydrophone depth; at Kaneohe the noise was sampled after each shot arrival. In each case a particular sample was obtained by squaring and integrating the background noise for a 15-second period.

Discussion of Ambient Noise Results

(C) The noise at Kaneohe was reasonably uniform during the total period of the experiment. Figure 81 is typical of the results obtained at Kaneohe. These data were processed from magnetic tape and the portion of the curves to the left of 28°N represents tape noise from the low gain channels. This channel was used during the early portion of the propagation run because of the high signal levels received from the acoustic sources at close ranges. The remainder of the curve was obtained from the high gain channel and represents environmental background noise. The small variations exhibited are characteristic of results for all frequencies above 100 Hz. The degree of variability was slightly greater at lower frequencies. Spectrum levels above 200 Hz are not reported because tape noise at these frequencies appears to be the dominant noise source.

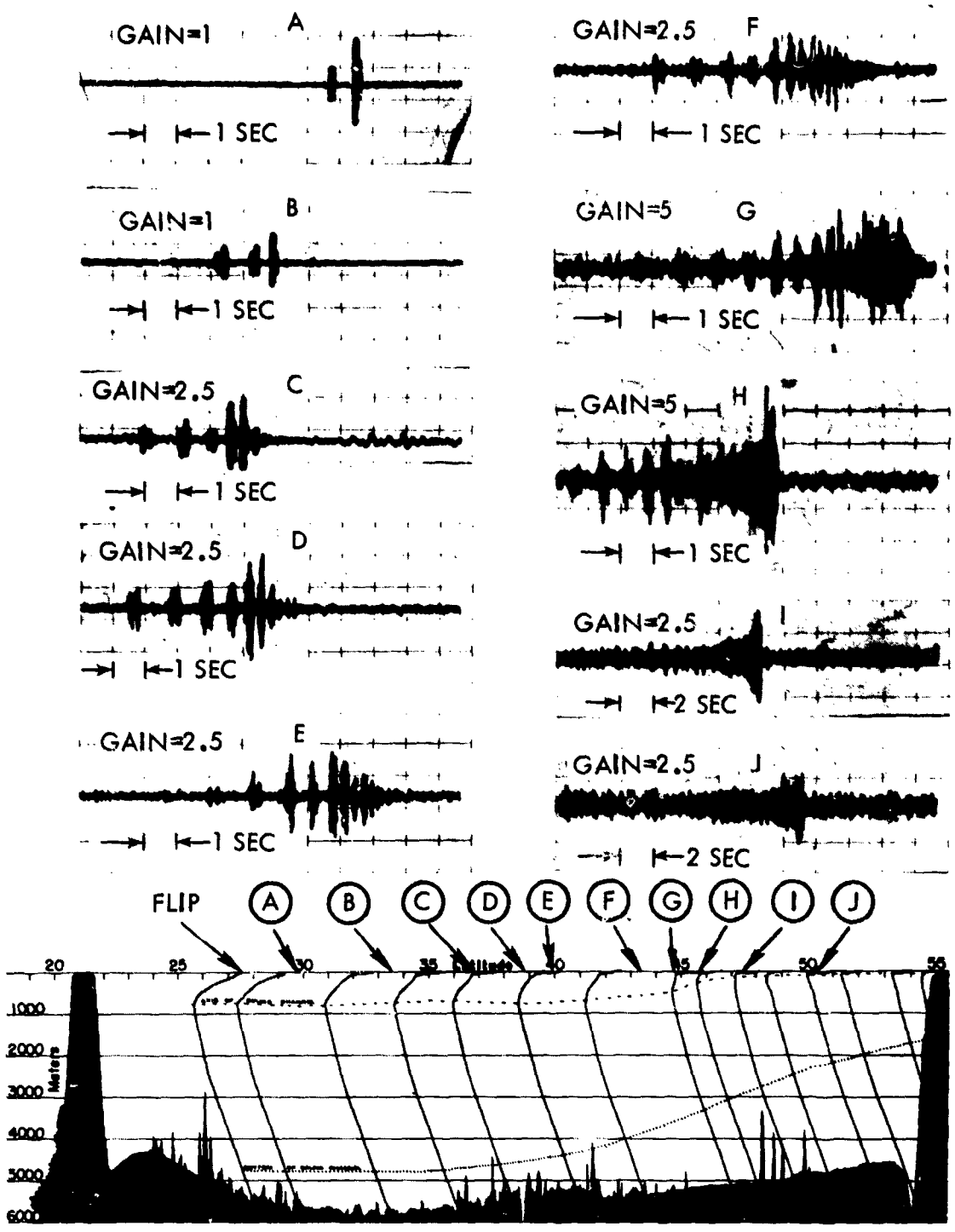

Fig. 77 – Received pulse shapes: source – 3 lb TNT; 500 ft; receiver – 2500 ft (C)

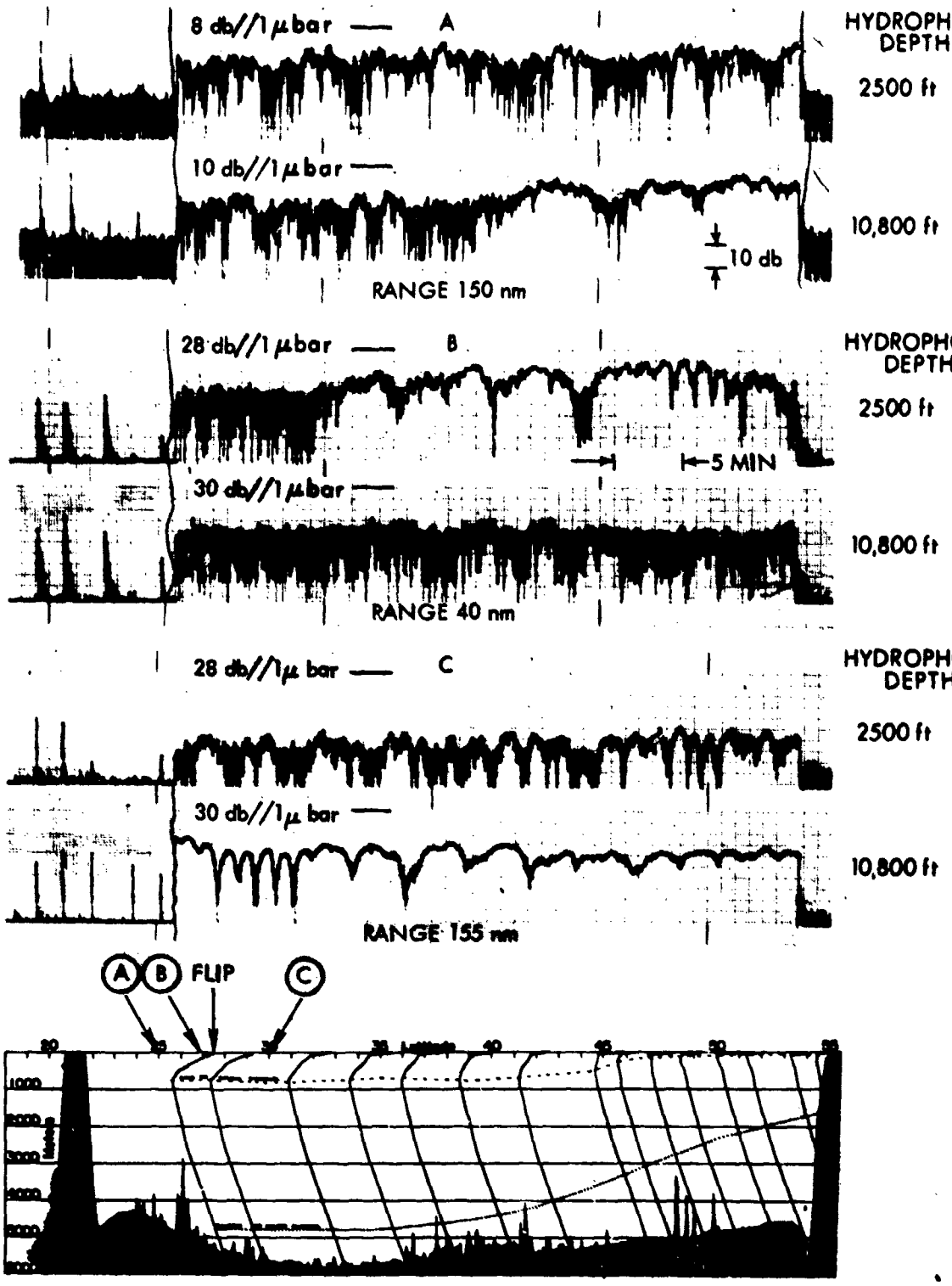

Fig. 78 — Recordings of 178 Hz CW signal level vs. time (C)

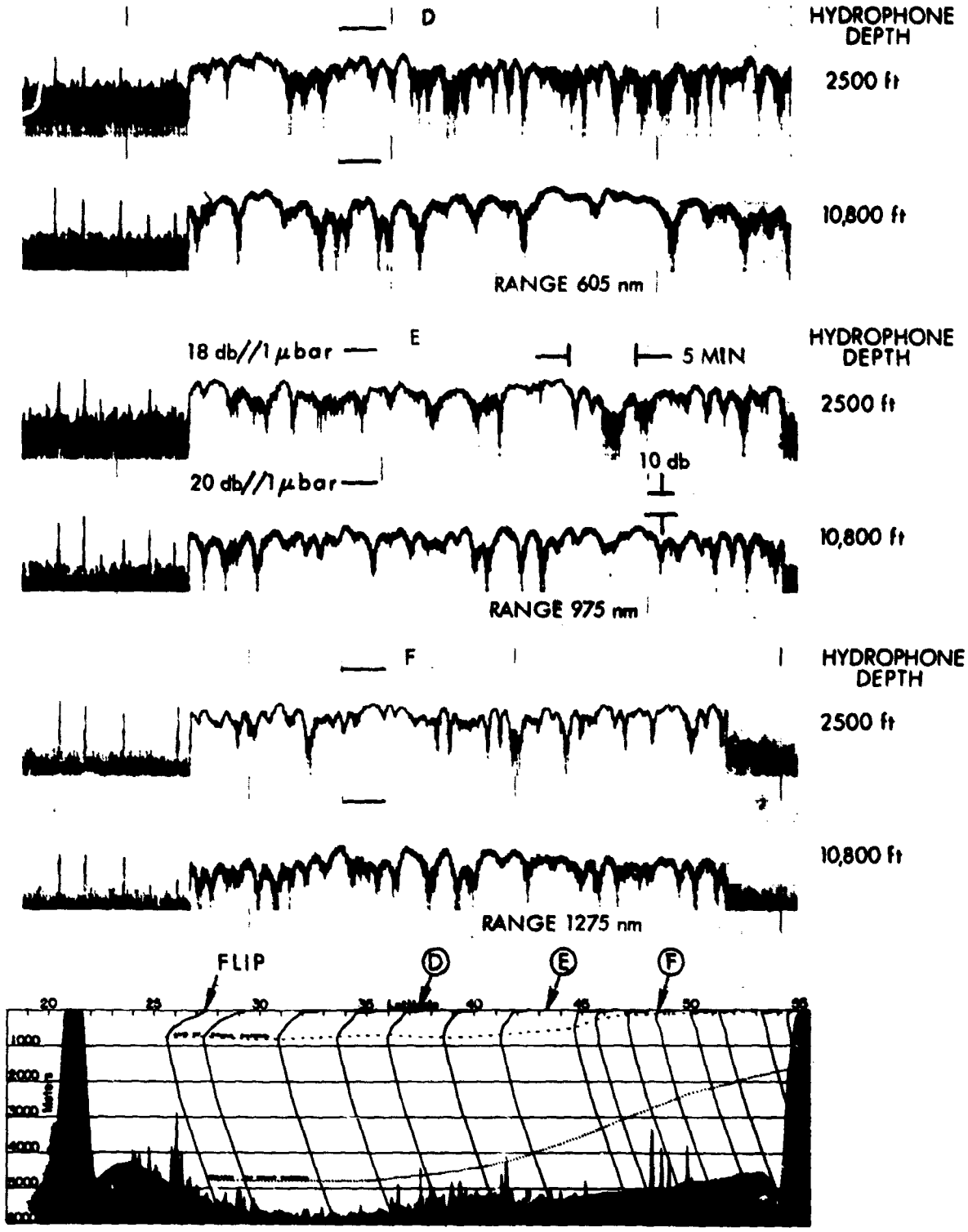

Fig. 78 (Continued) – Recordings of 178 Hz CW signal level vs. time (C)

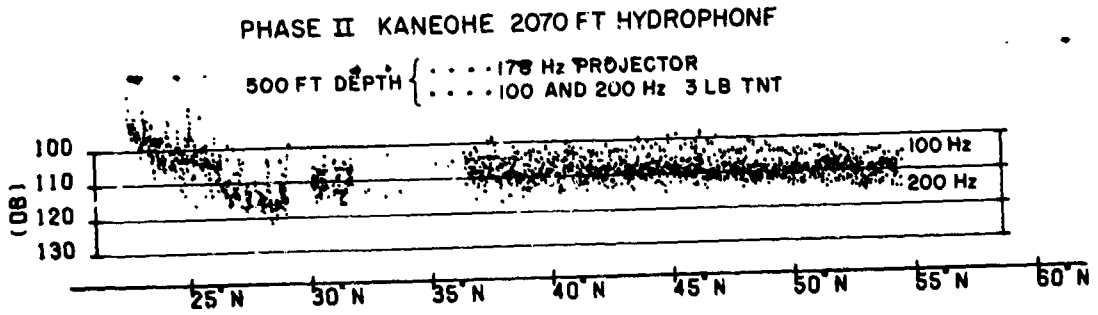

Fig. 79 – Comparison of projector and shot data (C)

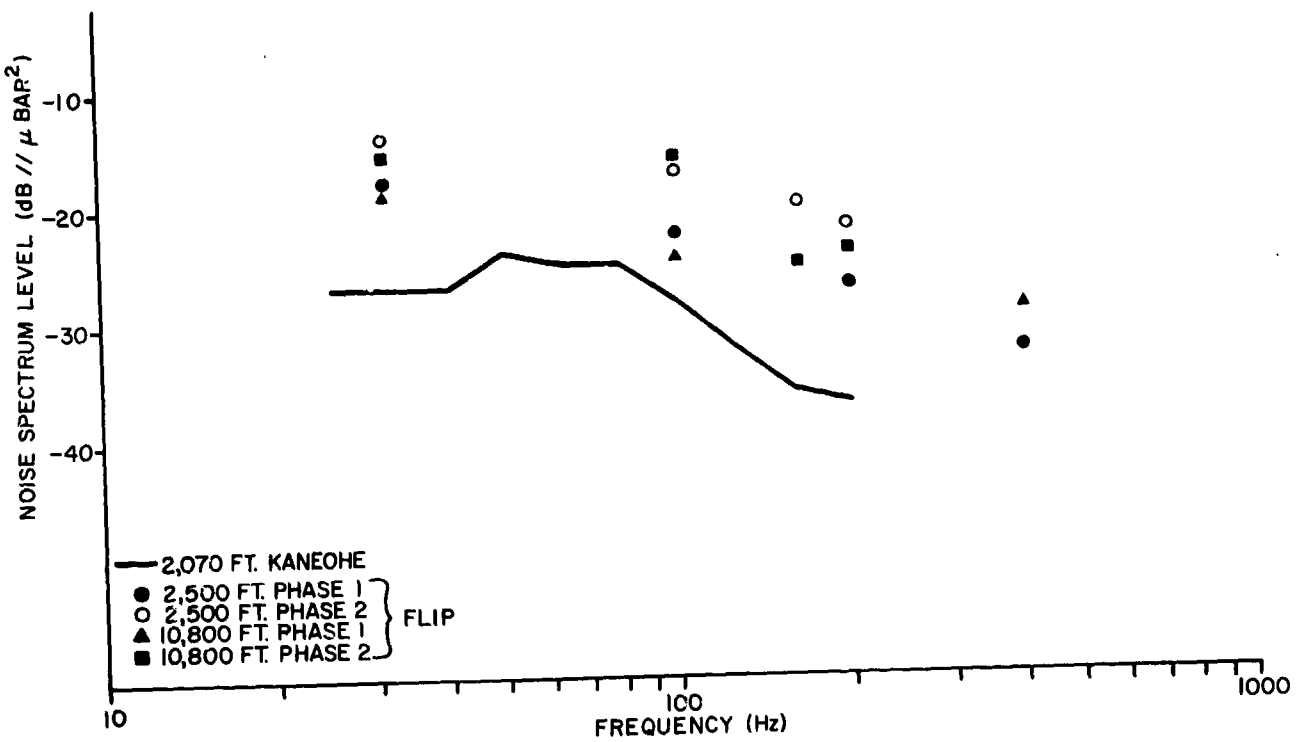

Fig. 80 – Noise spectrum level: noise levels measured at Kaneohe represent ambient sea noise. Those measured at FLIP may include the effects of some flow noise, vibration, or ship noise in addition. (C)

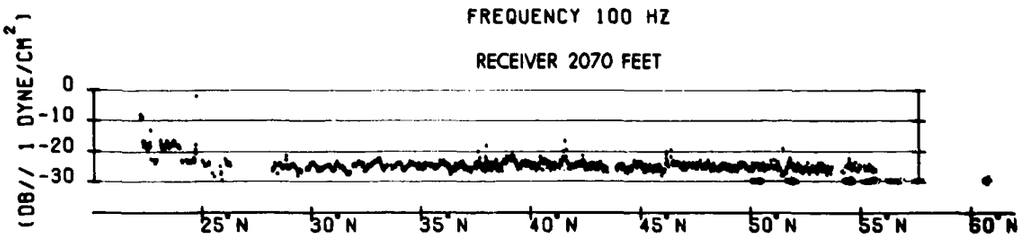

Fig. 81 – PARKA Phase 1 Noise Spectrum Level Kaneohe (C)

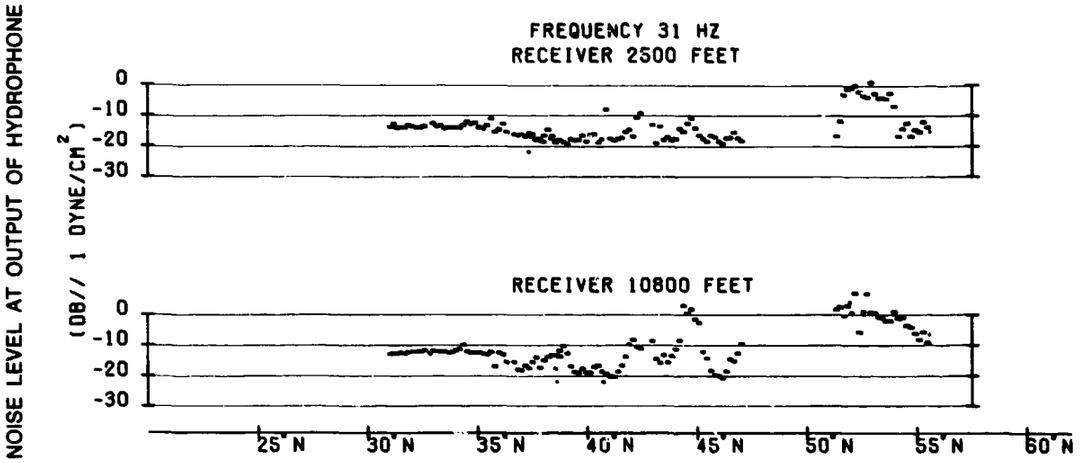

Fig. 82 – PARKA Phase 1 Noise Spectrum Level (C)

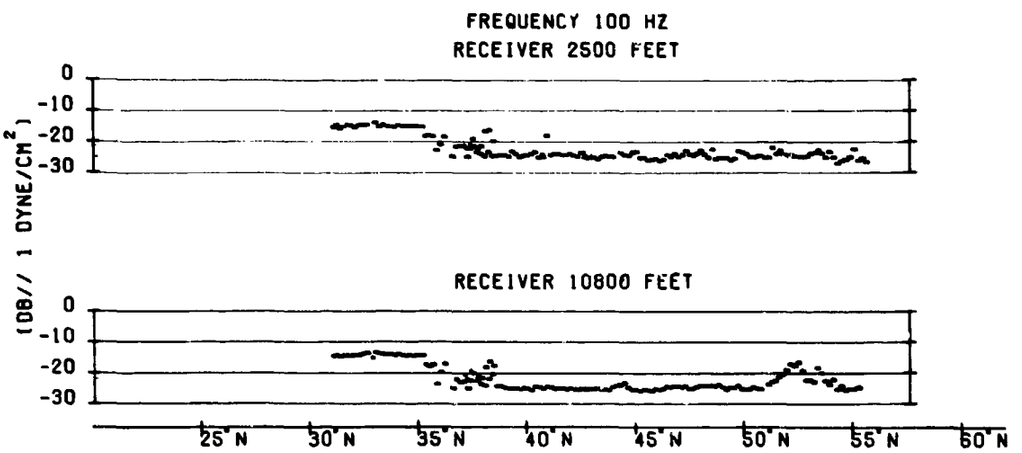

Fig. 83 – PARKA Phase 1 Noise Spectrum Level (C)

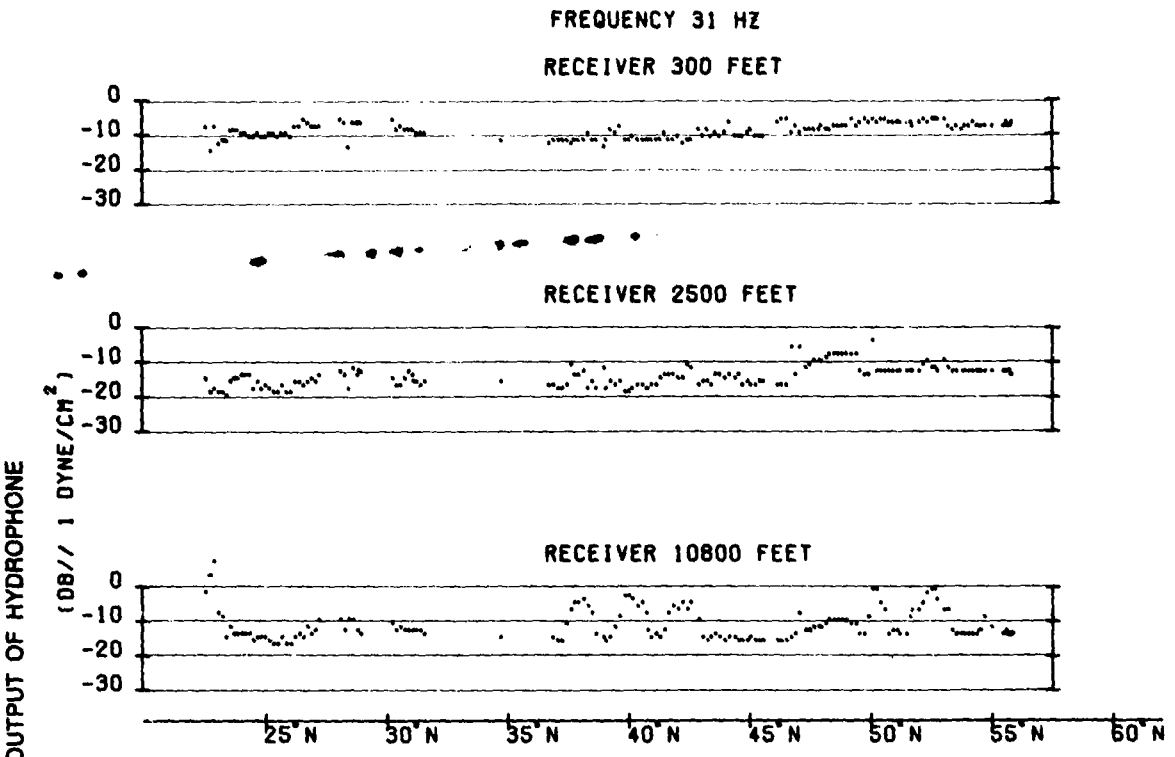

Fig. 84 – PARKA Phase 2 Noise Spectrum Level (C)

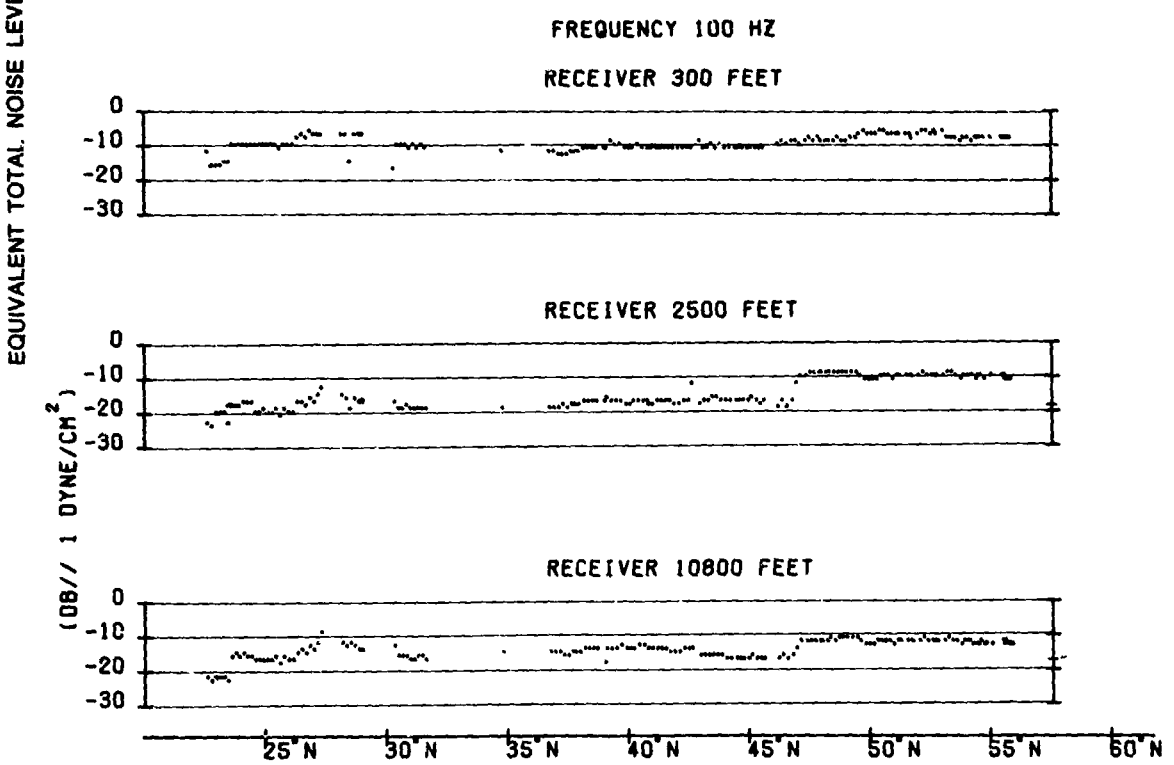

Fig. 85 – PARKA Phase 2 Noise Spectrum Level (C)

(C) The noise at FLIP/SANDS was not as uniform as at Kaneohe. Figures 82 and 83 are representative of the background noise environment for Phase 1 at FLIP. The 100 Hz curve is similar to those of the background noise observed at 200 Hz and 400 Hz. The early portion of these curves represents system noise occurring with the low gain settings when the received levels of the signals were high. To the right of 35°N the system gain was 20 dB greater and ambient sea noise was the dominant noise source. The cause of the strong fluctuations exhibited at 31 Hz during this period was not determined. Array vibration is suspected as the major cause of this 31 Hz noise. FLIP was tethered to SANDS for most of the PARKA I experiment with strong forces acting on FLIP because of local currents. The array on FLIP was characteristically tilted from the vertical in excess of 5°. Several tests with SANDS operating in various machinery modes (bow thruster on, main engines on, all propulsion secured, etc.) indicated that any resulting radiated noise had little influence on the background noise. Near the end of Phase 1, fluctuations became more intense and dominated the 100 Hz data on the 10,800 ft hydrophone. The noise results at the 2500 ft hydrophone for 100 Hz and 200 Hz did not exhibit these fluctuations at any time. A gap appears in the 31 Hz curve around 50°N due to channel modifications in the instrumentation system during the experiment.

(C) Figures 84 and 85 are 31 Hz and 100 Hz noise curves for FLIP hydrophones for Phase 2. A hardwire telemetry link was used at the start of Phase 2 up to 32°N at which time the experiment was interrupted. When the source ship was at 36°N the event continued with a sonobuoy transmitter providing the telemetry link. While the sonobuoy transmitter was in use, the 31 Hz data exhibited wide fluctuations on the 10,800-foot hydrophone while the shallower phones and the 100 Hz data on the 10,800-foot hydrophone did not appear to be affected.

(S) At 178 Hz (1 Hz bandwidth filter) and 200 Hz (not shown) the noise level increased on all hydrophones during this period but did not fluctuate. The hardwire telemetry link was again used from about 43°N to the end of the experiment. During this period, the noise exhibited little variability at first but at 46°N, the level began to rise appreciably at all frequencies on the 2500 and 10,800 ft hydrophones. At this same time, strong line components were observed on the low frequency spectrum analyzer (LOFAR display). It was determined that this latter effect was due to oscillations in the hydrophone electronics but the cause could not be localized.

(C) The summary results shown in Fig. 80 were determined from observations made during periods when the noise exhibited stable minimum levels. These corresponded to data at 40°N during Phase 1 and at 45°N during Phase 2. Where comparison between Phase 1 and Phase 2 can be made, it is noted that the Phase 2 noise levels are higher. The Phase 1 data agree favorably with results obtained at Kaneohe. While the minimum levels may actually represent ambient sea noise, free from cable strumming, flow noise and nearby ship noise, it is not certain that this is the case, and the results should not be so interpreted.

Bibliography

(U) Christian, Ermine A., Source Levels for Deep Underwater Explosions, J. Acoust. Soc. Am., Vol. 42, No. 4, 905, Oct. 1967.

(U) Thorp, William H., Analytic Description of the Low Frequency Attenuation Coefficient, J. Acoust. Soc. Am., Vol. 42, No. 1, 270, July 1967.

(U) Weston, David E., Proceedings Physical Society, LXXVI, 2, pp. 233-249, 1960.

Introduction

(U) The comparisons now available are shown in Figs. 86 through 90 in which the measured losses (red dots) are overprinted on the computed loss plots from pp. 30-33. The scale of presentation is useful for the comparison of average loss values. It is also useful for comparing such gross features as the convergence zones. It is not generally useful for comparing such details as the focusing (or defocusing) caused by irregular bottom topography. In this report the comparison will be limited to the larger or more obvious features and no precise analysis is attempted. Because of FLIP's drift, the actual ranges corresponding to the measured data points are not quite the same as for the computed values. The former were based on navigation and acoustic travel time, while the latter assumed FLIP remained fixed at a median position.

Average Loss

60 ft source and 2500 ft hydrophone
(Fig. 86)

(C) At 100 Hz (A) the region from 0 to about 600 n.m. is characterized by convergence zones with marked peaks and troughs in the curves, particularly for the computed values. From 0 to about 250 n.m. the troughs agree, but not the peaks; then there is a relative shift so that the peaks agree instead from about 400 to 600 n.m. The agreement is good, within 0 to 2 dB, from about 600 n.m. to the end of the track at 1700 n.m.

(C) At 200 Hz (B) the peak and trough agreement is a little better from 0 to 400 n.m. but the discrepancy in the troughs is still large from 400 to 600 n.m. From 600 n.m. on, there is a steadily increasing difference, amounting to 7 or 8 dB at 1700 n.m. This could be due to use of too large an attenuation coefficient, as will be considered in the discussion section which follows.

(C) At 400 Hz (C) the discrepancies in the troughs for ranges 0 to 600 n.m. are very large. From 600 n.m. on, there is a steadily increasing average deviation similar to that for 200 Hz (B), and greater in magnitude, 18 dB at 1200 n.m.

60 ft source, 10,800 ft hydrophone
(Fig. 87)

(C) At 100 Hz (A) the computed curve lies above the measured values by about 10 dB (less loss). The difference steadily decreases with range to 0 dB at 1700 n.m. The peak to trough amplitudes agree quite well.

(C) At 400 Hz (C) the computed curve agrees well at shorter ranges, but shows increasingly greater loss with increasing range, to about 10 dB difference at 1200 n.m.

500 ft source, 2500 ft hydrophone
(Fig. 88)

(C) At 100 Hz (A) the agreement is very close, except perhaps from 1500 to 1700 n.m., and there the computed curve indicates a 2 or 3 dB greater loss.

(C) At 200 Hz (B) the agreement is good out to about 1000 n.m. From there to the end of the track the calculated loss increases steadily to a difference of about 8 dB at 1700 n.m.

500 ft source, 10,800 ft hydrophone
(Fig. 89)

(C) At 100 Hz (A) the agreement is good (0 to 2 dB) over the entire range.

(C) At 200 Hz (B) the agreement is excellent except for the range from about 1000 n.m., in which the maximum difference is less than 4 dB.

178 Hz CW projector at 500 ft depth
(Fig. 90)

(C) This figure shows the computed and measured values for the 178 Hz sinusoidal signal as received at the two suspended FLIP hydrophones and a bottomed MILS hydrophone at Kaneohe. The agreement is generally at least as good as for the charge data presented in Figs. 86-89, and perhaps somewhat better at the closer ranges.

(U) A rough summary of the differences between calculated and measured values is given in Table IV. This obviously cannot be a very precise description; the only tendency one can see toward a pattern in the differences is in the increasingly greater discrepancy with increasing frequency at long ranges (600-1700 n.m.), and with range at the higher frequencies (200 and 400 Hz).

Convergence Zones

(C) Detailed comparisons of measured and computed loss can be made but they are limited by the scale of these figures. The convergence zones are evident on all results, both measured and computed. The computed convergence zone separation appears to be slightly greater than the measured, by perhaps the order of 1 or 2 percent.

(C) At 100 Hz the lowest measured losses in convergence zone peaks are generally greater than the computed by 0 to 8 dB. A few measured peaks agree with the computed ones, but thus far none of the measured peaks has less loss than the corresponding computed one.

(C) At 178 Hz many measured losses are equal to or less (by as much as 5 dB) than the computed ones on convergence zone peaks.

(C) At 200 Hz and 400 Hz the comparison is similar to that for 178 Hz. The measured losses are not less than the computed ones by appreciably more than 5 dB, nor does there seem to be any marked trend with frequency.

(C) For data received from the north at FLIP the largest measured losses in regions between convergence zones are equal to or less than the computed ones. This difference increases with frequency and with range up to about 400 n.m. At 100 Hz the largest difference is about 18 dB; at 400 Hz about 55 dB. At this writing the available Kaneohe computed losses are too few for comment.

Discussion

(C) The most striking result of the comparison of measured and computed propagation loss is the greater computed loss compared with measured loss, which increases with frequency and range. In the section on Acoustic Results, analysis of the measured data alone suggested that the losses attributable to absorption were considerably less than those of Thorp (1967), the latter of which were used in the FNWC model. The discrepancy in Table III agrees within about 2 dB of the comparisons of measured and computed losses described above. Thus, if the apparent coefficients observed experimentally in PARKA I were used in the computation, the agreement with measured values would be greatly improved. Computed losses with a revised absorption term will be discussed in a later report.

(C) Over long distances in three of the four plots of 100 Hz propagation loss (except for Fig. 78) it is not profitable to debate whether there is any difference between average measured and average computed loss. Nevertheless, there are sections of the plots where the discrepancy becomes large enough

to constitute a serious problem when the requirement is to distinguish between sites where a difference of 3 dB may be very important. No explanation is available for these differences. Possibilities are (1) failures of interpolation methods in modelling horizontal gradients in sound velocity, and (2) recognized inadequacy in modelling diffraction effects in steep gradients. The marked discrepancy at all but the longest ranges in Fig. 78 (100 Hz) may possibly be due to a combination of the sensitivity of propagation loss to depth for this source/receiver combination and an error in the depth of the hydrophone.

Convergence Zone Comparisons

(C) The small discrepancy between the separations of convergence zones of the measured and computed losses is either a result of a small systematic error in measuring range at sea, or it is due to using slightly erroneous sound velocity structure. A thorough analysis of errors is not available for PARKA I at this writing. In the balance of the discussion, the discrepancy will be regarded as nonexistent. Measured and computed losses in convergence zones will be compared as though the local point of minimum measured loss coincided exactly with the peak of the corresponding computed convergence zone.

(C) The marked tendency for measured 100 Hz peak loss to be greater than the computed loss suggests that the policy of rounding off the L-factor (see p. 13) at a value of 250 is inadequate for 100 Hz, and 500 might be better. At all higher frequencies 250 appears to give good results, but could possibly be improved by change to about 100. These are crude estimates subject to revision on more detailed examination.

(C) The serious failure of the model to compute the correct loss between convergence zones appears to be due to one or more of three possible factors: (1) errors in bottom loss estimates, (2) the lack of accounting for leakage paths, or (3) inadequacy of the model in accounting for the shape of the convergence zone. These loss plots were all computed assuming a bottom loss which is somewhat greater than is suggested by other short range comparisons of PARKA I data with geographical observations in this region.

Summary and Conclusions

(C) 1. A comparison of a number of propagation loss vs. range plots shows agreement between measured and computed average losses within 0 to 3 dB at 100 Hz.

(C) 2. At 200 and 400 Hz there is evidence that attenuation in the model is too high by a factor amounting, for example, to about 18 dB in 1200 n.m. at 400 Hz. The model can readily be modified to incorporate this change.

(C) 3. A 1 to 2 percent discrepancy is noted between measured and computed convergence zone spacing. This may or may not be significant depending on the outcome of analysis of errors.

(C) 4. Comparison of measured and computed peaks suggests that small frequency dependent modifications be made in the rounding off policy for computing loss in convergence zones.

(C) 5 Comparison of measured and computed losses in the troughs between convergence zones suggests that too high a bottom loss has been assumed in the model, and that leakage paths may need to be taken into account.

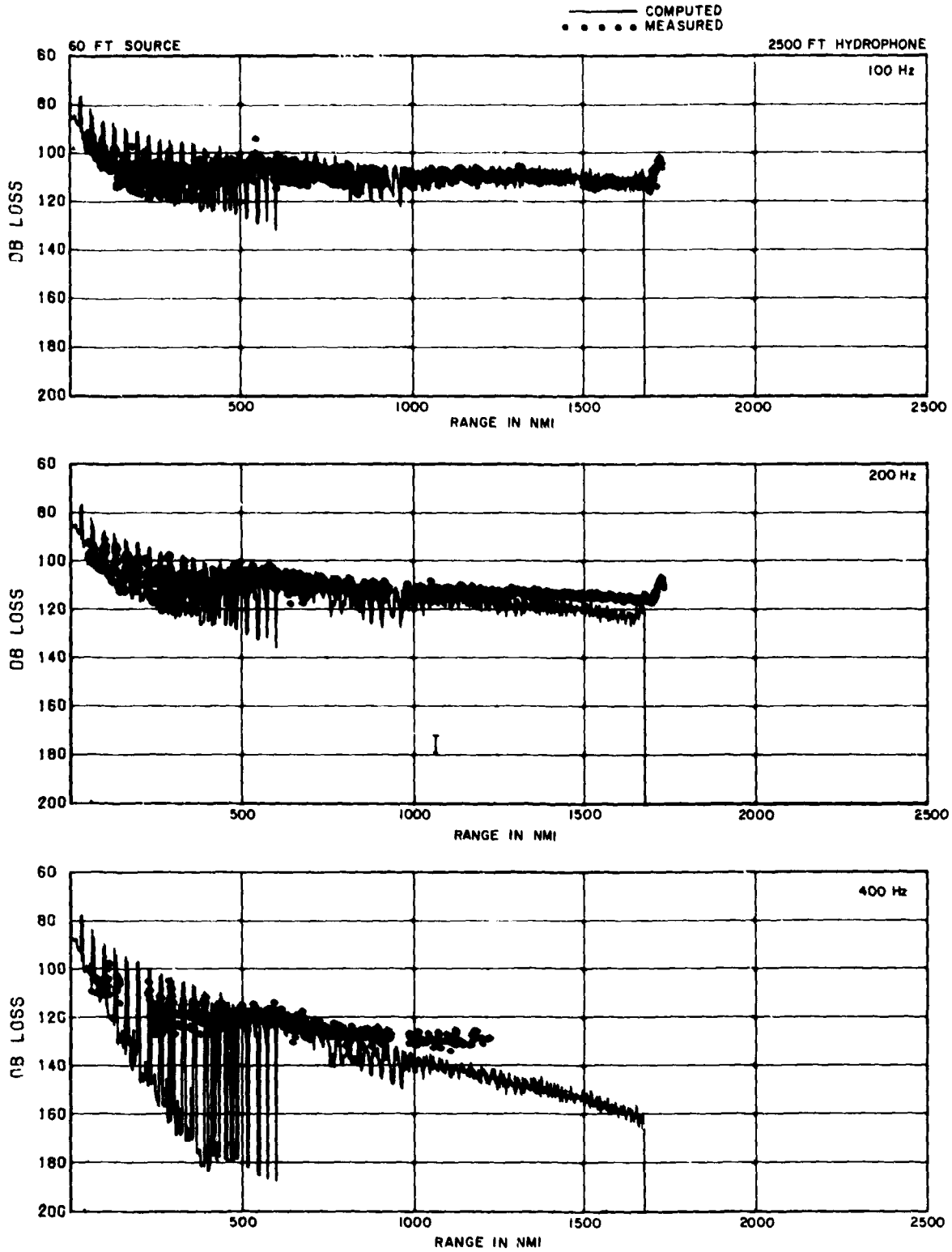

Fig. 86 — Comparison of computed and measured transmission loss (C)

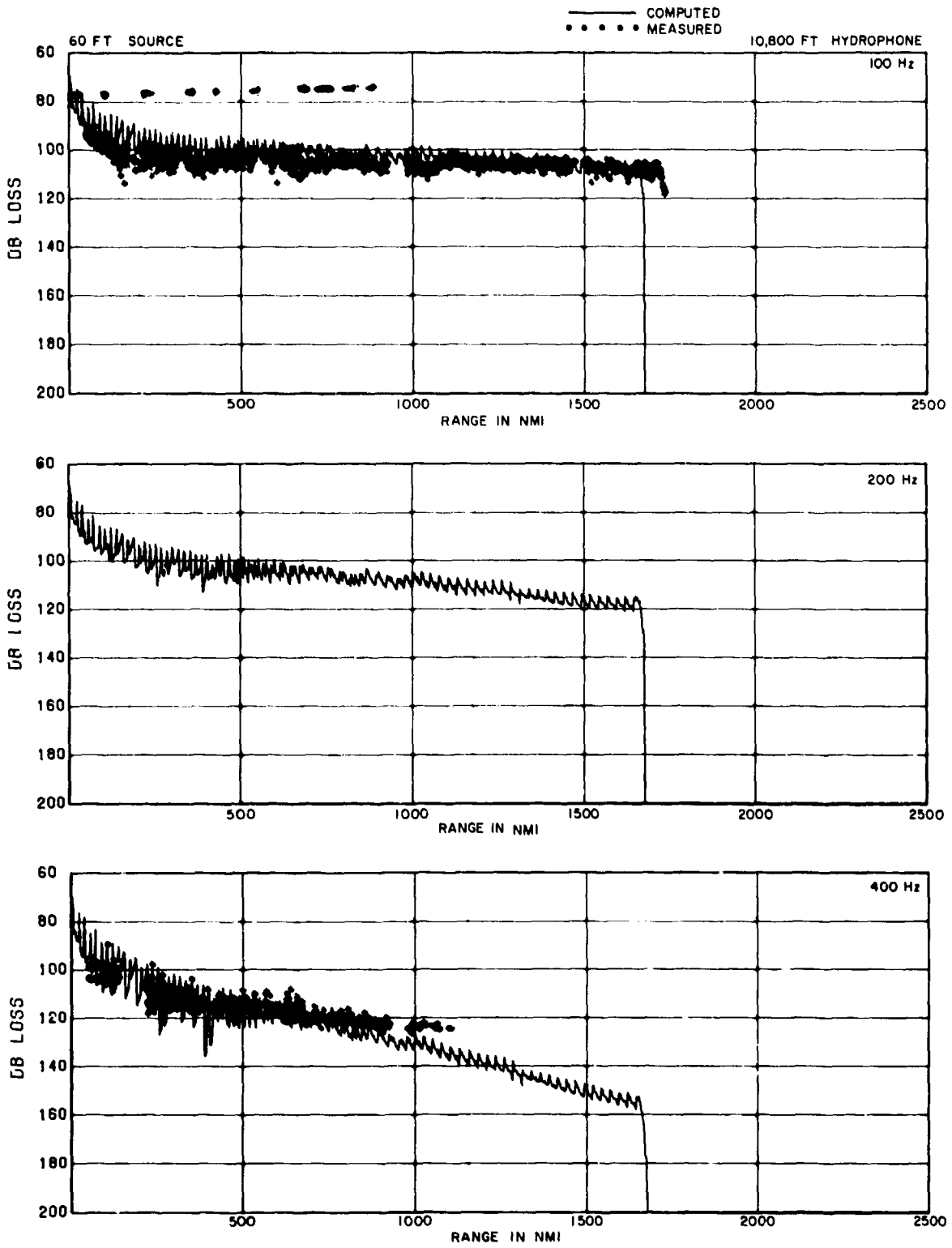

Fig. 87 – Comparison of computed and measured transmission loss (C)

MEASURED AND COMPUTED PROPAGATION LOSS

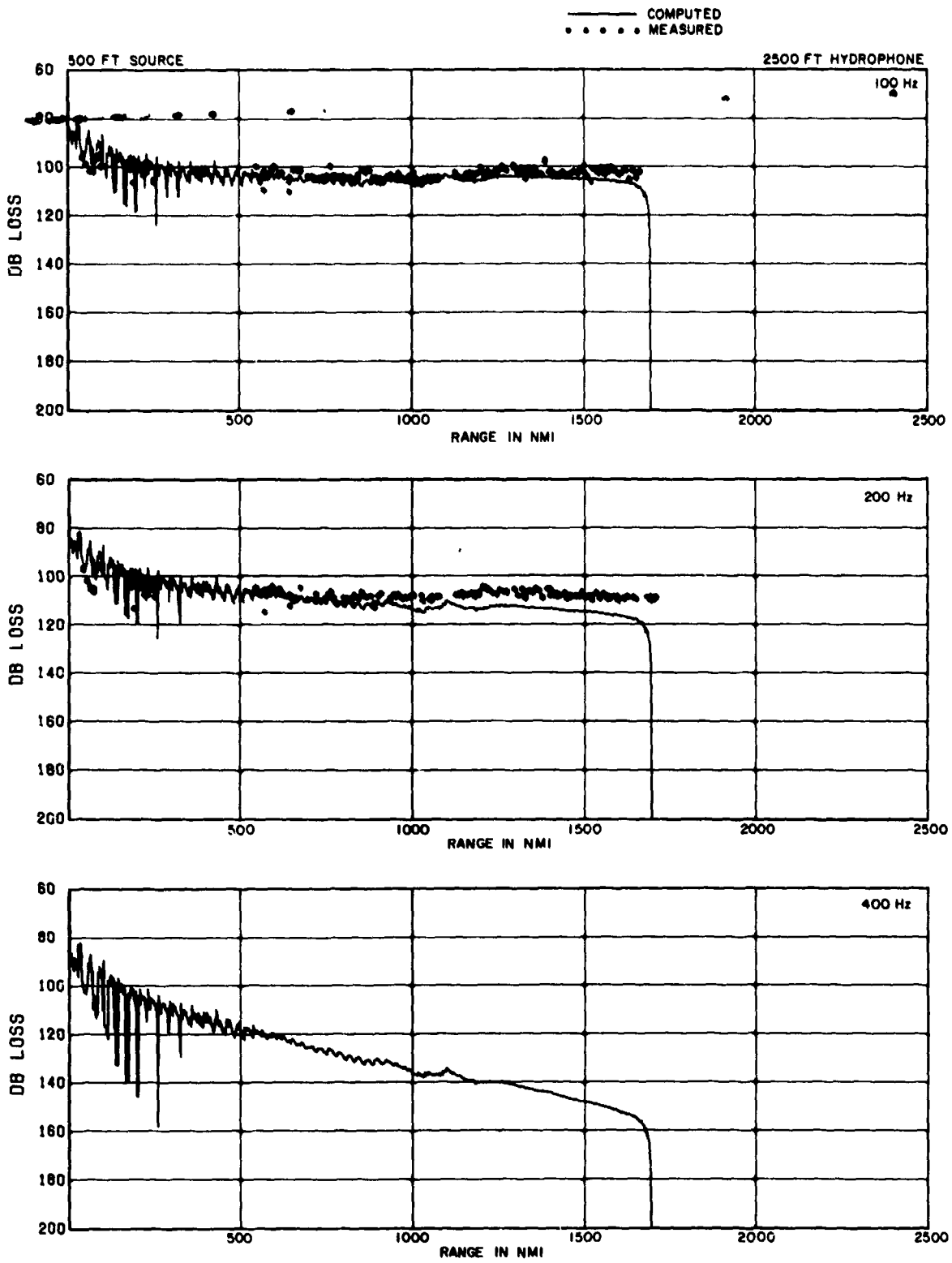

Fig. 88 — Comparison of computed and measured transmission loss (C)

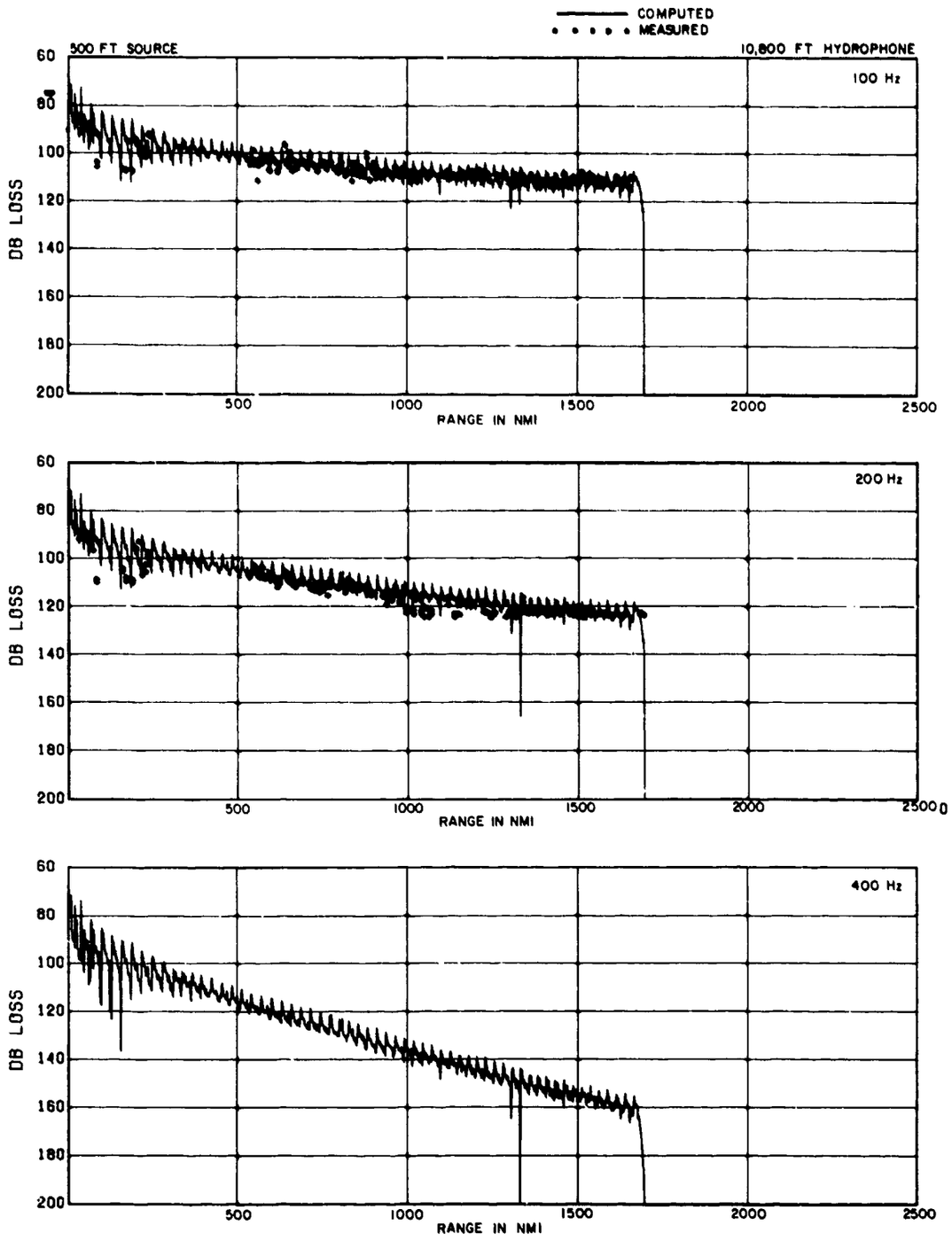

Fig. 89 — Comparison of computed and measured transmission loss (C)

MEASURED AND COMPUTED PROPAGATION LOSS

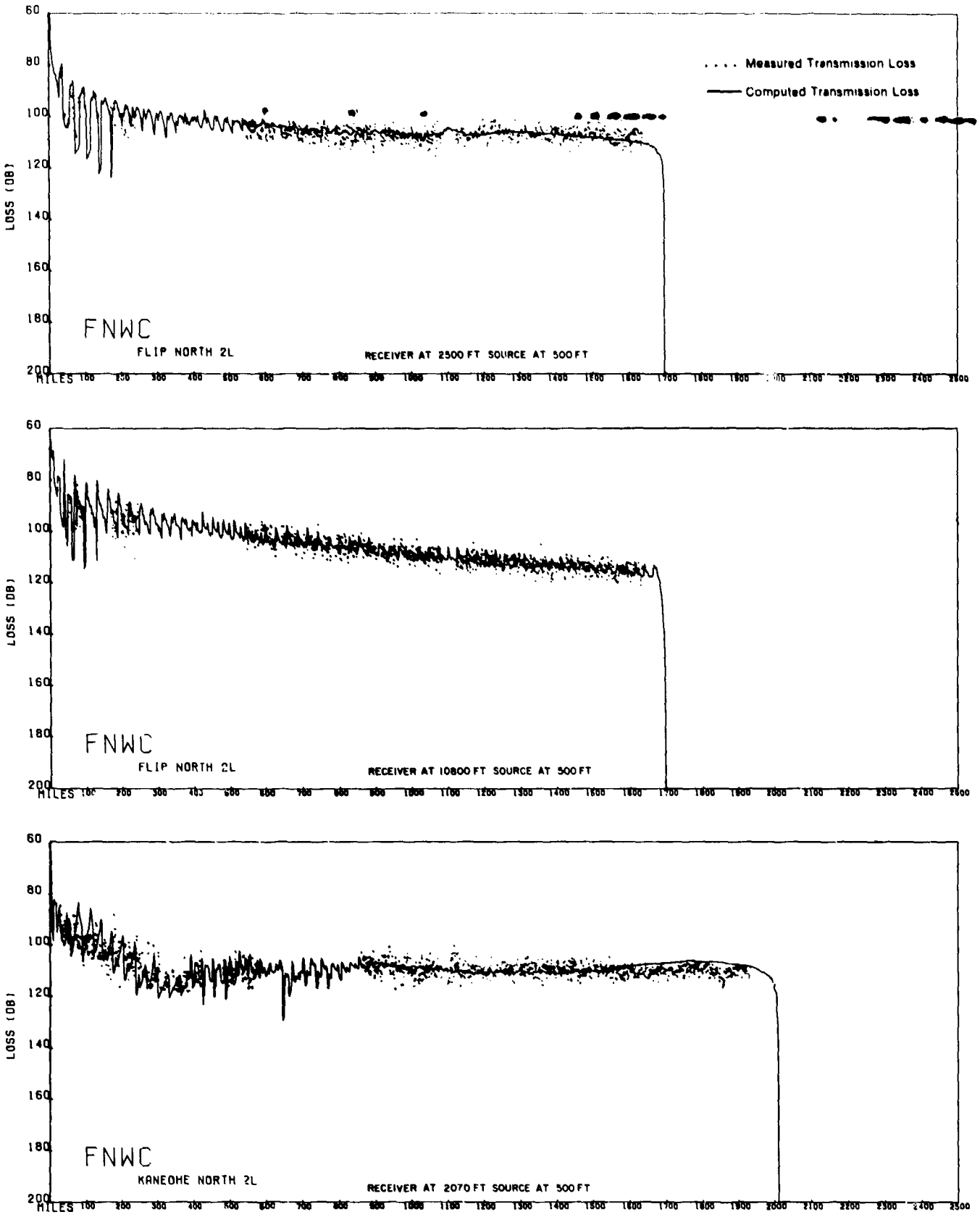

Fig. 90 — Comparison of measured and computed transmission loss (C)

TABLE IV
Differences Between Computed and Measured Values
of Propagation Loss (Figs. 86-89)

60 ft Source and 2500 ft Hydrophone				
	0-250 nm	250-600 nm	600-1200 nm	1200-1700 nm
100 Hz	Troughs 0-5 dB Peaks 10 dB	Troughs 5-20 dB Peaks 0-10 dB	0-1 dB in averages	0-1 dB in averages
200 Hz	Peaks 0-5 dB Troughs 0-5 dB	Peaks 0-5 dB Troughs 2-20 dB	6 dB in averages	Increasing from 6-10 dB in averages
400 Hz	Peaks 4 dB Troughs 0-55 dB	Peaks 0-4 dB Troughs 55-65 dB	Increasing from 0-14 dB in averages	(No data)
60 ft Source and 10,800 ft Hydrophone				
	0-250 nm	250-600 nm	600-1200 nm	1200-1700 nm
100 Hz	5-10 dB	5 dB	3-5 dB	0-3 dB
400 Hz	0-1 dB	0-3 dB	Increasing from 3-10 dB in averages	(No data)
500 ft Source and 2500 ft Hydrophone				
	0-250 nm	250-600 nm	600-1200 nm	1200-1700 nm
100 Hz	Limited data, generally agree	(No data)	0-1 dB in averages	0-3 dB in averages
200 Hz	Limited data, general agreement	(No data)	0-3 dB in averages	Increasing from 3-10 dB in averages
500 ft Source and 10,800 ft Hydrophone				
	0-250 nm	250-600 nm	600-1200 nm	1200-1700 nm
100 Hz	Limited data with equal scatters	(No data)	0-1 dB in averages	0-2 dB in averages
200 Hz	Limited data, general agreement	(No data)	0-2 dB in averages	0-2 dB in averages

CONFIDENTIAL

AD 506209L

CLASSIFICATION CHANGED
TO: CONFIDENTIAL
FROM: SECRET
AUTHORITY:
DoD 5200.1-R
Oct 80

CONFIDENTIAL

DEPARTMENT OF THE NAVY
OFFICE OF NAVAL RESEARCH
800 NORTH QUINCY STREET
ARLINGTON, VA 22217-5660

IN REPLY REFER TO
5510/1
Ser 93/160
10 Mar 99

From: Chief of Naval Research
To: Commander, Naval Meteorology and Oceanography Command
1020 Balch Boulevard
Stennis Space Center MS 39529-5005

Subj: DECLASSIFICATION OF PARKA I AND PARKA II REPORTS

Ref: (a) CNMOC ltr 3140 Ser 5/110 of 12 Aug 97

Encl: (1) Listing of Known Classified PARKA Reports

1. In response to reference (a), the Chief of Naval Operations (N874) has reviewed a number of Pacific Acoustic Research Kaneohe-Alaska (PARKA) Experiment documents and has determined that all PARKA I and PARKA II reports may be declassified and marked as follows:

   Classification changed to UNCLASSIFIED by authority of Chief of Naval Research letter Ser 93/160, 10 Mar 99.

   DISTRIBUTION STATEMENT A: Approved for public release. Distribution is unlimited.

2. Enclosure (1) is a listing of known classified PARKA reports. The marking on those documents should be changed as noted in paragraph 1 above. When other PARKA I and PARKA II reports are identified, their markings should be changed and a copy of the title page and a notation of how many pages the document contained should be provided to Chief of Naval Research (ONR 93), 800 N. Quincy Street, Arlington, VA 22217-5660. This will enable me to maintain a master list of downgraded PARKA reports.

3. Questions may be directed to the undersigned on (703) 696-4619, DSN 426-4619.

Peggy Lambert

PEGGY LAMBERT
By direction

Copy to:
NUWC Newport Technical Library (Code 5441)
NRL Washington (Mary Templeman, Code 5227)
NRL SSC (Roger Swanton, Code 7031)
DTIC (Bill Bush, DTIC-OCQ)

LISTING OF KNOWN CLASSIFIED PARKA REPORTS

Operation Plan, Pacific Acoustic Research Kaneohe-Alaska PARKA Experiment, Undated, ONR, 48 pages
(NUSC NL Accession # 49531)

Fleet Research Project 109 PARKA II, Undated, COMASWFORPAC-OPORD-303-69, Antisubmarine Warfare Force, Pacific Fleet, Unknown # of pages
(NUSC NL Accession # 093561)

Preliminary Operation Plan Pacific Acoustic Research Kaneohe-Alaska PARKA Experiment, June 1968, ONR, Unknown # of pages
(NUSC NL Accession # 023063)

LRAPP Briefing Report on the PARKA Series, May 1969, MC Report 001, Maury Center for Ocean Science (ONR), 20 pages
(NUSC NL Accession # 023375)

Bathythermograph Traces from PARKA, 20 May 1969, NUSL-TM-2213-118-69, 7 pages
(DTIC # B952 259)

Bathymetric Strip Charts in the North Pacific Ocean for Project PARKA II, 20 June 1969, Naval Oceanographic Office, Unknown # of pages
(NUSC NL Accession # 051659)

PARKA II Experiment Utilizing Sea Spider ONR Scientific Plan 2-69, 26 June 1969, MC-PLAN-01, 172 pages
(DTIC # B020 846)

PARKA I - Acoustic Processing and Results, 28 July 1969, USL Technical Memorandum No. 2210-015-69, NUSC New London, 115 pages
(NUSC NL Accession # 202993-001) (NRL SSC Accession # 85009134)

A Scheduled At-Sea Simulation of Adaptive Beamforming, 19 September 1969, NUSL-TM-2211-162-69, 23 pages
(DTIC # B026 991)

Biological Data Collected on the PARKA I Transit, 23 October 1969, NUSL-TM-2213-262-69, 15 pages
(DTIC # B952 263)

PARKA I Experiment, November 1969, MC Report 003, Volume 1, Maury Center for Ocean Science (ONR), 84 pages
(NRL Accession # 466930) (NRL SSC Accession # 85004881) (DTIC # 506 209)

ENCLOSURE (1) TO CNR LTR
5510/1 SER 93/160 DTD
10 MAR 99

DEPARTMENT OF THE NAVY
OFFICE OF NAVAL RESEARCH
875 NORTH RANDOLPH STREET
SUITE 1425
ARLINGTON VA 22203-1995

IN REPLY REFER TO:

5510/1
Ser 321OA/011/06
31 Jan 06

MEMORANDUM FOR DISTRIBUTION LIST

Subj: DECLASSIFICATION OF LONG RANGE ACOUSTIC PROPAGATION PROJECT (LRAPP) DOCUMENTS

Ref: (a) SECNAVINST 5510.36

Encl: (1) List of DECLASSIFIED LRAPP Documents

1. In accordance with reference (a), a declassification review has been conducted on a number of classified LRAPP documents.

2. The LRAPP documents listed in enclosure (1) have been downgraded to UNCLASSIFIED and have been approved for public release. These documents should be remarked as follows:

   Classification changed to UNCLASSIFIED by authority of the Chief of Naval Operations (N772) letter N772A/6U875630, 20 January 2006.

   DISTRIBUTION STATEMENT A: Approved for Public Release; Distribution is unlimited.

3. Questions may be directed to the undersigned on (703) 696-4619, DSN 426-4619.

BRIAN LINK
By direction

Subj: DECLASSIFICATION OF LONG RANGE ACOUSTIC PROPAGATION PROJECT (LRAPP) DOCUMENTS

DISTRIBUTION LIST:

NAVOCEANO (Code N121LC – Jaime Ratliff)
NRL Washington (Code 5596.3 – Mary Templeman)
PEO LMW Det San Diego (PMS 181)
DTIC-OCQ (Larry Downing)
ARL, U of Texas
Blue Sea Corporation (Dr.Roy Gaul)
ONR 32B (CAPT Paul Stewart)
ONR 321OA (Dr. Ellen Livingston)
APL, U of Washington
APL, Johns Hopkins University
ARL, Penn State University
MPL of Scripps Institution of Oceanography
WHOI
NAVSEA
NAVAIR
NUWC
SAIC

Declassified LRAPP Documents

Report Number	Personal Author	Title	Publication Source (Originator)	Pub. Date	Current Availability	Class.
ARLTR7952	Focke, K. C., et al.	CHURCH STROKE 2 CRUISE 5 PAR/ACODAC ENVIRONMENTAL ACOUSTIC MEASUREMENTS AND ANALYSIS (U)	University of Texas, Applied Research Laboratories	791029	ADC025102; NS; AU; ND	C
Unavailable	Van Wyckhouse, R. J.	SYNBAPS. VOLUME I. DATA BASE SOURCES AND DATA PREPARATION	Naval Ocean R&D Activity	791201	ADC025193	C
NORDATN63	Brunson, B. A., et al.	ENVIRONMENTAL EFFECTS ON LOW FREQUENCY TRANSMISSION LOSS IN THE GULF OF MEXICO (U)	Naval Ocean R&D Activity	800901	ADC029543; ND	C
NORDATN80C	Gereben, I. B.	ACOUSTIC SIGNAL CHARACTERISTICS MEASURED WITH THE LAMBDA III DURING CHURCH STROKE III (U)	Naval Ocean R&D Activity	800915	ADC023527; NS; AU; ND	C
NOSCTR664	Gordon, D. F.	ARRAY SIMULATION AT THE BEARING STAKE SITES	Naval Ocean Systems Center	810401	ADC025992; NS; AU; ND	C
NOSCTR703	Gordon, D. F.	NORMAL MODE ANALYSIS OF PROPAGATION LOSS AT THE BEARING STAKE SITES (U)	Naval Ocean Systems Center	810801	ADC026872; NS; AU; ND	C
NOSCTR680	Neubert, J. A.	COHERENCE VARIABILITY OF ARRAYS DURING BEARING STAKE (U)	Naval Ocean Systems Center	810801	ADC028075; NS; ND	C
HSECO735	Luehrmann, W. H.	SQUARE DEAL R/V SEISMIC EXPLORER FIELD OPERATIONS REPORT (U)	Seismic Engineering Co.	731121	AD0530744; NS; ND	C; U
MPL-C-42/76	Morris, G. B.	CHURCH ANCHOR EXPLOSIVE SOURCE (SUS) PROPAGATION MEASUREMENTS FROM R/P FLIP (U)	Marine Physical Laboratory	760701	ADC010072; AU; ND	C; U
ARLTR7637	Mitchell, S. K., et al.	SQUARE DEAL EXPLOSIVE SOURCE (SUS) PROPAGATION MEASUREMENTS. (U)	University of Texas, Applied Research Laboratories	760719	ADC014196; NS; AU; ND	C; U
NORDAR23	Fenner, D. F.	SOUND SPEED STRUCTURE OF THE NORTHEAST ATLANTIC OCEAN IN SUMMER 1973 DURING THE	Naval Ocean R&D Activity	800301	ADC029546; NS; ND	C; U
NOOTR230	Bucca, P. J.	SOUND VELOCITY CONDITIONS DURING THE CHURCH ANCHOR EXERCISE (U)	Naval Oceanographic Office	751201	NS; AU; ND	C;U
ONR SP 2-69; MC PLAN-01	Unavailable	PARKA II EXPERIMENT UTILIZING SEA SPIDER, ONR SCIENTIFIC PLAN 2-69 (U)	Maury Center for Ocean Science	690626	ADB020846; ND	U
Unavailable	Unavailable	PARKA I EXPERIMENT	Maury Center for Ocean Science	691101	AD0506209	U
USRD CR 3105	Unavailable	SEA SPIDER TRANSPONDER TRANSDUCER	Naval Research Laboratory	700505	ND	U
MC PLAN 05; ONR Scientific Plan 1-71	Unavailable	ATLANTIC TEST BED MEASUREMENT PROGRAM (U)	Maury Center for Ocean Science	701020	ND	U
ACR-170 VOL.1	Hurdle, B. G.	PROJECT NEAT- A COLLABORATIVE LONG RANGE PROPAGATION EXPERIMENT IN THE NORTHEAST ATLANTIC, PART I (U)	Naval Research Laboratory	701118	ND	U
MC-003-VOL-2	Unavailable	THE PARKA I EXPERIMENT. APPENDICES- PACIFIC ACOUSTIC RESEARCH KANEOHE-ALASKA (U)	Maury Center for Ocean Science	710101	ND	U